Chair of Reservoir Engineering

Master's Thesis

Understanding Wettability Changes during Alkali-Polymer through Spontaneous Imbibition Data

Vladislav Arekhov

May 2019

AFFIDAVIT

I declare on oath that I wrote this thesis independently, did not use other than the specified sources and aids, and did not otherwise use any unauthorized aids.

I declare that I have read, understood, and complied with the guidelines of the senate of the Montanuniversität Leoben for "Good Scientific Practice".

Furthermore, I declare that the electronic and printed version of the submitted thesis are identical, both, formally and with regard to content.

Date 26.05.2019

Signature Author
Vladislav, Arekhov
Matriculation Number: 11702304

Danksagung / Acknowledgement

I would like to dedicate my Master Diploma to my parents, Oksana Arekhova and Viacheslav Arekhov, who were supporting me at all ups and downs.

Furthermore, I would like to express my gratitude to the oil company OMV, which sponsored my studies and gave opportunity to receive proper high-level education. Particularly I would like to thank Dr.-Ing. Rafael Hincapie, who supervised my thesis and motivated me throughout entire project. Another word of gratitude I would like to express to Dr. Torsten Clemens. His advices during technological discussions helped me to come up with new ideas and improve the content of my thesis.

Also I would like to say thank you to my university professor and supervisor, Prof. Ott. His explanations of the physical phenomenons and physical background helped me to understand the problem properly.

Kurzfassung

Es ist bekannt, dass der Benetzungszustand der inneren mineralischen Oberflächen im Gestein die Speicher- und Fließeigenschaften einer Lagerstätte beeinflussen. Zudem wurde vorher bewiesen, dass das Einspritzen von Chemikalien in die Struktur zu einer Veränderung der Benetzungsfähigkeit führt. Die Ölcharakteristik wie etwa die TAN (total acid number) kann die Benetzungsfähigkeitsveränderung auch verbessern oder verringern. Ziel dieser Untersuchung ist es, die Auswirkung von alkalischen, polymeren und alkalisch-polymeren Lösungen auf die Benetzungsfähigkeit mit Hilfe von spontanen Sättigungstests zu untersuchen. Die Daten, die bei Amott Imbibitionsstests erhalten werden, werden durch die Anwendung von numerischer Simulation des kapillaren Saugprozesses und analytischer Lösung einer Gleichung, ähnlich wie Fick'sches Gesetz, analysiert. Ein detaillierter Vergleich von Gesteinsproben unterschiedlicher Mineralogie, Ölen mit verschiedenen TAN-Zahlen und Lagerstättenwasser unterschiedlicher Zusammensetzung wird gemacht. Die Experimente wurden sowohl mit gereinigten wasserbenetzenden Bohrkernen als auch mit Proben mit wiederhergestelltem verwässerten Ölzustand. Die Ergebnisse zeigen einen großen Einfluss von Chemikalien nicht nur auf die ultimative Erdölproduktion sondern auch auf die Produktionsrate im Laufe der Zeit. Die Untersuchung hat gezeigt, dass die Verwendung von Chemikalien die kapillaren Kräfte im Bohrkern beeinflusst, was mit der Veränderung der Benetzungsfähigkeit direkt übereinstimmt. Der Rahmen, der in diesem Projekt vorgestellt wird, kann dazu verwendet werden, die relativen Benetzungsfähigkeitsänderungen unter Anwendung von verschiedenen EOR Mitteln zu evaluieren.

Abstract

It is well known that the wetting state of the rock's internal mineral surfaces affects storage and flow characteristics of the reservoir. Moreover, it has been previously shown that injection of chemicals into the formation leads to alteration of the wettability. The oil characteristic such as the TAN (total acid number) also determines the wetting state of the reservoir. The aim of this study is to examine the effect of alkaline, polymer and alkali-polymer solutions on wettability by means of spontaneous imbibition tests. The data obtained from Amott imbibition tests were analyzed using numerical simulation of the capillary suction process and analytical solution of an equation similar to Fick's law of diffusion. A detailed comparison is made between rock samples with various mineralogy, oils with different TAN numbers and brines with various composition. The experiments were done on cleaned water-wet core plugs as well as on samples with restored oil-wet state. The results illustrate a large influence of chemicals not only on ultimate oil production, but also on the rate of production over time. The investigation has revealed that the application of chemicals influences capillary forces in the core plug, which can be directly correlated to wettability alteration. The framework presented in the project can be used to evaluate relative wettability change with the application of different EOR agents.

Abbreviations

EOR	Enhanced Oil Recovery
TAN	Total Acid Number
AN	Acid Number
TSN	Total Soap Number
IFT	Interfacial Tension
Pa	Pascal
s	second
m	meters
N	Newton
D	Darcy
ASP	Alkali-Surfactant-Polymer
rad	radian
kg	kilogram
Sx	Saturation of the phase x
Vx	Volume of the phase x
AHWI	Amott-Harvey Wettability Index
WI	Wettability Index
o	oil phase
w	water phase
SEM	Scanning Electron Microscope
NH	Nordhorn (Outcrop Core)
ml	millilitres
rpm	revolution per minute
Eq.	Equation
St. Dev.	Standard Deviation
St. U.	Saint Ulrich (oil)
Kro	Oil relative permeability
ft	foot
RCA	Routine Core Analysis

Table of content

Page

1 INTRODUCTION 1

2 FUNDAMENTALS AND LITERATURE OVERVIEW 3

2.1 Enhanced Oil Recovery Principles 3

2.2 Chemical EOR Mechanisms 5

2.3 Role of interfacial Tension in Wettability Evaluation - Generalities 7

2.4 Role of Wettability in Oil Recovery - Generalities 9

2.5 Summary 21

3 EXPERIMENTAL SETUP AND MATERIALS 23

3.1 Fluid Characterization 23

3.2 Core Plug Preparation and Analysis 26

3.3 Spontaneous Imbibition 34

4 EXPERIMENTAL RESULTS AND DISCUSSION 36

4.1 Fluid Characterization Results 36

4.2 Routine Core Analysis 39

4.3 IFT Measurement Results 43

4.4 Spontaneous Imbibition Results 47

5 DATA INTERPRETATION AND SIMULATIONS 58

5.1 Analytical Solution 58

5.2 Numerical Solution 72

6 CONCLUSION 76

7 REFERENCES 79

1 Introduction

Around 66% of the oil available is typically left behind in the reservoir due to technological or economic reasons [1]. For the majority of the cases, this oil can be only extracted by the use of additional methods that could provide external energy to the reservoir. Therefore, there is a substantial potential for increasing the oil production by implementation of enhanced oil recovery (EOR) methods. EOR affects the reservoir rock and/or reservoir fluids in order to increase displacement and sweep efficiency of oil [2]. There are different EOR methods described in the literature. This work focuses on chemical methods, namely, on the wettability alteration during Alkali-Polymer flooding.

A set of methods are available for defining wettability of the cores using laboratory approaches: contact angle measurements, Amott-Harvey method and USBM method [4]. A common disadvantage all available approaches is that they are either time consuming or cost intensive. The study presented here, attempts on defining wettability alteration in the core plugs based only on the spontaneous imbibition principle (Amott-Harvey method), by performing Amott imbibition tests.

The imbibition process is governed by the capillary suction phenomenon, which is directly related to the wettability state of the system and interfacial tension (IFT) between fluids. Obtaining both parameters for various experimental setups provides some basis for the determination of the relative wettability changes during the experiments.

Several parameters, affecting the wettability of the mineral surface, were studied throughout the project. First, the total acid number (TAN) of oil defines the efficiency of the alkaline flooding due to the amount of surfactants, which can be created in-situ after its reaction with alkali [34]. Two different oil types were used for the experiments, one of which is notable for a high TAN and the other one has a low content of organic acids (low TAN). Second, in order to detect the wettability alteration, the core plugs with two initial wetting states were used. It has been reported, that ageing of the core at reservoir temperature for around 800 hours leads to wettability shift from purely water-wet state of the cleaned core samples to the neutral or oil wet state [4]. The oil production behavior is being studied on the non-aged (water-wet) and aged (neutral to oil-wet) core plugs in order to detect the signs of the wettability alteration while chemicals (alkali, polymer and alkali-polymer solutions) are used.

Third, it is known that brine composition and mineralogy of the sample determine the extent of the wettability alteration [63-65, 71]. In order to study the effect of divalent ions and clay minerals on the wettability, the brine with two different compositions (with and without divalent ions) and two outcrop core plugs (with and without clay components) were investigated.

As a complementary and supportive evaluation, Interfacial tension was measured as a function of time over 300 minutes at temperature of 60°C. This allows to define both instantaneous and equilibrium IFT for different systems. While the IFT for brine-oil and polymer-oil systems does

not change with time, the interfacial tension between oil and alkali solution depends on the alkaline and oil acids consumption. A remarkable behavior of IFT for both oil types was observed. High TAN oil results in ultra-low equilibrium IFT after approximately 100 minutes from the start of the measurement, while applying the low TAN oil, the interfacial tension does not reach ultra-low values. Combining this data with spontaneous imbibition results helped to draw conclusions regarding the effect of chemicals on the wettability.

Subsequently, the obtained oil production data was analyzed by means of analytical and numerical solutions of an equation similar to Fick's law of diffusion. As a result, the capillary diffusion coefficients for the imbibition processes were estimated. They were further used to relate the shape of capillary diffusion function to a certain wettability state of the system and obtain saturation profiles within the core plug by solving the problem numerically.

Chapters and sections structure the work, in order to provide a complementary evaluation and interpretation of the data. In the first part of work, a thorough literature review on the corresponding topics is presented. Discussed topics includes: enhanced oil recovery principles, the mechanisms of chemical application, interfacial tension effects, wettability effects on oil recovery process, IFT and wettability measurement techniques. Then, the analytical solution of the capillary suction phenomenon is explained and numerical setup is presented. Later chapter contains the information about the equipment setup and measurement tools. Finally, results of the investigation are shown, containing: fluid characteristics, routine core analysis results, IFT measurement and spontaneous imbibition data. At last, the analysis of obtained data and numerical simulation results are presented.

2 Fundamentals and Literature Overview

Along this chapter, an overview of the relevant literature on wettability alteration is presented. First, the general description of enhanced oil recovery (EOR) methods is addressed. Further, the mechanisms associated to chemical injection, particularly Alkali, Polymer and Alkali-Polymer solutions are outlined. Subsequently, the effects of chemicals on interfacial tension (IFT) and wettability are explained; follow by a state-of-the-art technology for determination of these parameters.

2.1 Enhanced Oil Recovery Principles

EOR is defined as a process or technique affecting the reservoir rock and/or reservoir fluids to increase microscopic (displacement) and macroscopic (sweep) efficiency of oil displacement [2]. After primary or secondary stage of production, remaining oil is difficult to be produced due to insufficient viscous forces, dominating mobility of water over mobility of oil and capillary effects. Viscous and capillary forces determine the efficiency of displacement on pore scale. The relation between two forces is described by capillary number, which is defined as viscous forces over capillary forces [44].

$$N_c = \frac{u\mu}{\sigma} \tag{1}$$

, where:

N_c – Capillary number [-]

μ – Viscosity of displacing fluid [Pa*s]

u – Velocity of displacing fluid [m/s]

σ – Interfacial tension between displacing fluid and oil [N/m]

Thus, the first objective of EOR methods (on microscopic level) is increasing capillary number, namely increasing displacing fluid viscosity and velocity and decreasing interfacial tension between fluids. The link between residual oil saturation and capillary number was extensively studied in the industry. Lake, Larry W. (1989) established the so-called desaturation curve, which expresses this relationship (see Figure 1) [44]. One can see from the graph, that increasing capillary number up to a critical value does not affect residual oil saturation. However, at values larger than critical one, the residual oil saturation decreases. In addition, the effect of wettability on desaturation curve is presented. In case of oil-wet reservoirs, the capillary number must be increased significantly more to reach critical level.

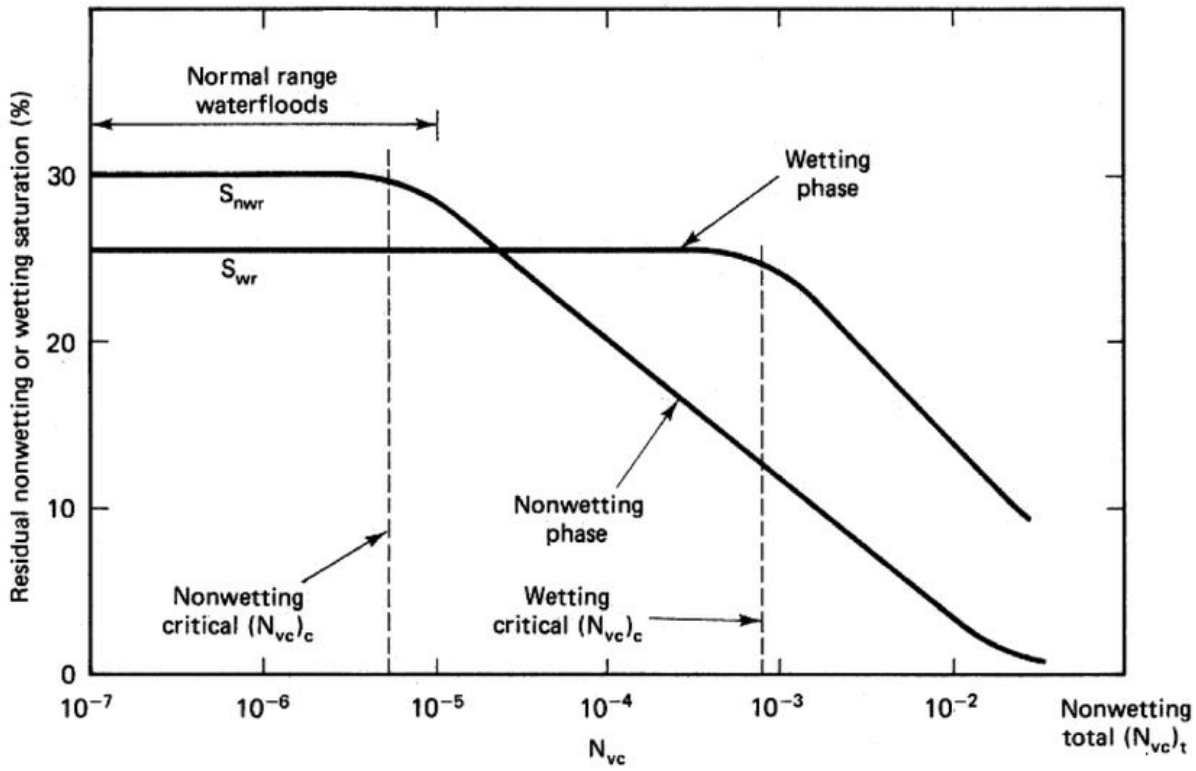

Figure 1: Capillary desaturation curve [44]

The second target of the EOR methods is to decrease mobility ratio. This goal is attributed to macroscopic sweep efficiency of the displacement process. Mobility of the fluid is defined as phase permeability divided into phase viscosity. The mobility ratio, in turn, describes the relation of displacing fluid mobility over the mobility of displaced fluid.

$$M = \frac{\lambda_{displacing}}{\lambda_{displaced}} = \frac{k_{r,displacing} \cdot \mu_{displaced}}{k_{r,displaced} \cdot \mu_{displacing}}, \tag{2}$$

where

M – Mobility ratio [-]

λ – Phase mobility [mD/Pa*s]

k_r – Phase relative permeability [-]

μ – Viscosity [Pa*s]

In case of high mobility ratio, the displacing fluid is more mobile than displaced. This leads to not stable displacement front and, consequently, viscous fingering. In the end, this results in large volumes of oil left behind the displacement front and early injection fluid breakthrough, which negatively affect the ultimate oil recovery (see Figure 2) [2].

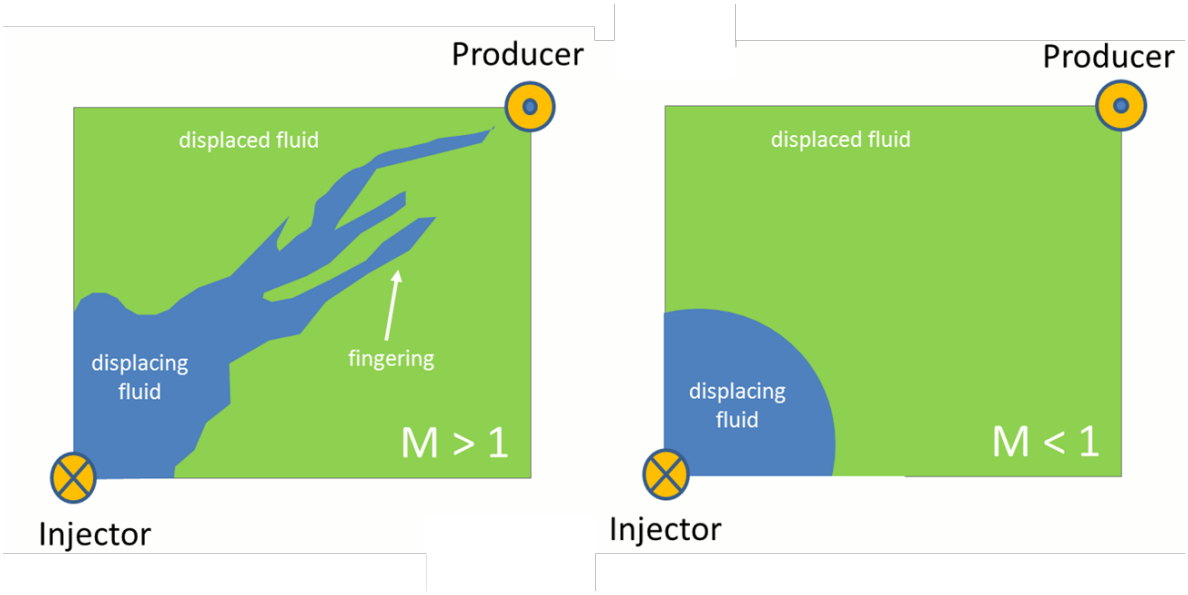

Figure 2 – Representation of the mobility ratio effect on sweep efficiency [45]

Summarizing the above, the main goal of every EOR method is improvement in microscopic (displacement) and/or macroscopic (sweep) efficiency. It can be done by increasing capillary number, which will lower the residual oil saturation, or by decreasing mobility ratio to stabilize front of the displacement.

2.2 Chemical EOR Mechanisms

There exist many different EOR methods: chemical, thermal, miscible flooding, ect. In this work, special attention is given to chemical techniques/processes, particularly on the application of Alkali, Polymer and Alkali-Polymer solutions.

The EOR objectives, defied before, might be directly linked to agents used for recovery improvement. Chemical application can affect both goals of EOR: as an increase of capillary number, as well as a decrease of mobility ratio.

In spite of the fact that the investigations of the use of alkali for flooding purposes started in the 1920's, the first field test was performed only in 1970's [46]. Many laboratory investigations have been performed to identify alkali-flooding effects on incremental oil recovery. Results have proven the effectiveness of alkali solution usage for flooding purposes. The increased oil production has been reported by various authors [7, 31, 33]. In addition to that, full field studies of alkali, alkali-polymer and alkali-surfactant-polymer (ASP) injection have provided optimistic results. ASP flooding implementation on oil fields in China have shown an average 15% increase in oil recovery [32]. Another field pilot-hole test was performed by Shell in 1989 in several wells of White Castle filed. 38% of incremental oil recovery was achieved by ASP flooding [33].

Additional oil production during alkaline flooding is attributed to two main mechanisms: low interfacial tension (IFT) between fluids and wettability alteration [32]. Both effects promote the increase in capillary number, leading to incremental oil recovery. Thus, in order to find out an effect of wettability change during chemical flooding, both mechanisms shall be considered.

Lowering of the interfacial tension with the addition of alkali solution occurs due to in-situ saponification mechanism. Crude oil composition plays an important role during alkaline flooding. Its efficiency mainly depends on the amount of natural acids in the oil, which can be neutralized by alkali. This finally leads to an in-situ soap creation and, consequently, to lowering in IFT (see Figure 3) [34, 68, 75].

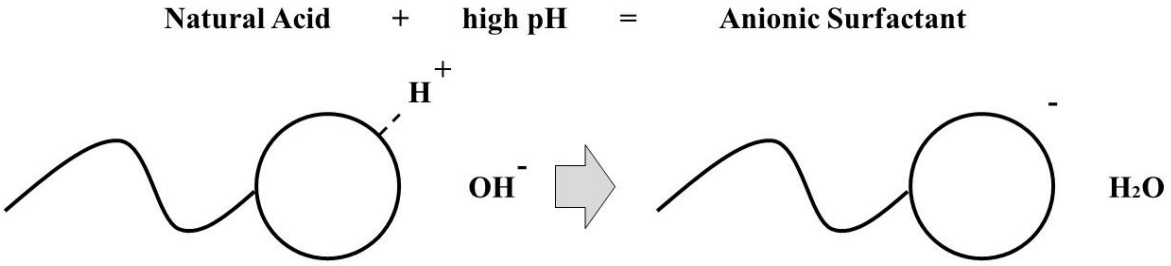

Figure 3 – Creation of in-situ surfactants

There are different parameters that could be used to describe or determine the potential for alkali flooding, such as Total Acid Number (TAN) number of oil. The most commonly used is the TAN number. The measurement of oil TAN number is performed applying titration with potassium hydroxide (KOH). Finally, the TAN number is reported as the amount of KOH needed in order to neutralize 1 g of oil. Although recent studies could not find a correlation between incremental oil recovery due to alkali application and TAN number, its effect is indisputable [59]. The parameter obtained by titration does not differentiate between weak acids, which do not contribute to in-situ soap generation, and strong acids. Therefore, the acid number (AN) can be used to better define the potential of alkali application with a certain oil type [35]. A number of research projects have focused onto confirming IFT reduction during alkali application. It was reported, that for incremental oil recovery an ultra-low IFT in a range of 10^{-3} mN/m shall be achieved [33, 34, 36].

A second type of chemicals studied are polymers. According to Pye [47], the first polymer flooding studies were carried out in the middle of 1960's. The idea behind polymer injection is very simple. Polymer solution has a higher viscosity than water, which directly affects displacing fluid mobility, lowering the mobility ratio [48]. Thereby, the viscosity of the water phase is increased by adding polymer. The major focus of polymer flooding is improvement of macroscopic (sweep) efficiency. However, the polymer retention and adsorption as well as viscoelastic behavior of the polymer solutions add significant complexity to the process, affecting also microscopic (displacement) efficiency. When combining Alkali-Polymer flooding,

the compatibility and interaction of all chemicals are crucial for a successful recovery process [6, 69]. Some studies have claimed, that the effect of polymer flooding on wettability is minor [49], whereas other authors have stated a significant effect of polymers, changing the wettability of the rock to more water-wet [50]. Generally, a wettability change is attributed to polymer adsorption. For instance, the detachment of the oil droplet is explained by diffusive-reptation of polymer chains mechanism. This behavior tends to modify the properties of the rock, changing the disjoining pressure at the wedge and allowing oil droplet to be released (see Figure 4) [51].

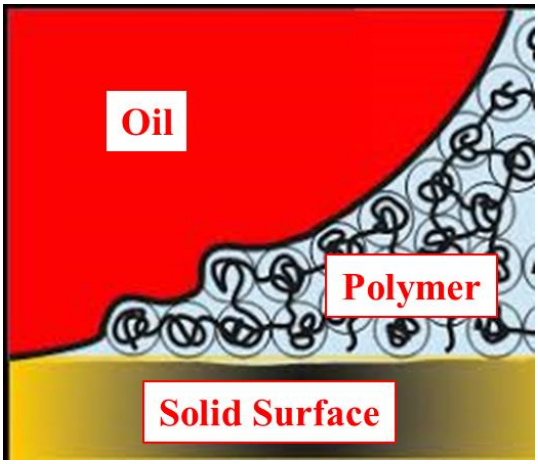

Figure 4 – Wettability change due to polymer application [50]

2.3 Role of Interfacial Tension in Wettability Evaluations - Generalities

2.3.1 IFT Definition

Interfacial tension is commonly defined as a force per unit length, which acts along an interface of two immiscible fluids [30]. The SI unit is mN/m. IFT can be described by Young's equation (see Figure 5).

In presence of two fluids, there appears a surface tension between fluids and solid surface. These surface tension forces are not always equal. Therefore, interfacial tension force starts playing the role in order to stabilize the system [38].

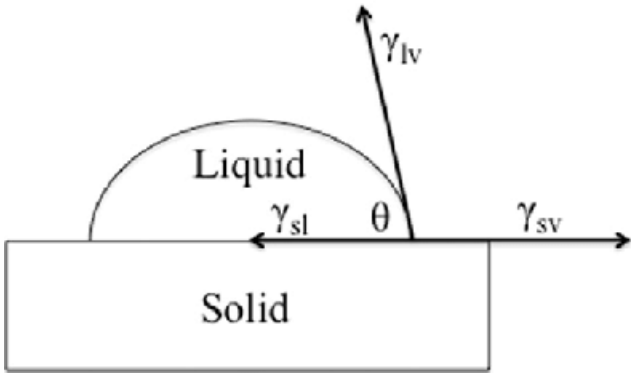

Figure 5 – Young's equation schematics

$$\gamma_{sl} + \gamma_{lv} * cos\theta = \gamma_{sv} \quad (3)$$

γ_{sl} – surface tension between solid and the first fluid [N/m]

γ_{sv} – surface tension between solid and the second fluid [N/m]

γ_{lv} – interfacial tension between fluids [N/m]

θ – contact angle [°degree]

Note that, interfacial tension widely depends on temperature, oil and water composition and slightly on the pressure. Therefore, it is important to measure IFT at the reservoir temperature.

The role of IFT in wettability evaluations have been widely reported in the literature. Recent studies have shown that in order to recover residual oil, the IFT shall be decreased until ultra-low values in an order of 10^{-3} N/m [33]. Due to the low IFT, the irremovable oil with large forces at the interface is being tuned into movable oil of easy deformation. [7]. Furthermore, it was proven that transient IFT plays a bigger role in release of the residual oil than equilibrium IFT [34]. The rapid change in local IFT might induce deformation of the interfacial films and, combining with the help of fluid driven shear forces, the residual oil starts moving forward. [7, 52].

2.3.2 IFT Spinning Drop Measurement Method

Vonnegut in 1942 proposed a method of measuring interfacial tension between two immiscible fluids by the rotation of a vessel at a defined rotational speed [37]. Due to the centrifugal forces involved, the fluid with lower density is pushed towards the center and forms a droplet. Interfacial tension forces act against the centrifugal force, which leads to a certain shape of a droplet at force equilibrium. The droplet shape will define an interfacial tension value between fluids (see Figure 6).

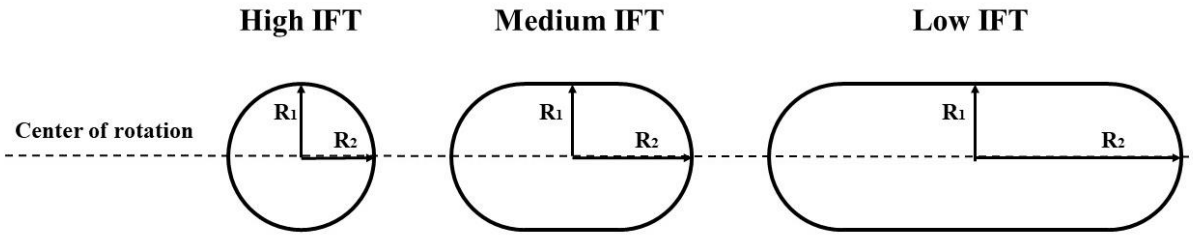

Figure 6 – Shape of spinning drop related to interfacial tension

When the length of a droplet is much larger than the droplet radius (4:1 ratio), the droplet shape can be approximated as a cylinder. This allows to consider only the radius of a droplet. Vonnegut derived the following equation for IFT calculation:

$$\sigma = \frac{\Delta\rho\omega^2}{4} R^3 \tag{4}$$

σ – Interfacial tension [N/m]

$\Delta\rho$ – density difference [kg/m^3]

ω – rotational speed [rad/s]

R – radii of curvature [m]

2.4 Role of Wettability in Oil Recovery - Generalities

2.4.1 Wettability as per Definition

Generally, the term wettability describes the preference of a solid to contact one wetting liquid (gas) rather than another non-wetting liquid (gas) [11]. In petroleum reservoir engineering, wettability describes the preference of oil or water to “stick” to the reservoir rock. However, due to the complex porous structure, it is not always possible to define preferential wetting phase. Usually, what is called “wettability” in oil industry refers to an “average” preference of fluid to be in contact with reservoir rock [26]. There exist four types of wettability: 1) when the rock is water-wet, the rock tends to adsorb water molecules on the surface. Water occupies in tendency smaller pores. 2) In opposite case, oil-wet rocks show the preference to hold oil molecules on their surface. Moreover, there exist also two intermediate wettability states: mixed wet and neutral wet systems. 3) Mixed wet appears due to reservoir heterogeneity. While one mineral exhibits water-wet behaviour, another mineral acts as an oil-wet rock. Another cause of mixed wettability state is a hysteresis of the minerals with respect to exposure by initial heterogeneous fluid distribution. This leads to a mixed wettability state, where wettability varies spatially on a microscale level. 4) Neutral wettability is addressed to type of rocks, which do not give a preference to any of fluids and may adhere them equally.

It is very important to note, that wettability describes only the preference of rock to be in contact with molecules on the surface and it does not depend on the saturation of fluids in the reservoir. For example, after hydrocarbon migration into the reservoir trap, the rock still can be water-wet, while the saturation of water stays at connate water saturation level. Wettability can be demonstrated in this case by imbibition process. Supplying additional water into the system (e.g., implementing waterflooding), the water will imbibe into the rock, displacing oil, indicating that the formation “prefers” to hold water [3]. The data, presented in this report, attempts to investigate wettability alteration based on this principle. By performing multiple spontaneous imbibition tests, the effort is given to detect wettability changes in the core plugs, submerged into different chemical solutions.

2.4.2 Wettability on a Pore Scale

As previously stated, wettability is an important factor, which directly affects the effectiveness of oil production in the reservoir. Generally, one of the fluids in the reservoir will be a wetting fluid, meaning that it will occupy smallest pores and spread along the rock surface. Non-wetting fluid, in turn, will stay in the center of largest pores and form initial globules, which fill several pores. This will affect both storage and flow characteristics of the reservoir rock. In order to capture the influence of wettability on storage and flow capacity, both, primary drainage and primary imbibition should be tracked in detail.

Different authors have reported [3, 60], that the reservoir before hydrocarbon migration is believed to be strongly water-wet, the reason behind is that mineral surfaces are charged/polar and hence initially terminated by polar water molecules (see Figure 7a). When oil migrates inside the pores, it flows through the center leading to connate water saturation. There exists only a thin layer of water on the rock surface (see Figure 7b). As soon as imbibition process starts, the water, imbibing into the pore, goes preferentially to the already existing water films, and therefore swelling them. Some part of the oil is displaced to the next pore at a higher rate, translating into a high relative permeability to oil. However, the residual oil saturation in this case is larger. Due to a snap-off of water in a small pore throat, the oil cluster gets disconnected. Oil, remaining in the pore, is not movable as long as viscous forces does not increase enough to push the oil through a small capillary [12].

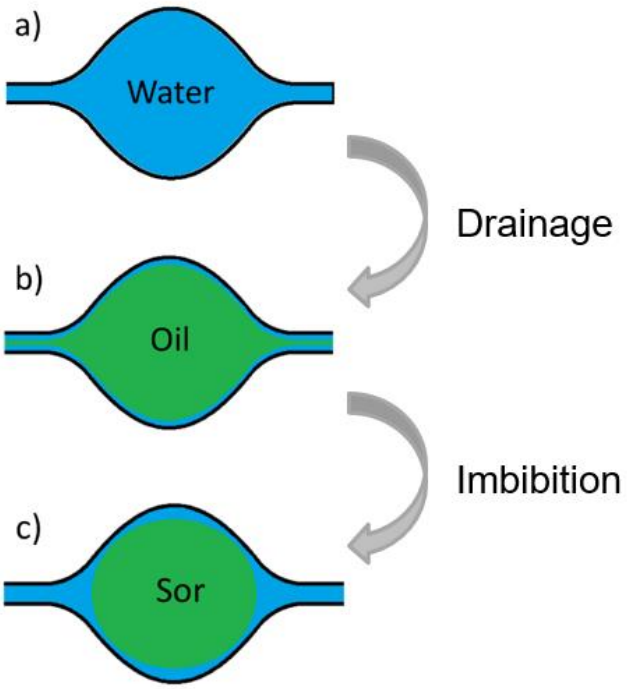

Figure 7 – Water-wet rock storage and flow behaviour

The opposite happens for the case of oil-wet rock behavior; relative permeability to oil stays very low, but the final oil recovery exceeds the one in case of water-wet rock. An example of this can be seen from Figure 8.

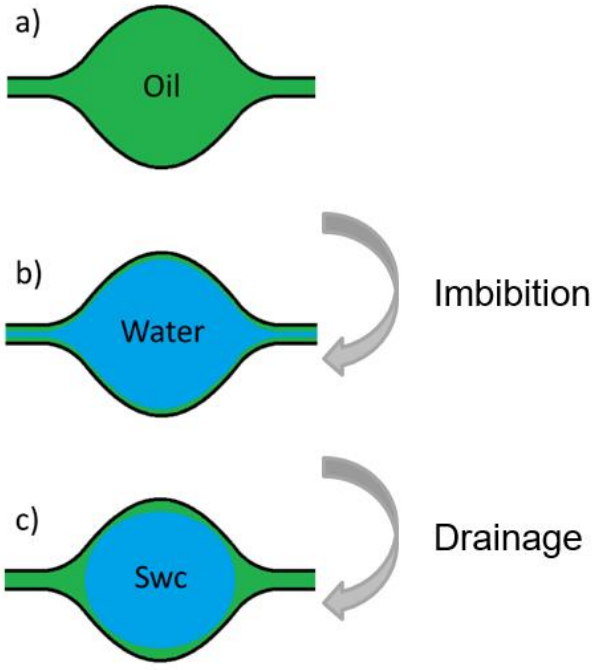

Figure 8 – Oil-wet rock storage and flow behaviour

Consequently, wettability controls the shape and distribution of residual oil. Whereas, on one hand, in water-wet rocks, residual oil is entrapped in the form of irregular strings, cakes and beads, which are mainly located in larger pores. On the other hand, in oil-wet system, the residual oil stays in small pores or pores with dead ends [34]. Although, most industry efforts focus on altering oil-wet rock to water-wet, which would promote oil production rate, some of the researches claim that an optimum wettability of the rock is not oil-wet nor water-wet, but something in between [7,13].

2.4.3 Wettability States Associated to Oil Production

Despite the fact that originally the reservoirs are water-wet, initial natural state of the reservoir at a start of production can be oil-wet. Nutting (1934) first realized that a big amount of producing fields are actually strongly oil-wet [14]. For instance, Bradford sands, Ordovician sands can serve as examples of strongly oil-wet reservoirs [15, 16]. Chilingar and Yen (1983), performed contact-angle measurement using 161 limestone and dolomite cores. The results showed, that around 80% of all cores exhibit oil-wet behavior [17]. The author`s findings suggested that wettability of the initially water-wet rock changes over time. Literature point out, that the main reason of wettability alteration is the adsorption of polar compounds of crude oil and/or deposition of the organic matter on the mineral surface [11, 18, 19, 70]. The charged components in oil, which are adsorbed on the surface, generally contain hydrocarbon end and polar end. The polar end either directly adsorbs on the mineral surface or connects via divalent cations. The cation acts as a bridge between exchangeable cations on mineral surface and functional group of oil. This mechanism is known as cation bridging (see Figure 9).

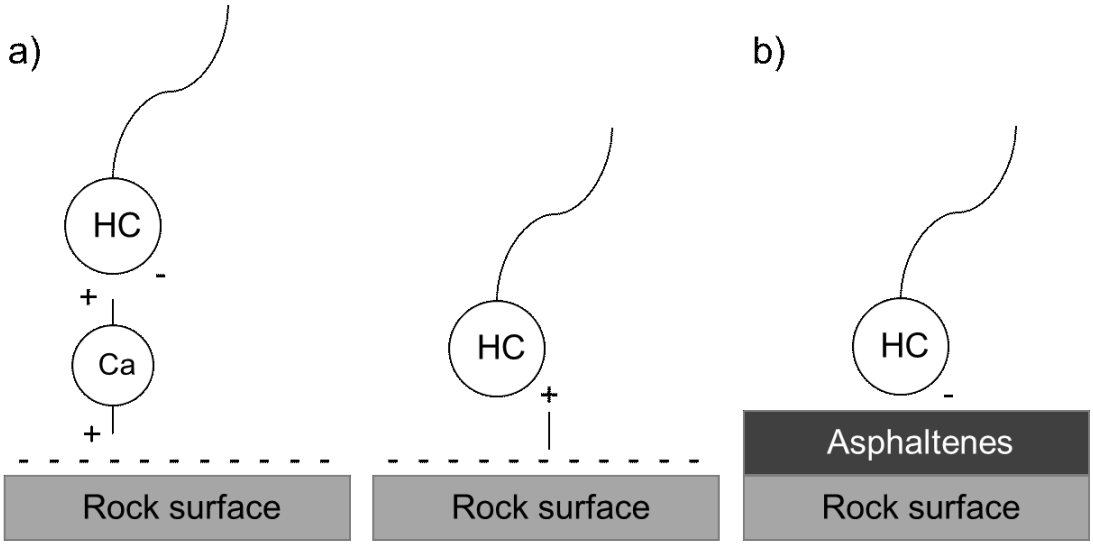

Figure 9 – Wettability change due to polar molecule adsorption (a) and organic matter precipitation (b)

As previously described, the oil, migrating into the reservoir rock, does not contact a mineral surface initially. There exists a thin interstitial water film, coating the rock surfaces. Under certain conditions, this water layer can rapture, which will lead to contact between oil and

minerals. Hall and Melrose (1983) established a theoretical model for water film stability. The electrostatic forces, which appear from electrical double layer at the interfaces between water-oil and water-mineral, stabilize the water films. Thickness of water film reduces as more oil migrates into the pore. As soon as critical water thickness is reached, the film at larger pores becomes unstable and finally raptures, allowing oil-mineral contacts [20, 21]. Moreover, various studies have proven that some of these polar components are capable to diffuse through the thin water layer and contact a mineral surface [22, 23]. Other than oil composition, wettability alteration depends on pressure, temperature, mineral surface, ion composition and pH [3]. The process described above is crucial for laboratory experimental evaluations. It is important to understand the initial state of the core before the start of testing. Depending on the objectives of the studies, there are three initial states used in core analysis: native-state, cleaned and restored-state cores [4].

Native-state Core: As reported in the literature, the best results were observed using native state wettability of core for analysis. “Native” means that the wettability influence is minimized and the core plug sample depicts similar characteristics as in the reservoir. The native state of a core plug sample is difficult to achieve. A special oil-filtrate type mud shall be used to ensure no changes in original connate water saturation as well as no invasion of mud. These cores are difficult to handle and operate. Therefore, it is not common practice to use native-state cores for the laboratory analysis [24].

Cleaned Core: It is believed, that after a proper cleaning, all fluids and adsorbed organic components are removed and the strongly water-wet state of the core is established.

Restored-state Core: In this case, an attempt is made to restore the native state of the core. First, the core is cleaned and subsequently fully saturated with brine. By that, the crude oil is injected into the core until irreducible water saturation is achieved. Finally, the core needs to be aged at reservoir temperature. Different researches have shown that the pressure influence during ageing process is not significant, therefore ageing can be done at atmospheric pressure [61]. Regarding the time of ageing, different durations have been reported in the literature, depending on the parameters of the rock, brine and crude oil [7, 61].

Note that in this work, cleaned cores as well as restored-state cores after 30 days ageing time were investigated. Full description of used samples can be found in Chapter 3.2.

2.4.4 Wettability Measurement Techniques

Current state-of-the-art technology in wettability measurements consists of three main methods: contact angle measurements, Amott-Harvey method and USBM method.

- Contact Angle

Generally, the contact angle test is performed using the sessile drop method or the modified sessile drop method. In sessile drop method, one fluid (usually oil) is placed on a polished rock

surface in presence of second fluid (usually brine). After equilibration, an angle between solid surface and fluid interfaces is measured through the higher density fluid. The measured angle corresponds to the preference of one fluid to spread over the surface [25] (see Figure 10).

In case of the modified sessile drop method, there are two polished rock surfaces and a fluid droplet (usually oil) attached in between. Moving one of the rock planes, one can obtain contact angle change due to displacement, which correspond to advancing and receding contact angles. During a drainage process, when oil displaces water, receding contact angle plays a bigger role, whereas during imbibition process, advancing contact angle is more important. Both need to be studied to properly describe physical means [26]. The advancing contact angle is larger than receding contact angle, which affects the displacement process significantly [27, 28].

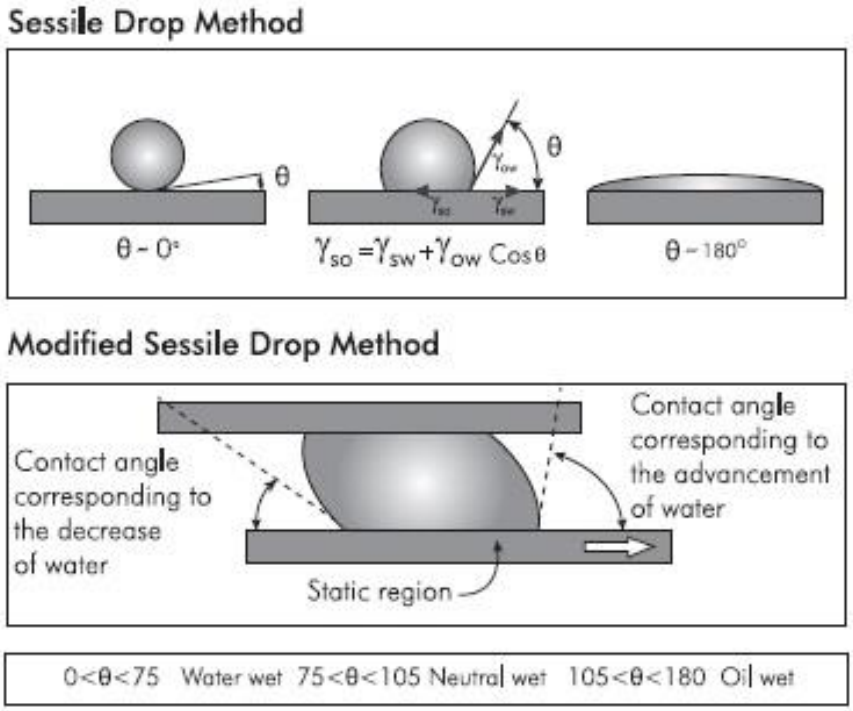

Figure 10 – Sessile drop contact angle measurements [26]

Contact angle evaluations have a strong advantage over core wettability measurements, due to the surface is not affected by mud filtrate, natural oil surfactants and other components altering wettability (e.g. tensoactives). Furthermore, it is a simple test, which allows to investigate effects of pressure, temperature and brine chemistry. One possible downside of this measurement is that it does not represent the complex pore structure and cannot exhibit mixed wettability state due to mineral composition.

The results of contact angle measurement are reported as a value of angle, which further can be used to define wettability state of the surface. Generally, measured angle and wetting condition relation can be assumed as it is presented in Table 1.

Table 1 – Contact angle to wettability state relationship [4]

	Water-Wet	**Neutrally-Wet**	**Oil-Wet**
Minimum	0°	60 to 75°	105 to 120°
Maximum	60 to 75°	105 to 120°	180°

- Amott-Harvey method

The second industry standard for defining rock wettability is Amott-Harvey method. This combines spontaneous imbibition and spontaneous drainage in Amott cell and forced displacement in centrifuge or Hassler cell in order to measure an “average” wettability of a core plug.

The physical definition of drainage and imbibition depend on the type of wetting fluid. Drainage refers to a reduction of wetting phase saturation, while imbibition to an increase. Due to the complexity of reservoir rocks and possible oil- and water-wetness of the surface, it was decided in petroleum industry to use the term drainage for decrease in water saturation and imbibition for increase in water saturation [4].

The Amott-Harvey method is based on a physical observation that a wetting phase spontaneously imbibes into the core without any additional force, while a non-wetting phase expels. This can be described by capillary pressure curve. (see Figure 11).

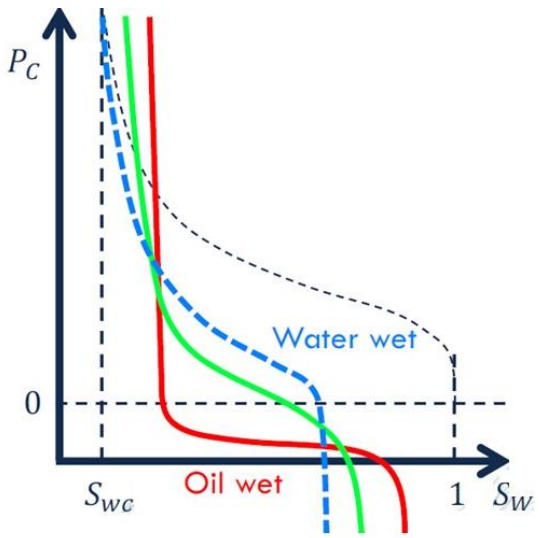

Figure 11 – Capillary pressure curve [76]

Capillary pressure at the initial core state (at connate water saturation) is large. When the core is placed into the excess of water, capillary pressure gradually drops to zero. The amount of oil expelled identify a wetness of rock.

In order to gather data for wettability evaluation and analysis, experimental workflow follows four main steps shown as follow. Moreover, a schematic representation of the process can be seen from Figure 12:

1. Spontaneous Brine Imbibition

   The core sample is initially at irreducible water saturation, placed into Amott cell. This will allow water to further imbibe under capillary pressure. Therefore, as the water imbibes, oil is expelled. The production of oil is measured over time until no more production is obtained. The specific period of the imbibition highly depends on the rock and fluid properties. According to industry experience, the imbibition period should not be smaller than 480 hours [4].

2. Forced Brine imbibition

   At this stage, the brine is forced into the core by either centrifuging or using a core holder (e.g. Hassler Cell). Centrifuging is a preferred option, because of the viscous instability and capillary end effect during core flooding, which can affect measured forced imbibition volumes. Note that, the displacement shall be as long as not further oil production is obtained.
   Finally, the core shall be at residual oil saturation, what is difficult to achieve in practice. Having performed the first two steps, a water-wetting index can be evaluated.

   $$\delta w = \frac{Vw_{si}}{Vw_{si}+Vw_{fi}} \quad (5)$$

   Vw_{si} – Volume of brine spontaneously imbibed

   Vw_{fi} – Volume of brine forcibly imbibed

   For a water-wet rock, water wetting index is close to 1.

3. Spontaneous Oil Drainage

   The core sample is placed once again into the Amott cell, but this time filled with oil. The volume of oil spontaneously imbibed into the core is recorded. If the core is oil-wet, a significant amount of water should be displaced at this stage.

4. Forced Oil Drainage

   At this point, the oil is pushed into the core by centrifuging or using core-flooding displacement. The process is completed until irreducible water saturation is reached

and the volume of oil entering the system is calculated. Having done that, the oil wetting index can be estimated.

$$\delta o = \frac{Vo_{si}}{Vo_{si}+Vo_{fi}} \tag{6}$$

Vo_{si} – Volume of brine spontaneously imbibed

Vo_{fi} – Volume of brine forcibly imbibed

For an oil-wet rock, water wetting index is close to 1.

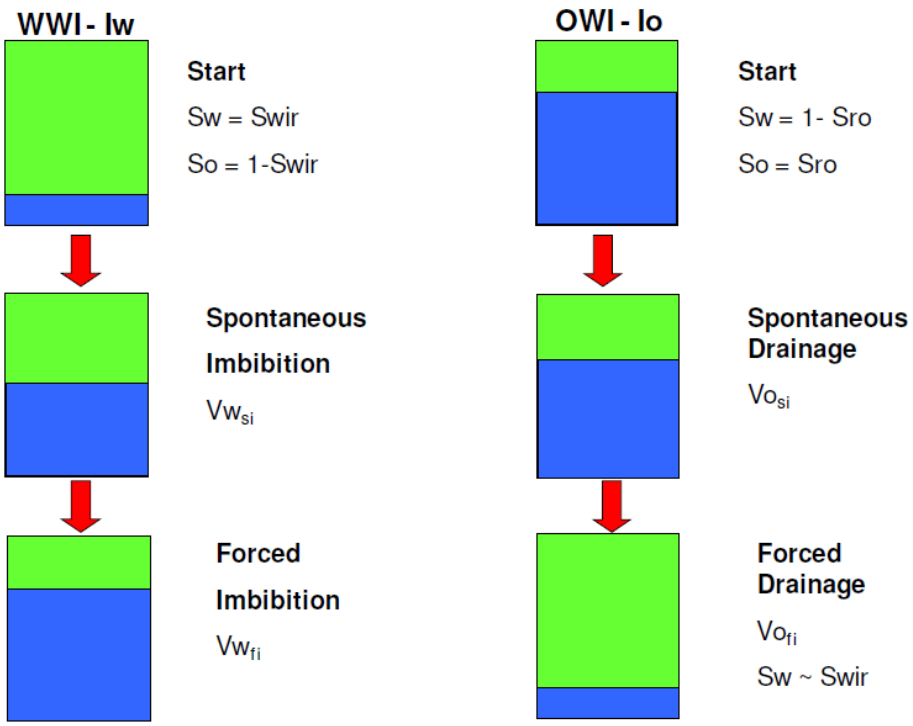

Figure 12 – Schematic of Amott-Harvey test (green – oil, blue – water) [4]

The Amott-Harvey wettability index is defined as following:

$$AHWI = \delta w - \delta o \tag{7}$$

Wettability index vary between -1 and +1. Table 2 summarizes the relation between wetting indices and wetting condition.

Table 2 – Amott-Harvey wetting indices

Index	Water-Wet	Neutral-Wet	Oil-Wet
δw	+1	0.5	0
δo	0	0.5	+1
$AHWI$	+0.3 to +1	-0.3 to +0.3	-0.3 to -1

- USBM method

The United States Bureau of Mines (USBM) measures the average wettability of a core sample. The method is based on thermodynamic principles and it compares the work (*PdV*) needed to displace one fluid by another. As per its principle, the work required to displace the non-wetting fluid from the core sample should be less than in the opposite case. By building capillary pressure curves for both, first imbibition and second drainage would help determining the required *PdV*, which per definition is equal to the area under the curve (see Figure 13).

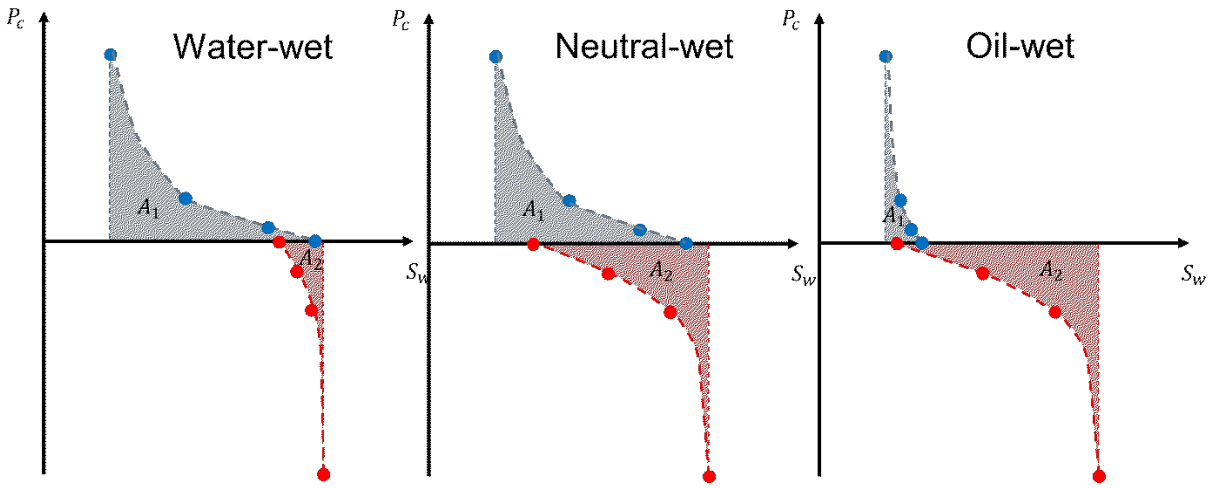

Figure 13 – Capillary pressure curve for primary imbibition (red) and secondary drainage (blue)

The point on a curve can be measure using a centrifuge apparatus. Applying different rotational speeds, which correspond to capillary force, the amount of expelled phase is measured and the corresponding capillary pressure point is obtained. In the USBM test, there is no spontaneous imbibition measurements, but it is estimated during centrifuging at low rotational speed.

The USBM method relates a ratio of areas to a wetting state of the core.

$$WI = \log \frac{A_1}{A_2} \tag{8}$$

Table 3 represents the relation of USBM wettability index and corresponding wetting state of the core. The more absolute value of the wettability index the more preference of the fluid to be held by a rock.

Table 3 – USBM wetting indices

	Water-Wet	**Neutral-Wet**	**Oil-Wet**
WI	Positive	Zero	Negative

In the present work, the focus is given to evaluate wettability only by using the first step previously described -Spontaneous imbibition process, the first step of Amott-Harvey method. The forced imbibition part of the technique is necessary to compare different rock types with various flow and storage properties. If similar rock samples are used, the information, obtained only from spontaneous imbibition may be directly related to wettability effects. Furthermore, the rate of oil production during spontaneous imbibition process is being analyzed by analytical diffusion model.

2.4.5 Capillary Suction Phenomenon

It is widely agreed in the literature that spontaneous imbibition process happens under the impact of capillary forces and governed by an equation similar to Fick's law of diffusion, when the impact of convection and buoyancy is negligible [53-56]. Darcy's law for two-phase flow system with the assumption of negligible convection and buoyancy can be written as following:

$$\phi \frac{\partial S_w}{\partial t} = -\nabla \left[\frac{1}{{\lambda_w}^{-1} + {\lambda_o}^{-1}} \nabla P_c(S_w) \right] \tag{9}$$

ϕ – Porosity [-]

S_w – Water saturation [-]

K – Absolute Permeability [m^2]

$\lambda_{w,o}$ – Mobility of water/oil [-]

P_c – Capillary pressure [Pa]

The above equation can be rewritten as diffusion equation:

$$\frac{\partial S_w}{\partial t} = D_c \nabla^2 S_w \qquad with \qquad D_c = \frac{1}{\phi} \frac{1}{{\lambda_w}^{-1} + {\lambda_o}^{-1}} \frac{\partial P_c}{\partial S_w} \tag{10}$$

Where D_c is so-called capillary diffusion coefficient, which defines the rate with which displacing fluid imbibes into the core plug, depending on core permeability, phase mobilities and capillary pressure effects.

- Analytical Solution

At constant capillary diffusion coefficient, the solution of above equation for a cylindrical geometry is well known [57,58]. The normalized oil saturation is defined as:

$$S_o^* = C_{ps} C_{cyl} \qquad with \qquad S_o^* = \frac{S_o - S_{of}}{S_{oi} - S_{of}} \tag{11}$$

$$C_{ps} = \sum_{n=0}^{\infty} \frac{8}{(2n+1)^2 \pi^2} exp\left[-D_c (2n+1)^2 \pi^2 \frac{t}{4l^2}\right] \tag{12}$$

$$C_{cyl} = \sum_{n=1}^{\infty} \frac{4}{r^2 q_n^2} exp[-D_c q_n^2 t] \tag{13}$$

S_o^* – Normalized oil saturation [-]

C_{ps} – Concentration for the plane sheet solution [-]

C_{cyl} – Concentration for the cylinder solution [-]

S_{of} – Final oil saturation [-]

S_{oi} – Initial oil saturation [-]

D_c – Capillary diffusion coefficient [m^2/s]

q_n – the positive roots of the $J_0(rq_n) = 0$ equation, being the first type Bessel function of order zero

r – Core plug radius [m]

l – Core plug half-length [m]

t – time [s]

The boundary condition for the current solution is constant saturation at the outlet equal to $S_o^* = 0$ and the assumption of homogeneous saturation distribution within the core plug and time zero. Despite the fact, that the author, who first presented the analytical solution for this problem, claims the validness of the solution without limitations on time after the diffusion process started [58], the other studies have stated, that the solution is applicable only for early time steps [56].

- Numerical Solution

The equation (10) was solved numerically using simulation platform OpenFOAM. Axial mesh type was used in order to solve the equation for cylindrical shape mesh. The numerical mesh with applied boundary conditions used for simulation is displayed on the Figure 14.

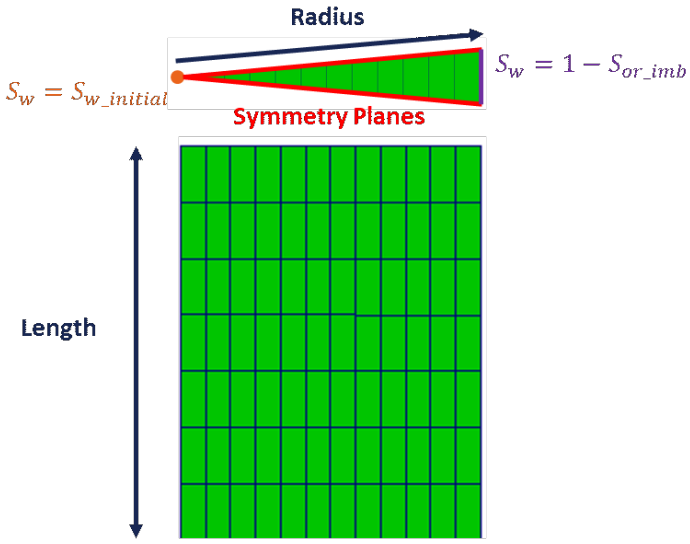

Figure 14 – Axial numerical mesh with the top-view (top) and side-view (bottom) and applied boundary conditions

The top, bottom and side of the numerical mesh were set as outlets with the saturation equal to final water saturation. The saturation at the middle of the core plug (left side of the mesh) is set to a value of initial water saturation. The block size is chosen to be 1 mm in length and width, which was validated by comparison to analytical solution of the capillary diffusion equation.

The results of analytical and numerical calculations and comparison to observed data are presented in Chapter 5.

2.5 Summary

During chemical flooding processes application, the major mechanisms of additional oil production are believed to be low interfacial tension (IFT) and wettability alteration. Both parameters shall be accounted for in order to attribute the observed oil production behavior to certain physical drives. Performing spontaneous imbibition tests on water-wet cleaned cores help to establish a baseline of oil production and determine the effect of decreased IFT due to in-situ surfactants formation. Further investigations on restored wettability cores after 5 weeks ageing time may demonstrate the effect of wettability change during chemical flooding. In the current study, two oils with low and high TAN number were used with the purpose of evaluating the influence of in-situ soaps on wettability alteration. Furthermore, cores with different mineralogy and brines with various composition were analyzed.

3 Experimental Setup and Materials

In this chapter one can find all relevant information about the preparation of the experiments, used materials and equipment and data obtained from routine analysis of oils, brines and cores.

3.1 Fluid Characterization

In order to understand the behaviour of the fluids during the main set of experiments, it is imperative to characterize the fluids. Density and viscosity of all used fluids were determined using industry state of the art techniques and reliable equipment. Moreover, IFT measurement technique is described and explained.

3.1.1 Density and Steady-Shear Viscosity Evaluation

- Density Measurements

Density of fluids were measured using Anton Paar densitymeter device (see Figure 15). The device works on oscillating U-tube principle. Density is determined based on an electronic measurements of oscillation frequency. The sample is placed into a container with oscillation capacity, which frequency is controlled by the mass of the sample. The device is known for its accuracy, which is claimed to be 1 kg/m^3. However, in order to omit measurement errors, each test was performed three times and the average value was used for further calculations. Additionally, the standard deviation was measured in order to control the reliability of the data.

Figure 15 – Anton Paar Density Meter [43]

- Steady-Shear Viscosity Measurements

Due to the usage of polymer and alkali-polymer solutions, viscosity should be measured at different shear rates, in order to define the rheological properties of the material. An Anton Paar rheometer MCR-302 was used to measure the shear viscosity data (see Figure 16). A double-gap system was used, which allows measurement of low to medium viscous solutions.

Figure 16 – Anton Paar Rheometer [43]

Accuracy of obtained data is the primary concern during every measurement. Besides thorough and accurate calibration of the device, the test was performed three to four times for every solution with average and standard deviation evaluation.

In order to ensure proper device calibration, the torque on the motor was measured/verified with an empty gap system before and after calibration (air check). One can see from the Figure 17, that torque values before calibration exceed the defined limits. After calibrating the device, the same “air check” procedure was performed. Figure 18 proves the correctness of the device adjustment. The torque value error is fluctuating close to zero, which is acceptable value of error for the equipment.

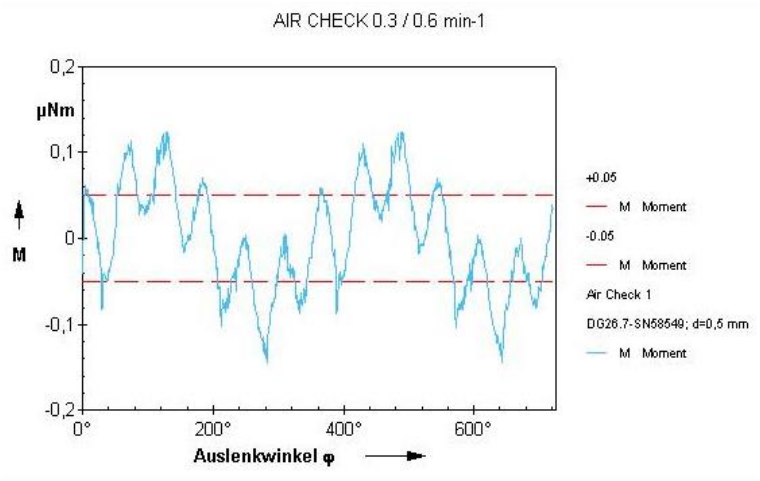

Figure 17 – Torque error check before device calibration

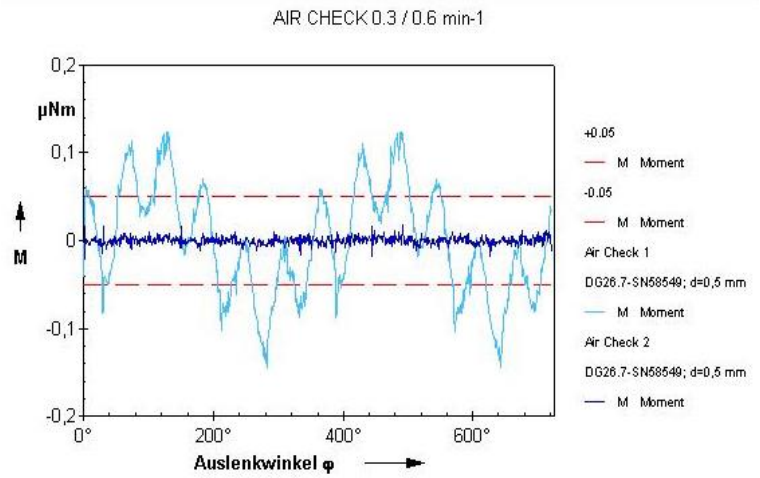

Figure 18 – Torque error check after device calibration

3.1.2 Interfacial Tension (IFT) Measurements

For IFT measurements, a KRUSS spinning drop tensiometer was used (shown in Figure 19). As a principle -for measuring with this device-, the heavy fluid (Water, Alkali, Polymer or Alkali-Polymer solution) is placed into the vessel using a piston and a rod. A droplet of oil is filled into oil holder and with the use of auxiliary tool; the oil holder is fixed into a vessel. Having done that, the rod shall be removed and vessel can be placed into the device. The equipment is presented on the Figure 20. Interfacial Tension was measured at 60°C and 7000 rpm based on the principle suggested by Sharma et al. (1989) [66].

Figure 19 – Used spinning drop tensiometer [42]

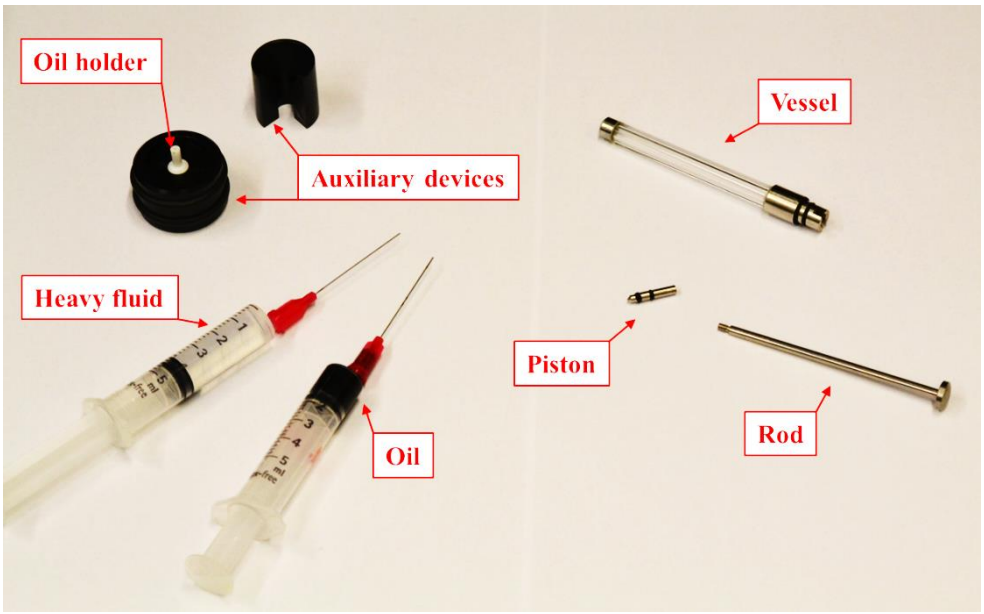

Figure 20 – Components of the IFT measurements device

3.2 Core Plug Preparation and Analysis

Two different types of rock were considered, to perform the investigations in this work. One main idea was to study the effect of mineralogy during the imbibition process. First, a Bentheimer outcrop rock from Nordhorn (Germany) was taken. This rock type was chosen due to several reasons: 1) permeability of the core plugs resembles the permeability ranges of the 16 TH formation -where Alkali-Polymer flooding is under investigations for implementation; 2) core plugs are highly similar in properties (observed ranges/differences of porosity and permeability values are narrow (see Chapter 4.2); 3) mineralogy of the rock is fairly simple – simplifying any additional uncertainties during the experimental analysis. Second, a Keuper

outcrop (Germany) was considered. Keuper was selected due to its high heterogeneity, as well as high content of clay materials. This in turn, enables observing the possible influence of clay particles on the wettability alteration process. An image of both core samples is shown on the Figure 21.

Figure 21 – Photo of Nordhorn (left) and Keuper outcrop rock (right)

3.2.1 Mineralogy Description

- Nordhorn Outcrop

The sample can be described as fine-medium-grained, porous sandstone that consists of quartz (96.6%), potassium feldspar (0.9%) and kaolinite (2.5%). Due to the mineralogical composition, the sandstone can be referred to as quartz arenite weakly cemented by quartz and clay materials. The quartz grains exhibit well developed quartz cement overgrowths (see Figure 22, left). The kaolinite is present as cement in pore space and as replacement within potassium feldspar. Under the SEM, the kaolinite exhibits a well-developed booklet structure (see Figure 22, right). The pore space consists predominately of primary interparticle pores [62].

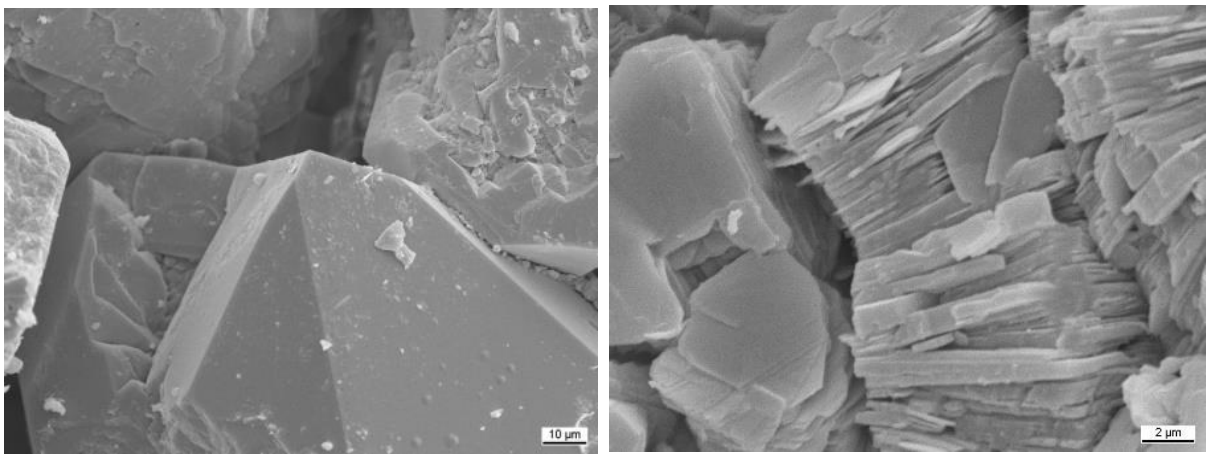

Figure 22 – SEM results on Nordhorn Outcrop Core [62]

Nordhorn outcrop rock is a very homogeneous sample, which is confirmed by thin-section analysis (see Figure 23).

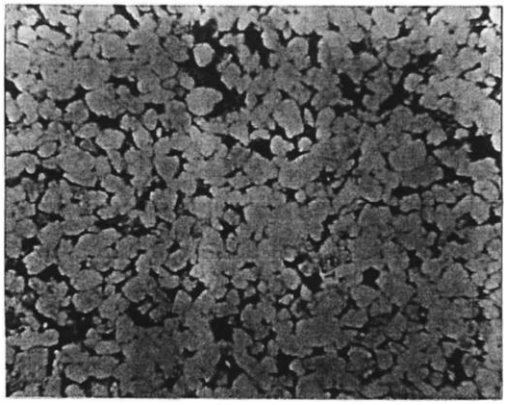

Figure 23 – This-section analysis of Nordhorn outcrop rock

- Keuper Outcrop

The sample is a reddish-brownish fine-grained sandstone. In some specific areas, black spots can be observed. Thin-section analysis has revealed that the sample is a well-sorted sandstone arenite, composed of quartz (88%), feldspar (1%), kaolinite (10%) and others materials (1%). The porous space is predominantly primary interparticle porosity. Only a minor part of the porous space is originated due to secondary porosity in feldspar.

3.2.2 Core Cleaning Procedure

All cores samples were cleaned using the Soxhlet extraction method. A schematic representation of the Soxhlet apparatus is shown on Figure 24. A mixture of azeotropes (methanol + toluene) is filled into the distillation flask. Having boiled, an azeotrope vapour rises up to the condenser and after devaporation drops to the extractor, where the core plug is

located. The level of azeotrope in the extractor rises until it reaches siphon. In the end, the contaminated cleaning mixture drops back to the distillation flask and the process is repeated once again. After one-day of cleaning in the Soxhlet apparatus, cores were dried in the vacuumed oven at 60 °C during 24 hours.

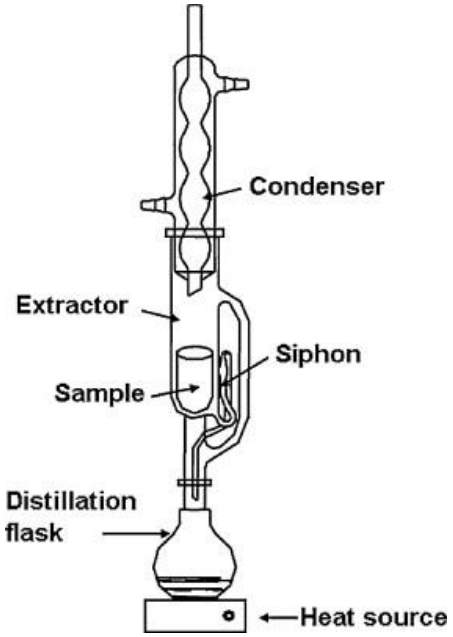

Figure 24 – Soxhlet extraction apparatus

3.2.3 Porosity

Porosity of the samples were measured with a Boyle's type porosimeter (see Figure 25). The method is based on the Ideal Gas Equation of State. First, Helium is injected into the first chamber, where the sample is located. After pressure stabilization, the valve leading to the second reference chamber (with known volume) is opened. Pressure drop is measured and, by applying Equation of State, the volume of gas can be determined. All measurements were repeated three times to ensure quality of the data.

Second, the bulk volume of rock was determined by mercury submergence technique. The sample was placed in the bath with mercury and the change of the mass was determined. The change of the mass is assumed to be directly related to the bulk volume of the sample.

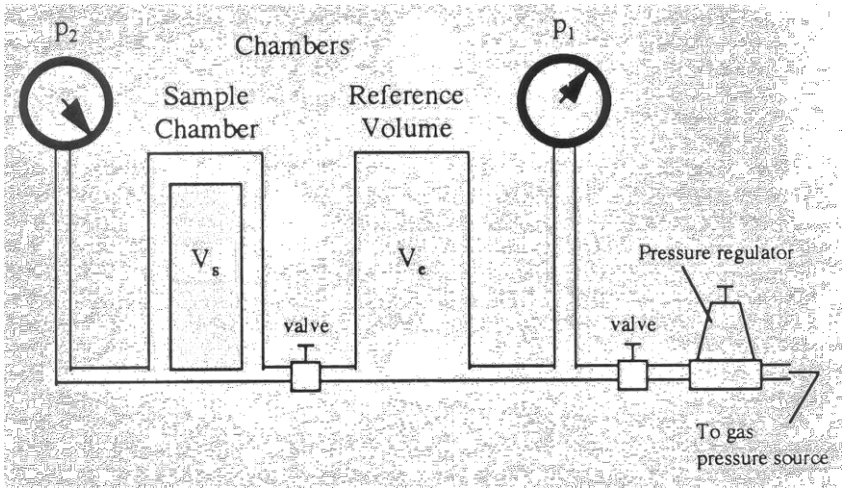

Figure 25 – Boyle's porosimeter schematics

3.2.4 Permeability to Gas - N_2

Values of permeability to gas were determined using Hassler cell type device. An image of the setup can be seen in Figure 26. Nitrogen was pumped into the core colder at rate of 2000 ml/min. The outlet was open to atmospheric pressure, while the inlet pressure was recorded. After considered pressure stabilization, permeability was computed using Darcy's law with a respective correction of Klinkenberg effect.

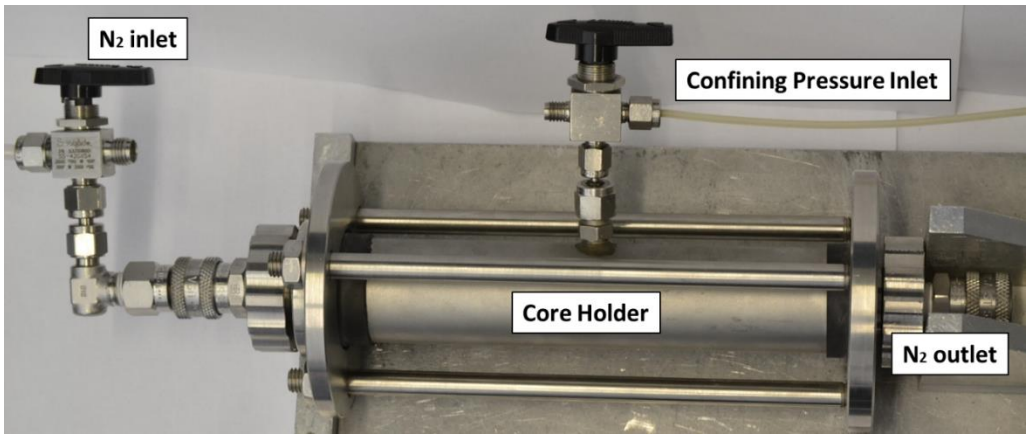

Figure 26 – N2 permeability measurement device

3.2.5 Permeability to Water

For pre-saturation and phase permeability measurement purposes, a saturation setup was built. Figure 27 and 28 show a schematic representation of the setup and an image, respectively.

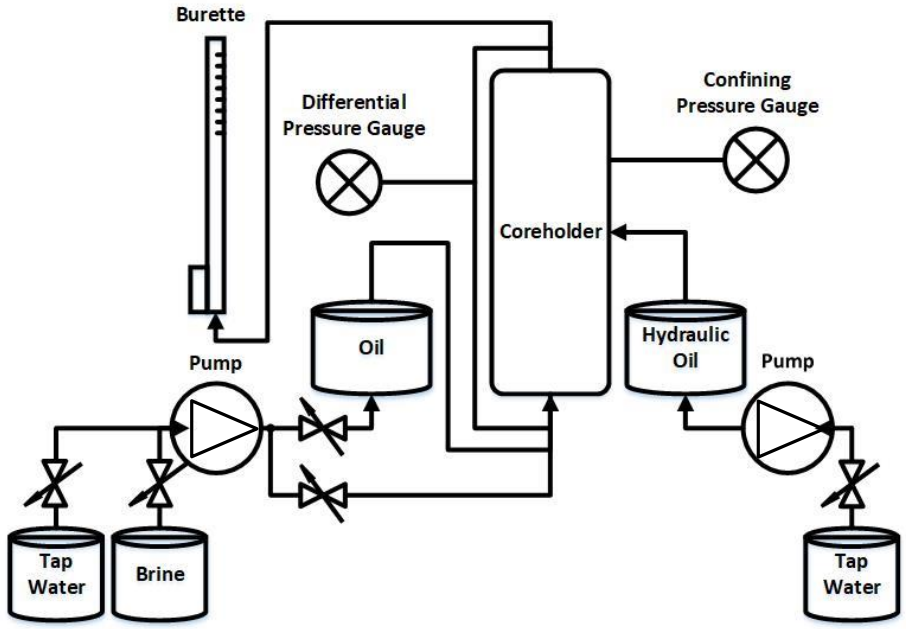

Figure 27 – Pre-saturation setup schematics

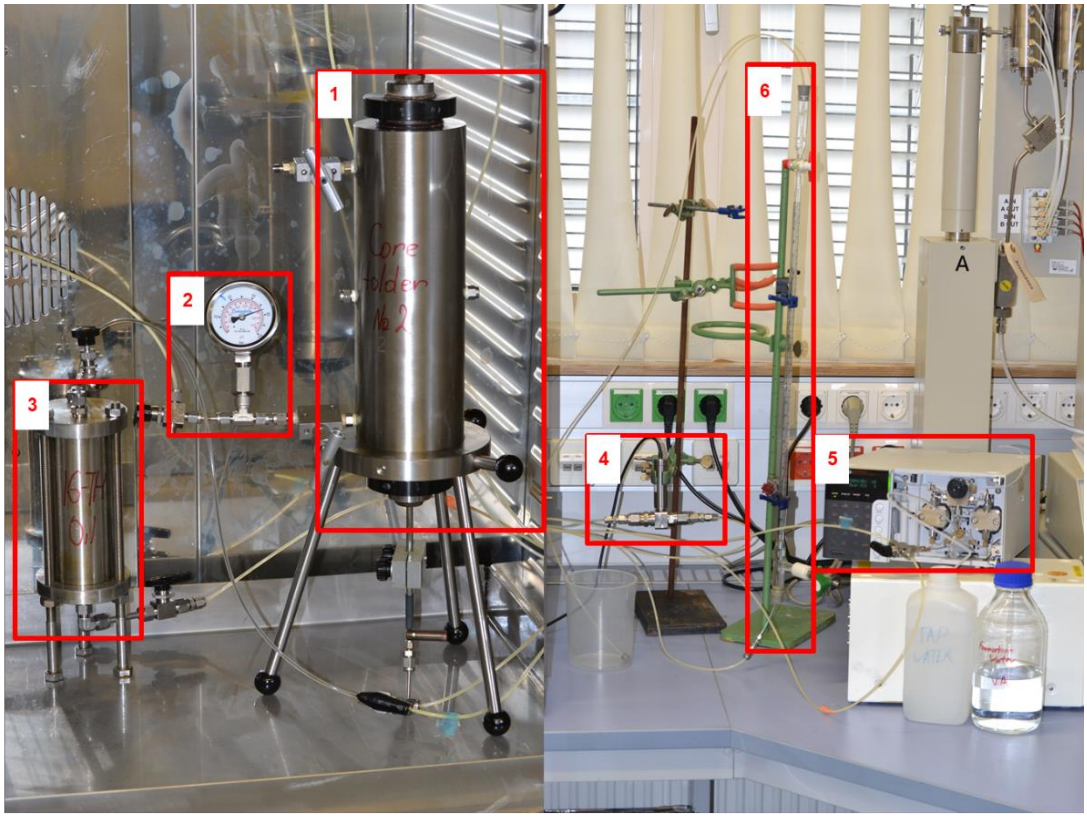

1. Core holder
2. Confining pressure gauge
3. Oil container
4. Differential pressure gauge
5. Pump
6. Burette

Figure 28 – Core Pre-saturation setup equipment

After water saturation under vacuum, the core is placed into the Hassler cell and differential pressure is recorded while using flow rate steps to inject the water. Values were considered after sufficient stabilization is observed. Further, the water permeability was evaluated applying Darcy's law. On the Figure 29 one can see an example of differential pressure response during water permeability measurement.

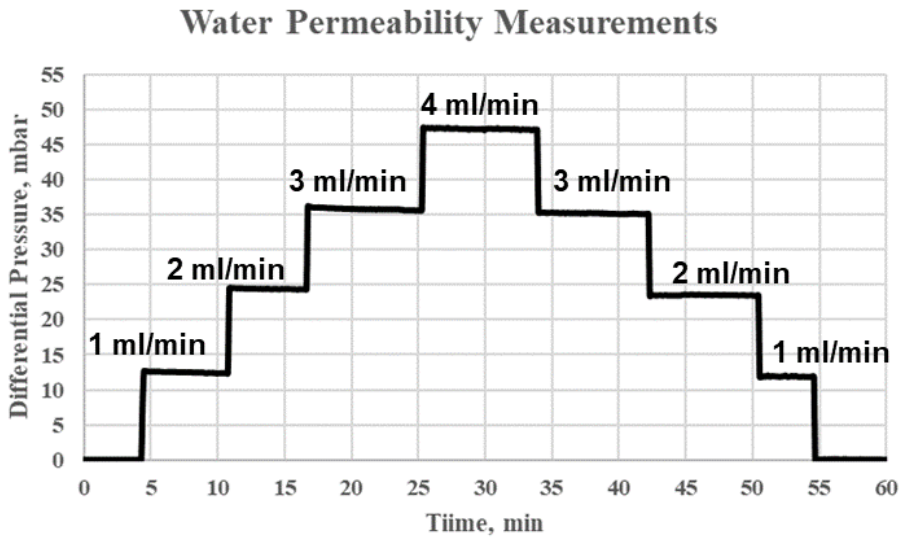

Figure 29 – Water permeability measurement (i.e. Core NH-113)

$$k_w = \frac{q_w \mu_w L}{\Delta P A} \tag{9}$$

k_w – Water permeability [mD]

q_w – Water injection rate [m^3/s]

μ_w – Water viscosity [Pa*s]

L – Core plug length [m]

A – Core plug cross-section area [m^2]

ΔP – Differential pressure along the core [Pa]

3.2.6 Oil Saturation and Relative Permeability

Oil saturation was completed using the same equipment shown on the Figure 27. Oil was injected over 15 hours at a rate of 0.05 ml/min, which corresponds to approximately 1.4 ft/day Darcy velocity. Once irreducible water saturation saturation was achieved, oil was injected at three (3) different rate steps, in an attempt of measuring the end-point oil relative permeability. The example is presented on Figure 30.

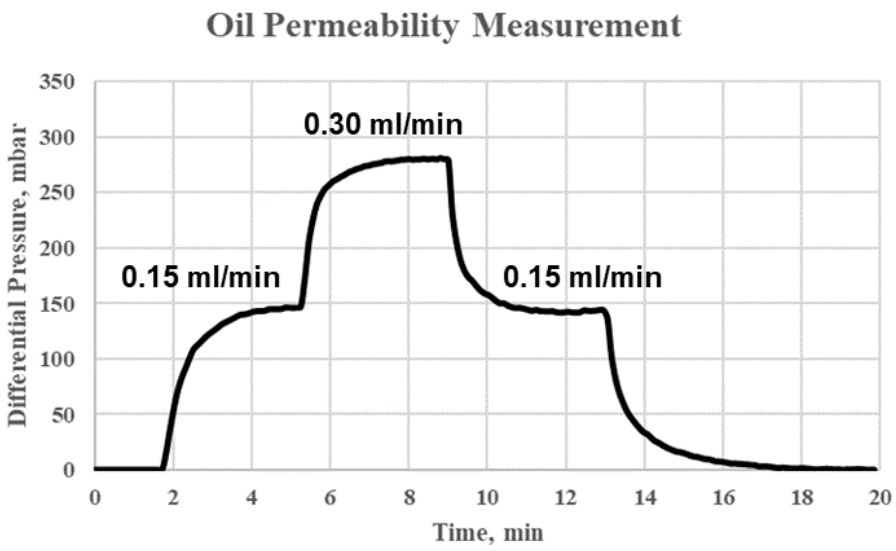

Figure 30 – Oil permeability measurement (i.e. Core NH-117)

Applying Darcy's law, relative oil permeability can be calculated.

$$k_o = \frac{q_o \mu_o L}{\Delta P A} \tag{10}$$

$$k_{o\,rel} = \frac{k_o}{k_w} \tag{11}$$

$k_{o\,rel}$ – Oil relative permeability [mD]

k_w – Water permeability [mD]

q_o – Oil injection rate [m^3/s]

μ_o – Oil viscosity [Pa*s]

L – Core plug length [m]

A – Core plug cross-section area [m^2]

ΔP – Differential pressure along the core [Pa]

Finally, oil and water saturation were evaluated. The amount of displaced water was measured using Burette and later transferred to initial oil and water saturation using the following equation (see Eq. 12, 13).

$$S_o = \frac{V_{disp.water}}{PV} \tag{12}$$

$$S_{wirr} = 1 - S_o \quad (13)$$

S_o – Oil saturation [-]

S_{wirr} – Irreducible water saturation after oil injection [-]

$V_{disp.water}$ – The volume of displaced water during oil saturation [ml]

PV – The plug pore volume [ml]

3.3 Spontaneous Imbibition

For spontaneous imbibition experiments, Amott cells were used. The design of the cell is simple, consisting of a vessel where the sample is placed, subsequently covered and measure the graduated tube. The schematic representation of the Amott cell is shown in Figure 31.

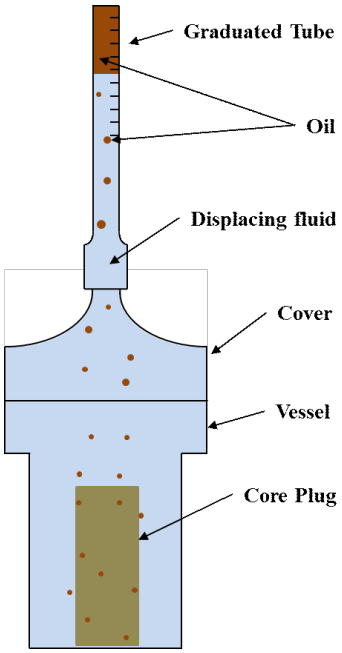

Figure 31 – Amott cell schematic

The experimental principle is straightforward; the core -saturated with oil until irreducible water saturation- is submerged into the displacing fluid. Oil production over time is recorded by measuring the volumes in the graduated pipette.

In order to replicate temperature reservoir conditions, Amott cells were placed in the oven at 60°C temperature. Amott cells in the oven are depicted on the Figure 32.

Figure 32 – Amott cell in the oven

4 Experimental Results and Discussion

In this chapter, parameters obtained during the experiments are presented and discussed. First, the fluid characterization parameters are shown for both types of oil and four different displacing fluids, followed by the routine core analysis (RCA) results. As previously described, RCA was performed on both rock types. Towards the end, results of the main experiments, IFT measurement and spontaneous imbibition experiments, are shown and described.

4.1 Fluid Characterization Results

- Oil

Two oil types have been used for the experiments performed in this work. One from 16th TH reservoir of Matzen field, Austria, (Badenian horizon) [29] and the other one from Saint Ulrich, Austria [57]. Both oils were chosen with the purpose of comparing behaviors based on their TAN (total acid number) number. The 16 TH oil is notable for its high TAN number, whereas the St. Ulrich oil is known for having a small amount of acids. All relevant oil properties are given in Table 4, measured at 25 °C as well as at reservoir temperature of 60°C.

Table 4 – Oil properties

Parameter	Units	16th TH		St. Ulrich	
		Average	St.Dev.	Average	St.Dev.
Density @25°C	g/cm^3	907.30	0.10	866.60	0.20
Density @60°C	g/cm^3	884.30	0.20	842.60	0.60
Viscosity @60°C	cP	11.90	0.10	6.00	0.10
TAN	Mg KOH/g oil	1.61	0.18	0.17	0.08

- Brine

Two synthetic brines were prepared to investigate the influence of brine composition on spontaneous imbibition process. First, a simplified brine was used without divalent cation, subsequently named here Test Water. The simplified composition mimics the injection water expected to be used during the process application, where Sodium bicarbonate is used to control the pH. Second, a brine with similar composition to the 16th TH reservoir was prepared (Formation Brine). Composition and main parameters of used brines can be seen from Table 5.

Table 5 – Brine properties and composition

Parameter	Units	Test Water		Formation Brine	
		Average	St.Dev.	Average	St.Dev.
Density @25°C	g/cm^3	1011.700	0.000	1012.000	0.000
Density @60°C	g/cm^3	997.100	0.100	1012.000	0.000
Viscosity @25°C	cP	0.964	0.032	0.954	0.030
Viscosity @60°C	cP	0.571	0.023	0.592	0.054
Components	**Units**	**Test Water**		**Formation Brine**	
NaCl	g/L	18.96		19.75	
$NaHCO_3$	g/L	1.85		-	
$CaCl_2 \cdot 2H_2O$	g/L	-		0.40	
$MgCl_2 \cdot 6H_2O$	g/L	-		0.66	
NH_4Cl	g/L	-		0.17	
$SrCl_2 \cdot 6H_2O$	g/L	-		0.06	
$BaCl_2 \cdot 2H_2O$	g/L	-		0.03	

- Chemical Solutions

Chemicals selection, optimization and definition of concentrations was previously performed and reported by Schumi et al. (2019) [39]. The evaluation was performed based on phase behavior, micro-model and coreflooding experiments, where an optimum alkali and polymer concentration as well as type of alkali and polymer to be used were defined. Additional information about selection of alkali, polymer and alkali-polymer can be found in the following papers [39-41].

Sodium Carbonate Na_2CO_3 at a concentration of 7000 ppm was considered as the alkali solution. FLOPAAM 3630S (HPAM Polymer) from SNF Floerger was dissolved in the specific brine with a concentration of 2000 ppm. The Alkali-Polymer solution was defined as a combination of the referred solutions. The main properties of the solutions can be found in

Table 6. Viscosity versus shear rate behavior are presented on the Figure 33 and 34 for 25 and 60 °C respectively.

Table 6 – Chemical solution properties

Parameter	Units	Alkali		Polymer		AP solution	
		Average	St.Dev.	Average	St.Dev.	Average	St.Dev.
Density @25°C	g/cm^3	1020.0	0.0	1013.0	0.0	1018.7	0.1
Density @60°C	g/cm^3	1005.2	0.1	998.5	0.0	1004.2	0.0
Viscosity @25°C	cP	0.999	0.028	27.786 @ 7,984 s^{-1}		25.905 @ 7,984 s^{-1}	
Viscosity @60°C	cP	0.559	0.024	19.536 @ 7,984 s^{-1}		18.054 @ 7,984 s^{-1}	

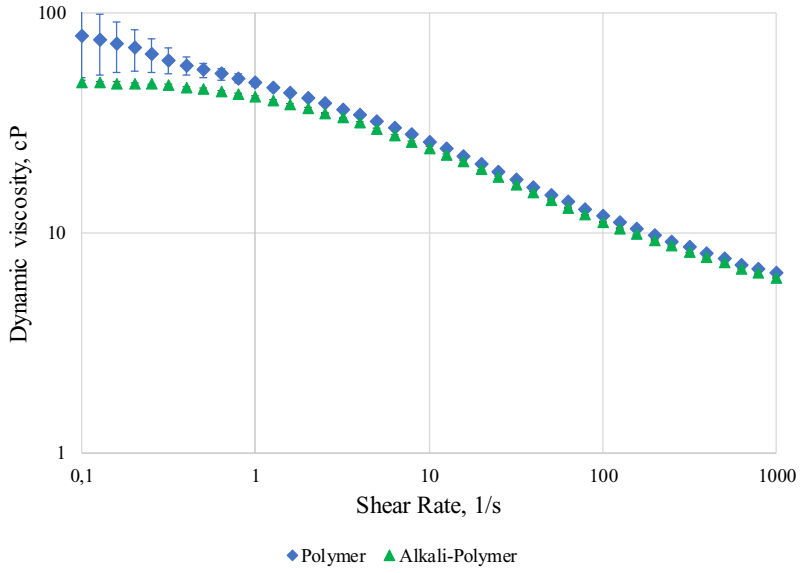

Figure 33 – Steady-shear viscosity of polymer (left) and alkali-polymer (right) versus shear rate at 25°C

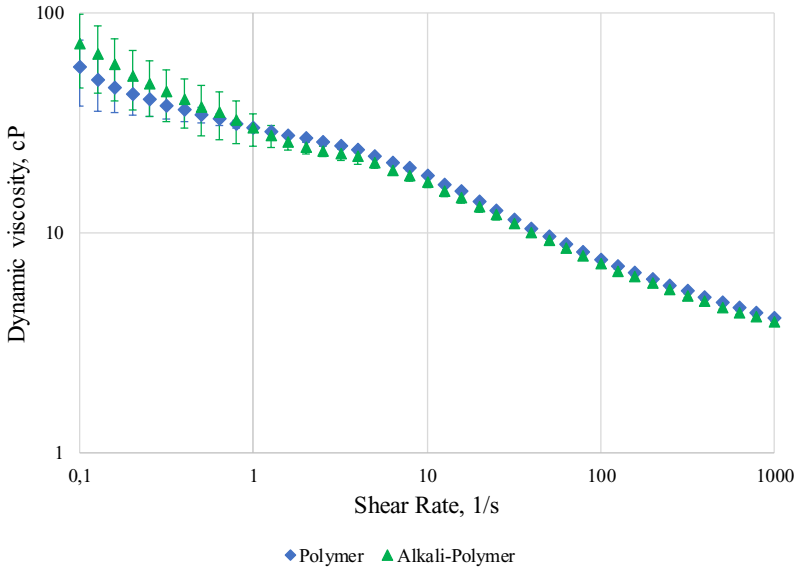

Figure 34 – Steady-shear viscosity of polymer (left) and alkali-polymer (right) versus shear rate at 60°C

4.2 Routine Core Analysis

In total 40 Nordhorn core plugs and 8 Keuper samples were analysed. The summary of porosity measurement related core data is listed in Table 7.

Table 7 –Average Properties of the Core plug used in this work

Parameter	Units	Nordhorn		Keuper	
		Average	St.Dev.	Average	St.Dev.
Length	cm	8.01	0.11	8.12	0.09
Diameter	cm	2.96	0.01	2.98	0.01
Bulk Volume	cm^3	54.42	0.87	55.76	0.73
Pore Volume	cm^3	13.07	0.26	12.75	0.22
Grain Volume	kg/cm^3	41.36	0.70	42.98	0.67
Porosity	%	23.96	0.35	22.79	0.34

Measured permeability to gas (N_2) provided consistent data when comparing the porosity-permeability correlation. (see Figure 35). The average permeability of the Nordhorn core plugs is 2313 with ±7% standard deviation, whereas for Keuper cores this value is significantly

smaller -with higher standard deviation- 1327 ±24%. This again supports highest level of heterogeneity of Keuper core plugs and similarity of NH cores.

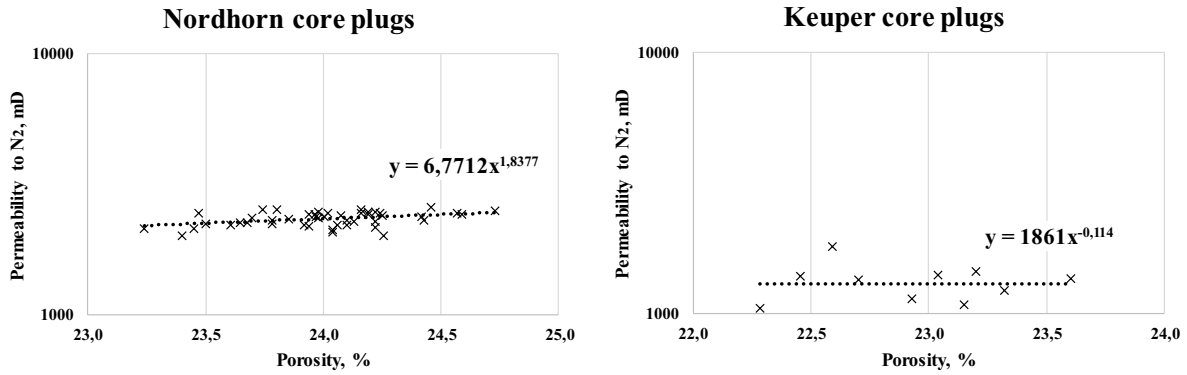

Figure 35 – Porosity-N2 permeability cross-plot for Nordhorn (left) and Keuper core plugs (right)

Multi-rate measurements allow to establish uncertainty ranges for each core plug. To verify the consistency of obtained results, a permeability to N_2 and permeability to water cross-plot can be plotted (see Figure 36).

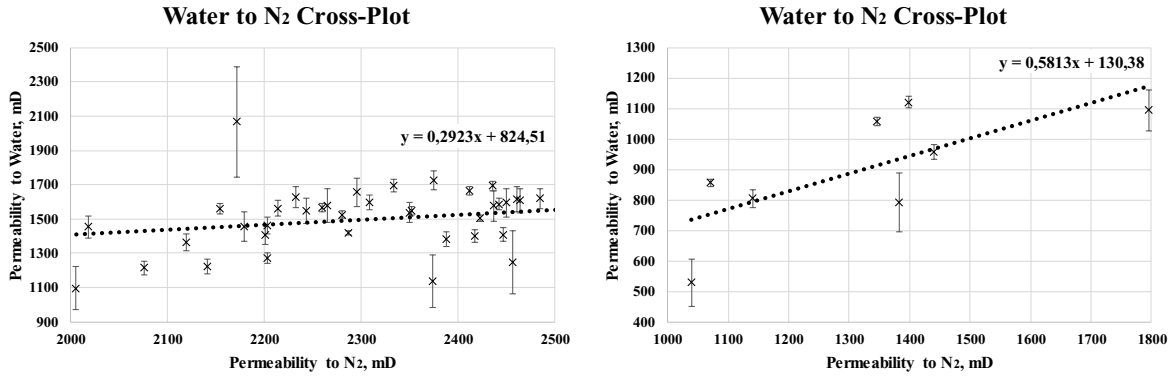

Figure 36 – Cross-plot permeability to Water and Gas for Nordhorn (left and Keuper core plugs (right)

From figure 36, one can see a few outliers having a high standard deviation in the water permeability measurements. Presumably, the possible errors can be associated to the pressure deferential device reading limits. Removing the outliers, a certain trend of permeabilities can be observed (see Figure 37). This supports the correctness of permeability evaluation.

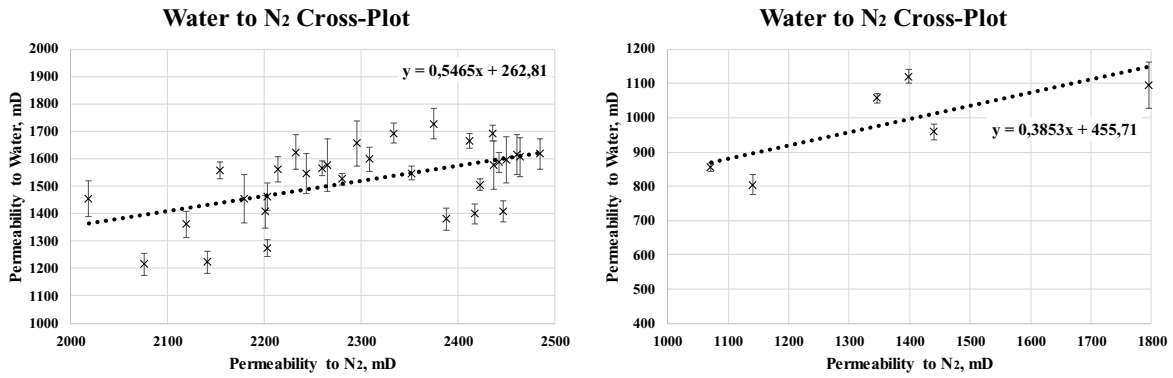

Figure 37 – Cross-plot permeability to Water and Gas without outliers for Nordhorn (left) and Keuper samples (right)

The average values and standard deviations for both cores type are presented in the permeability summary shown in Table 8. Similarly, to the water permeability, the standard deviation for each core plug was estimated and oil permeability was plotted versus nitrogen permeability (see Figure 38).

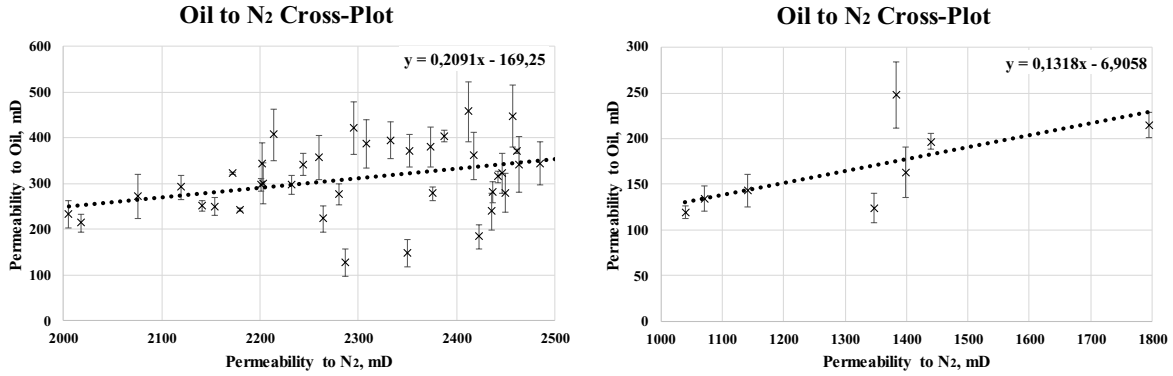

Figure 38 – Cross-plot permeability to Gas and Oil for Nordhorn (left) and Keuper core plugs (right)

A few outliers with high standard deviation can be observed. Removing them, a certain trend in data can be seen.

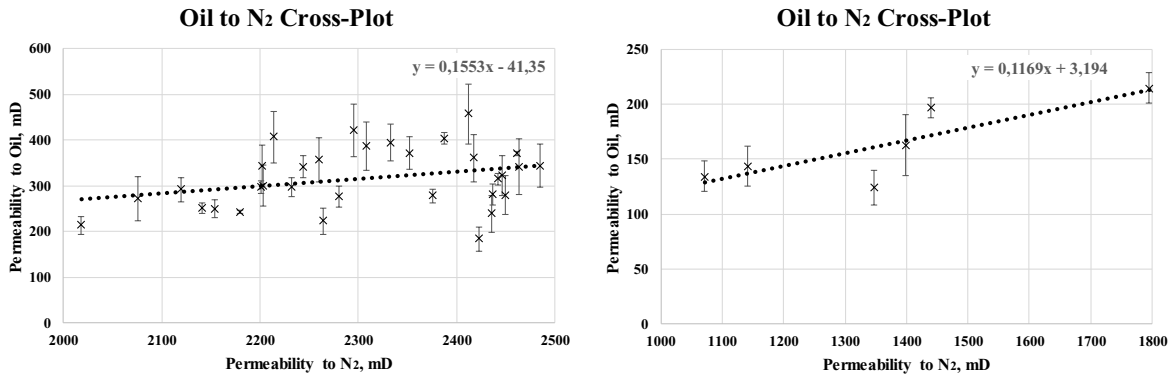

Figure 39 – Cross-plot permeability to Gas and Oil without outliers for Nordhorn (left) and Keuper samples (right)

Further, the relationship between irreducible water saturation and end-point oil relative permeability was verified (see Figure 40). One can observe a slight correlation between the two parameters for Nordhorn core plugs, whereas the Keuper samples does not show any correlation. One possible reason is the lack of scatter data, since a reduced number of Keuper core plugs were used for the analysis.

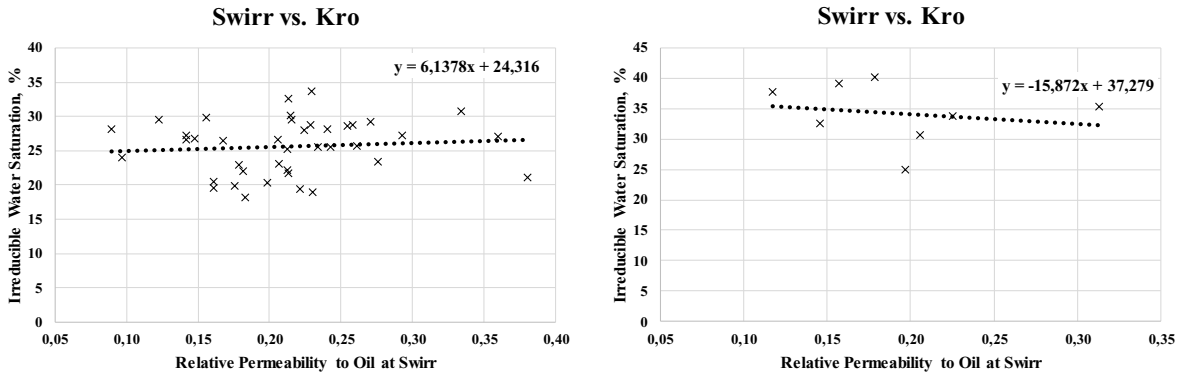

Figure 40 – Swirr versus Kro cross-plot for Nordhorn (left) and Keuper core plugs (right)

The overall results of two-phase analysis are summarized in Table 8. Data, obtained from the routine core analysis, depicted a reasonable standard deviation. A large number of core plugs were analyzed, which adds a confidence in the reliability of the data. When referring to saturation data, the irreducible water saturation in Keuper cores is significantly larger than in Nordhorn core plugs. This can be a result of more complex porosity distribution within the core plug and bigger amount of micro-pores. Despite the difference in irreducible water saturation values, the end-point relative permeabilities are similar.

Table 8 – Overall Comparison for Phase permeability and saturation data of the cores used in this work

Parameter	Units	Nordhorn		Keuper	
		Average	St.Dev.	Average	St.Dev.
Water permeability	mD	1500	190	902	198
Irreducible water saturation	%	25.60	4.00	32.50	4.40
Oil permeability	mD	314	79	178	51
End-point oil relative permeability	-	0.21	0.06	0.20	0.07
Initial oil saturation	%	74.40	4.00	67.50	4.40

4.3 IFT Measurement Results

Interfacial tension was measured twice for every solution, in order to define the uncertainty range. Obtained results have indicated the complexity of IFT measurements and high uncertainty associated to it, especially in case of high IFT systems (>1 mN/m). Similar claims were reported by Arnold (2018) [67]. Although, the exact values of the measured IFTs might not be strictly representative, they provide enough information for fluid comparison as an IFT indexer.

All experiments were conducted with the spinning drop tensiometer at 60°C with the rotational speed of 7000 rpm. The change of IFT was recorded/observed over 300 minutes, revealing both instant IFT values (right after the start of the experiment), as well as the equilibrium period of the IFT (expected to be stablished after the reaction between fluids). Observed standard errors during the experiments are possibly associated to the following reasons:

1. Different algorithms considered for the measurement, which is based on drop shape and fluid characteristics

   To better understand and properly depict the obtained data, two different algorithms were considered for the measurements (Vonnegut and Young-Laplace). For systems with interfacial tension more than 1 mN/m (Test Water and Polymer solutions), the Vonnegut algorithm could not be applied because of the oil droplet shape. As per

definition, in order to use Vonnegut's method, the ratio between length and width of the oil droplet should be 4:1, not fulfilled during the experiment. Therefore, Young-Laplace calculation algorithm was used. At the same time, for systems with IFT lower than 1 mN/m (Alkali and Alkali-Polymer solutions), the Young-Laplace method could not be used because of the highly elongated oil droplet. Hence, Vonnegut method was implemented this time.

2. Lack of proper temperature stabilization leading to malfunction of the device;
   From time to time, the recording camera stopped responding, which led to missing data for some period until the camera was setup again.

3. Collapse and/or junction of multiple oil droplets.
   Finally, yet importantly, the errors due to multiple oil droplets collision and separation were observed. Especially in case of low IFT (Alkali and Alkali-Polymer solutions), the droplets were not stable over time. Due to separation/collision of the droplets, its volume was changing and, consequently, the IFT measurement was affected.

The results of all experiments performed are presented in Figure 41 for comparison. Furthermore, each experiments (test kind) is detailed describe using images of the droplets size and the measured IFT with time at the same period. Data is shown from Figures 42 to 45.

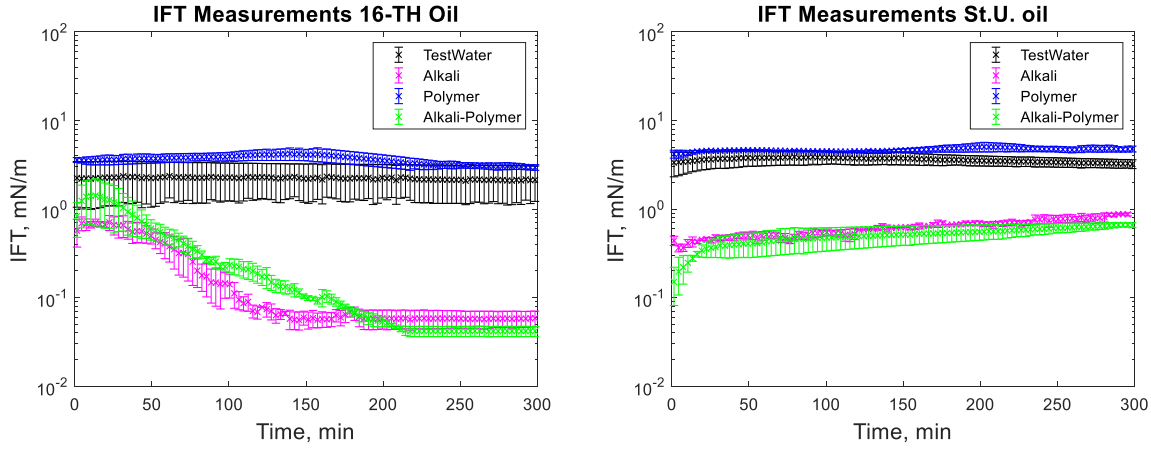

Figure 41 – IFT measurement for 16-TH (left) and Saint Ulrich oil (right) at 60°C [Alkali: 7g/L Na_2CO_3, Polymer: 2000 ppm FLOPAAM 3630S]

From Figure 41 it can be observed that in case of both high and low TAN oils, the effect of alkali on lowering of the interfacial tension is clear. However, the decrease of IFT for high TAN oil is more significant and the final equilibrium value reaches low IFT in a range of 0.05 mN/m. For all cases, the measured values of interfacial tension between oils and test water stay constant with time in a range between 1 and 3,5 mN/m for high TAN oil and 2 to 4,5 mN/m for low TAN oil.

Addition of polymer to the test water causes a slight increase in the measured IFT values. Whereas, the highest reduction of IFT was caused by the alkali interaction with high TAN oil. The application of alkali together with polymer is reflected in a slightly higher interfacial tension values. Presumably, the higher interfacial tension observed for Alkali-Polymer compare to the pure alkali solution is the smaller concentration of alkali (due to additional volume of the polymer) and slower diffusion of Na_2CO_3 molecules into the oil due to higher polymer solution viscosity.

One relevant observation to point out is the low instantaneous IFT observed for the case of alkali and alkali-polymer solution with high TAN oil. As per repeated experiments, the oil droplet elongates drastically within the first minutes of the measuring period (right after the start of the measurement), followed by a shrinking period again, delivering higher value of IFT. A similar behaviour was observed during the spontaneous imbibition evaluations, which will be further discussed.

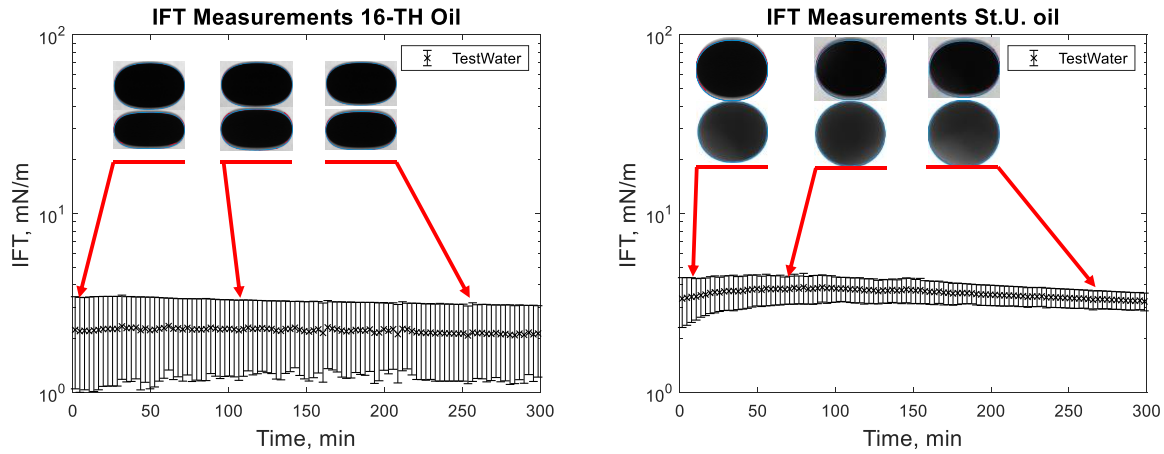

Figure 42 – IFT measurement for high TAN (left) and low TAN oil (right) with Test Water at 60°C

Figure 42 shows the behaviour of the oil droplet during IFT measurements with test water. One can note, that the droplet shape stays almost constant over the 300 minutes of experimental period. Only a slight increase in IFT was observed approximately at minute 50 for the experiment with a low TAN oil. Comparing the repeated measurements for the same solution, helped clarifying the effect of droplet size (oil) on the IFT value outcome. During the second measurement for high TAN oil, the oil droplet with smaller volume was formed. This led to smaller measured values of IFT and resulted in high range of uncertainty for the experiment.

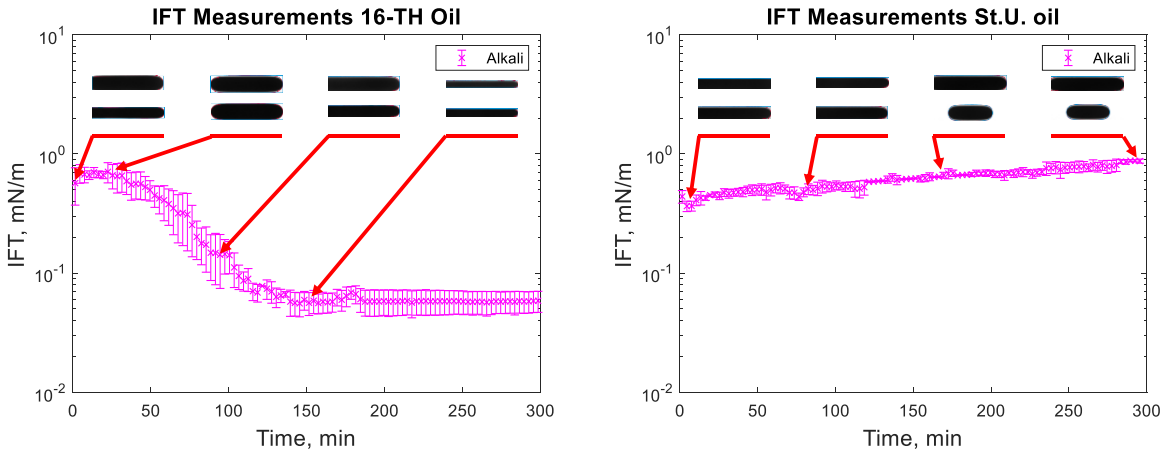

Figure 43 – IFT measurement for high TAN (left) and low TAN oil (right) with Alkali Solution at 60°C [Alkali: 7g/L Na_2CO_3]

During the experiments performed using alkali solutions, very different behaviours were observed for both, high and low TAN oil. First, instantaneous IFT for the high TAN oil reached very low values. As soon as the experiment starts, the droplet quickly elongates depicting a small interfacial tension. After a few minutes, the droplet starts to shrink again, increasing its IFT until reaching a peak and, having passed the highest value, starts to decrease again reaching equilibrium at a value of around 0.05 mN/m. Similar behaviour of interfacial tension was observed by Sharma, M.M. (1989) [73]. Using the low TAN oil led to a different outcome. The initial low value of IFT was monotonically rising over 300 minutes of investigation with almost linear trend. Such results can be explained by the interaction between alkali and natural acids of oil.

It is believed, that in the case of high TAN oil, there are enough acids to consume all available alkali in the solution. After a very fast reaction on the surface of oil droplet, the interfacial tension between fluids drops very fast. There are many anionic surfactants on the interface, which makes the alkali consumption slow down. There are no enough natural acids on the interface to continue creation of the surfactants. That is why, the IFT rises after a short period after the reaction. The observed data suggests the diffusion dominated system, when the neutralization of organic acids happens faster than molecular diffusion of alkali into the bulk of the solution. However, due to molecular diffusion, when the alkali contacts “fresh” oil from the bulk, new anionic surfactants are created. By rearrangement of the molecules, the concentration of surfactant equalizes, leading to decrease of IFT until equilibrium value, when all the alkali or natural acids are consumed. For the second oil, it was observed that the amount of natural acids is not sufficient for efficient IFT decrease. Initially created surfactants drop the IFT until minimum value. However, due to the lack of natural acids and small concentration of surfactants after rearrangement, the interfacial tension starts to increase again over time.

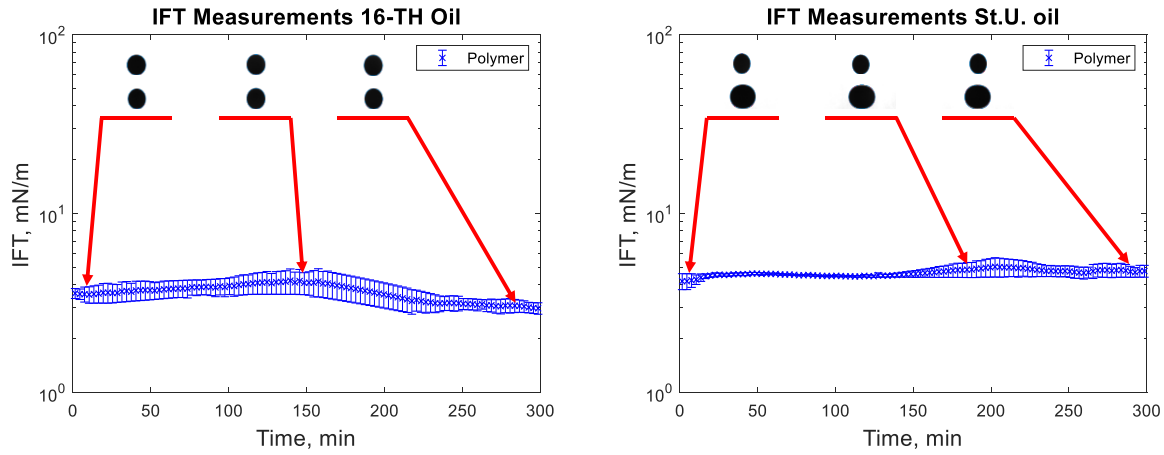

Figure 44 – IFT measurement for high TAN (left) and low TAN oil (right) with Polymer at 60°C [Polymer: 2000 ppm FLOPAAM 3630S]

During interfacial tension measurements with polymer solution, no significant changes in oil droplet shape were observed. A slightly higher interfacial tension comparing to test water was measured. The uncertainty range of the evaluated data can be related to the chosen measurement algorithm or the devise stabilization. Nevertheless, taking an average value of IFT would be a reliable approximation for oil-polymer system.

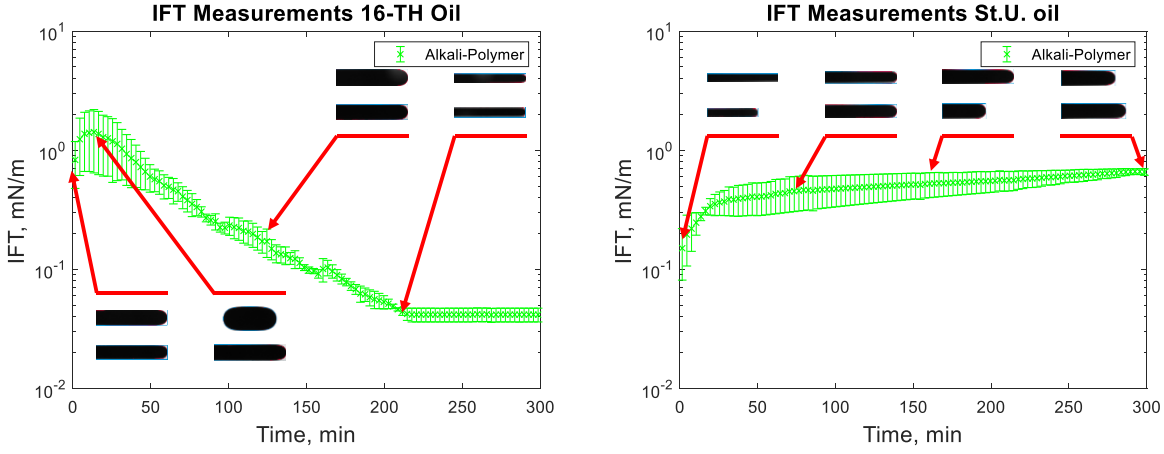

Figure 45 – IFT measurement for high TAN (left) and low TAN oil (right) with Alkali-Polymer at 60°C [Alkali: 7g/L Na_2CO_3, Polymer: 2000 ppm FLOPAAM 3630S]

Implementation alkali-polymer solution have delivered similar results to those of alkali mixture only. Instantaneous IFT for high TAN oil is very low. It can be seen by the elongated structure of the oil droplet. Then the droplet starts to shrink, representing a higher value of interfacial tension. Towards the end, the tension between fluids decreases again because of rearrangement of surfactant molecules in the droplet. Addition of polymer to the alkali solution

leads to diminishing the effect of IFT reduction and an increase of the observed IFT peak value. This might happen due to two reasons: 1) lower concentration of alkali due to additional volume of polymer; 2) delayed diffusion of Na_2CO_3 molecules into the oil due to higher polymer viscosity. Low TAN oil delivers very similar behaviour to the case with alkali-oil system. Initial low value of IFT gradually increases over time due to the lack of anionic surfactants on the interface between oil and the second fluid.

4.4 Spontaneous Imbibition Results

This section describes the results obtained for the multiple imbibition experiments performed along this work. The section includes several sub-sections that help comparing the effect of different parameters, namely: 1) Total Acid Number of oil; 2) Ageing effect; 3) Water composition; 4) Mineralogy. The graphical representation of studied cases is shown on the Figure 46. Most experiments were conducted twice in order to assess the uncertainty range related to test procedure.

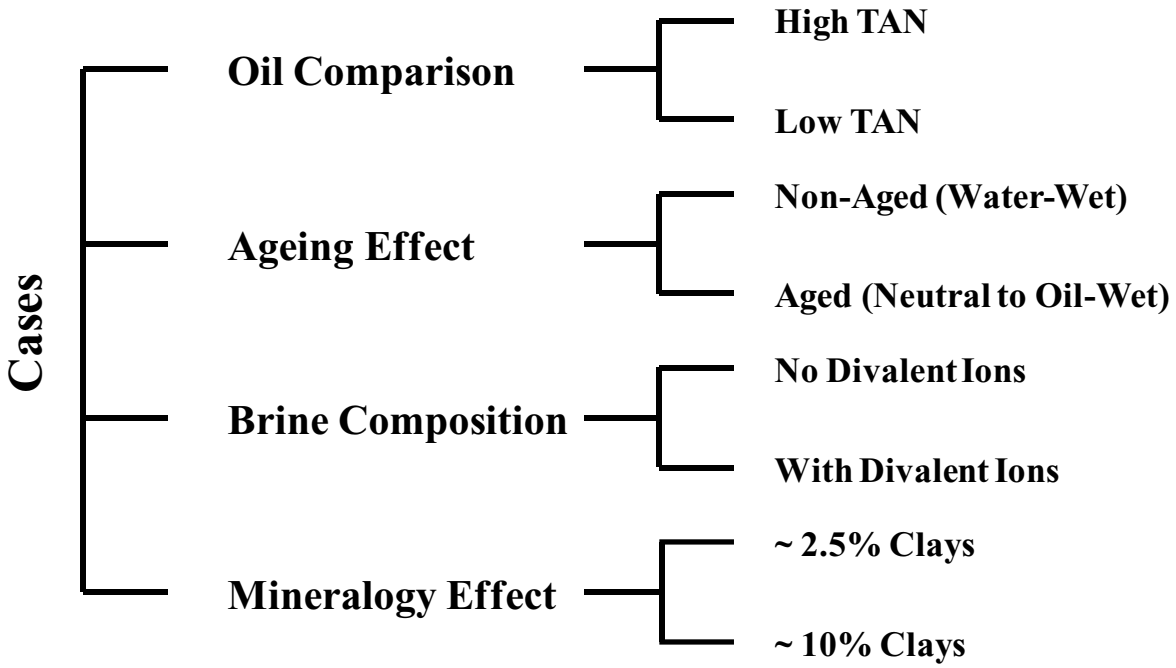

Figure 46 – Performed spontaneous imbibition tests and studied parameters

4.4.1 Non-Aged Nordhorn Core Plugs - Oil Type Comparison

The behaviour of oil production due the imbibition process was studied base on two factors: 1) Oil production time dependency (revealing how capillary forces over time will perform in the core plug); 2) Final oil recovery, which represents the total amount of oil trapped in the system. Both parameters are determined by wettability of the rock surface.

Figure 47 depicts the oil production behaviour over the first 24 hours. According to the observations in this work, this time is the most representative. After 24 hours of imbibition, only small changes in oil production were observed until the ultimate recovery was reached. On the top-left part of the graph (figure 47), the ultimate recovery values for each case is presented.

It can be seen from the figure 47, that regardless the TAN number of oil, the imbibition rate is larger using Test Water. The observed imbibition rate for the polymer, was slowed down due to the large molecules in the solution. Molecules move slowly into the pore system, which lead to a smaller imbibition rate. In the case of alkali and alkali-polymer solutions, the slower imbibition is explained by the reduction of IFT. Due to small interfacial tension, the capillary forces are reduced, which lead to slower process of imbibition.

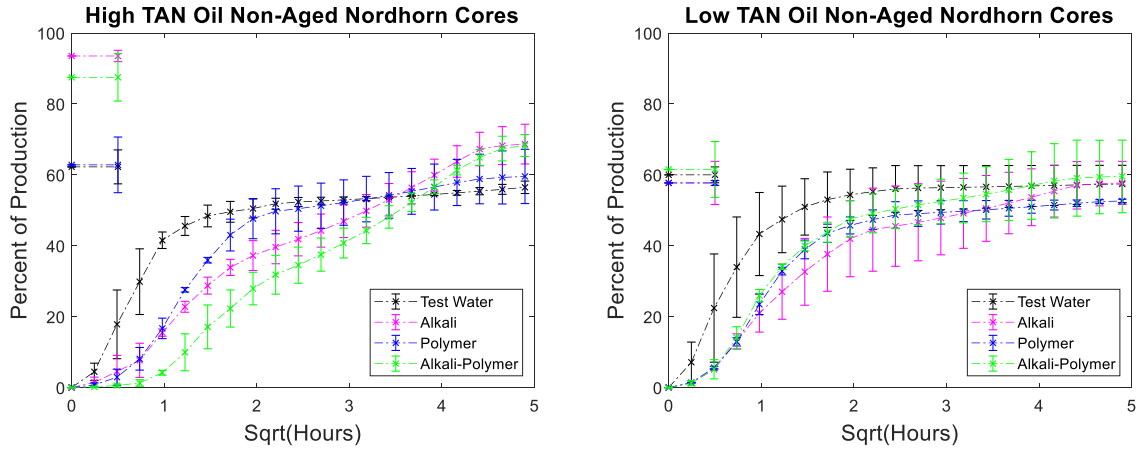

Figure 47 – Percent of production versus square root of time plot for Nordhorn core plugs using high TAN oil (left) and low TAN oil (right) at 60°C [Alkali: 7g/L Na_2CO_3, Polymer: 2000 ppm FLOPAAM 3630S]

The overall ultimate recovery (total recovery) obtained can be considered as remarkable results. For the case of low TAN oil, all chemical solutions provided similar total recovery in a small range of uncertainty. Whereas, in the case of high TAN oil, the use of alkali and alkali-polymer solutions, led to a larger amount of produced oil. Similarly, the ultimate recovery of test water and polymer was very much alike. The larger amount of total production in case of alkali and alkali-polymer solutions can be explained by lower values of equilibrium IFT. Reducing IFT until ultra-low values leads to destruction of the rigid oil films, stringing and drawing of oil. By this mechanism, the oil produced slower, but larger total amount can be released from the core.

4.4.2 Nordhorn Core Plugs - Ageing Effect

The same set of experiments was held with restored wettability state core plugs. Figure 48 shows the comparison between production from aged and non-aged Nordhorn core plugs.

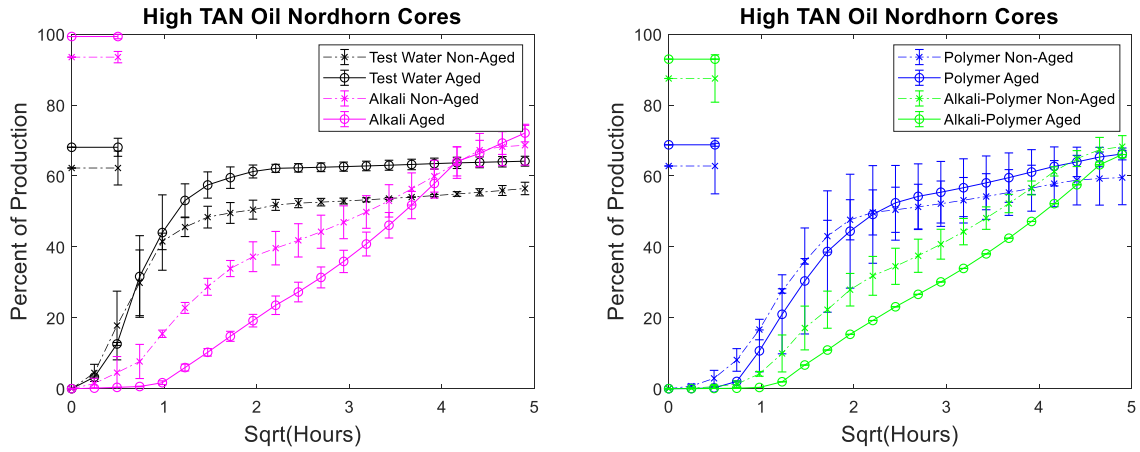

Figure 48 – Percent of production versus square root of time plot for Nordhorn non-aged and aged core plugs saturated with high TAN oil at 60°C [Alkali: 7g/L Na_2CO_3, Polymer: 2000 ppm FLOPAAM 3630S]

The effect of ageing can be clearly deduced from the observed oil production behaviour. In all cases, the early time production is slower comparing to non-aged core plugs. However, using test water and polymer as displacing fluids reflected slower production rate only within the first hour of imbibition evaluation. All other cases exhibit significantly slower initial production rate. This data confirms the change of rock surface wettability towards more oil-wet state. Additionally, it can be seen, that the effect of IFT reduction is significant during spontaneous imbibition process. Small capillary forces originated in case of alkali and alkali-polymer application allow to observe wettability change of the internal surface of rock minerals.

The ultimate oil production outcome can be explained by the oil droplet snap-off phenomenon. When the rock is water-wet, the invading fluid spreads around the surface, leading to large amount of oil left behind in the middle of the large pores. In case of oil-wet state, the oil initially covers the mineral surfaces. Submerging more oil-wet core plugs into different solutions, the invading fluid enters the middle of the pore throat, displacing larger amount of oil, then in case of water-wet core. This explains the incremental oil recovery for all cases with aged core plugs shown above. Oil recovery close to 100% in case of alkali implementation also confirms the wettability alteration. Initially oil-wet core plug is submerged into the alkali solution. Fluid enters large pores and displaces oil from the core plug. In-situ created surfactants cause the wettability alteration towards water-wet state. The invading fluid starts to spread around the inner surface of the pore throats. This leads to oil detachment from the mineral surfaces. Hence

the oil is displaced, despite of being trapped in small pores and “sticking” to the mineral surfaces.

Similar effects were observed during low TAN oil displacement process (see Figure 49).

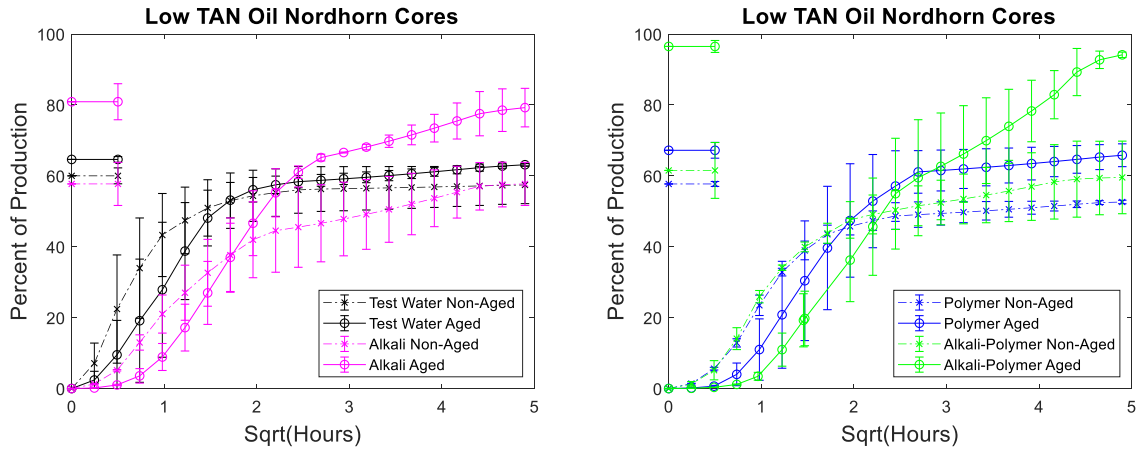

Figure 49 – Percent of production versus square root of time plot for Nordhorn non-aged and aged core plugs saturated with low TAN oil at 60°C [Alkali: 7g/L Na_2CO_3, Polymer: 2000 ppm FLOPAAM 3630S]

Results obtained from low TAN oil deliver similar behaviour and confirm previous statements. All the restored wettability core plugs exhibit slower oil production rate over first time of imbibition process, which further overrides non-aged core production and delivers higher ultimate recovery. As it was shown in Chapter 4.3, even small amount of crude oil acids was enough in order to decease interfacial tension between oil and displacing fluid. Decrease in IFT is not large enough to cause stringing of the oil in case of water-wet state. However, the surfactants, created in-situ, result in wettability alteration of the initially aged core plugs. As a result, oil is displaced not only from the middle of the larger pores (as in case of test-water and polymer imbibition), but also from the mineral surfaces. This assumption is confirmed by incremental oil production while using alkali and alkali-polymer displacing fluids for low TAN oil case.

4.4.3 Nordhorn Core Plugs - Water Composition Effect

Spontaneous imbibition tests were performed with cores initially saturated with brine, which contains high amount of divalent ions. The water composition is described in the Chapter 4.1. This part of the work was performed in order to study the effect of divalent ions on spontaneous imbibition process. However, only experiments with test water and alkali-polymer solution were conducted. Figure 50 depicts the comparison of oil production behaviour in non-aged Nordhorn core plugs in case of a brine with only monovalent and one with both mono and bivalents ions.

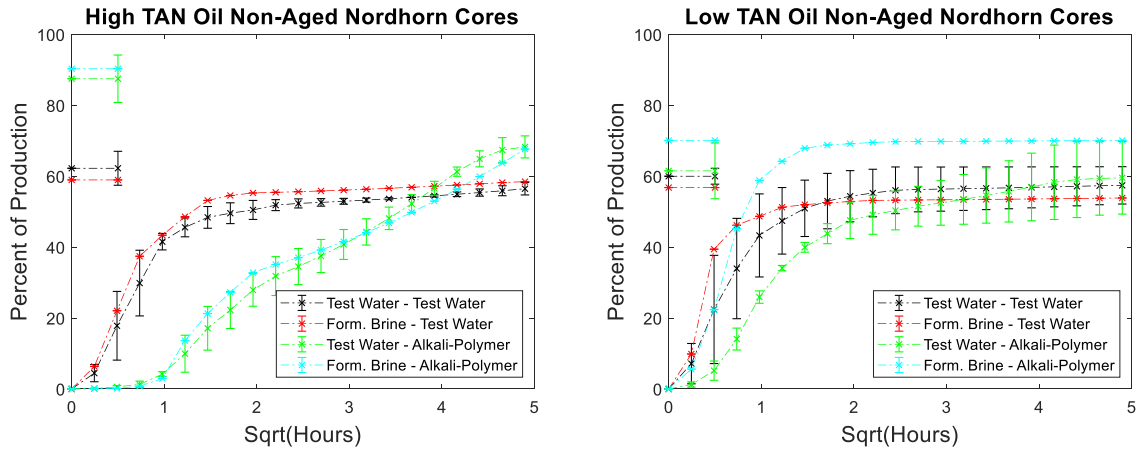

Figure 50 – Percent of production versus square root of time plot for non-aged Nordhorn core plugs (water composition comparison) for high Tan oil (left) and low TAN oil (right) at 60°C [Alkali: 7g/L Na_2CO_3, Polymer: 2000 ppm FLOPAAM 3630S]

Analysing the results, one can note, that there are not significant changes in oil production rate and ultimate oil recovery, when formation brine or test water were used for initial saturation. Only in case of low TAN oil, the recovery for the core initially saturated with formation brine and subsequently submerged into alkali-polymer solution is higher. This behaviour can be attributed to uncertainty while performing the measurement. As a next step, the core plugs, initially saturated with formation brine, were aged under reservoir temperature during 30 days in order to figure out the influence of divalent ion concentration on wettability change during ageing. The comparison of aged and non-aged Nordhorn core plugs can be seen on the Figure 51 for high TAN oil and Figure 53 for low TAN oil.

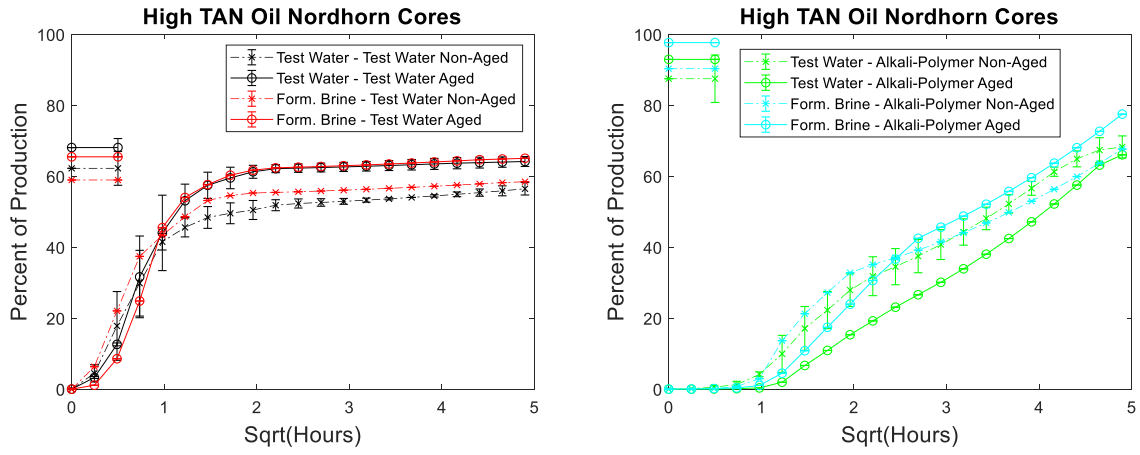

Figure 51 – Percent of production versus square root of time plot for non-aged and aged Nordhorn core plugs saturated with high TAN oil (water composition comparison) at 60°C [Alkali: 7g/L Na_2CO_3, Polymer: 2000 ppm FLOPAAM 3630S]

For the observations obtained in this work, when the core plug is placed into test water after saturation, composition of formation brine does not play a big role. As can be seen from the Figure 51 (left), the oil production profile follows the same path both, for formation brine and test water initial saturation in case of aged and non-aged cores. On the other hand, when the displacing fluid is alkali-polymer solution, the differences can be detected. A higher production rate can be observed, when formation water is used for primary saturation. This behaviour is logical and can be explained by surfactant-divalent ion-rock surface interaction [74]. As it was discussed in Chapter 2.4.3, the divalent ions might create “bridges” between negatively charged rock surface and polar oil components. On the other hand, the same divalent ions can promote wettability alteration with the use of anionic surfactants. When the alkali reacts with crude oil acids, the anionic surfactant with negatively charged head is formed. The negatively charged end of the surfactant can replace polar oil compound creating the bridge with mineral surface. This effect leads to faster wettability alteration towards water-wet state and higher oil production rate. This statement is supported by the results of similar experiments performed with low TAN oil. The oil production profiles for low TAN oil are presented on Figure 53.

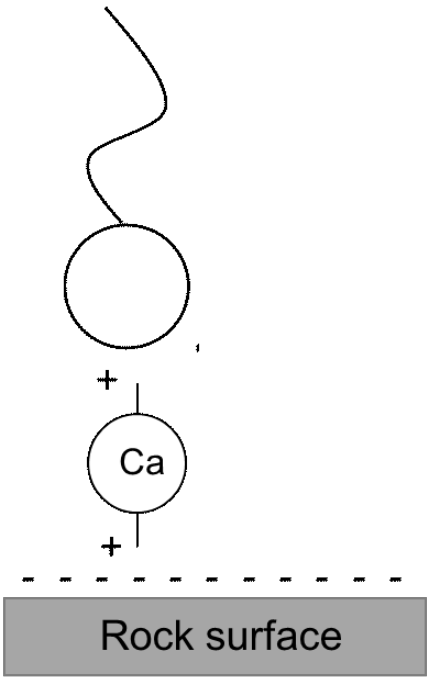

Figure 52 – Schematic process of wettability alteration due to anionic surfactant formation

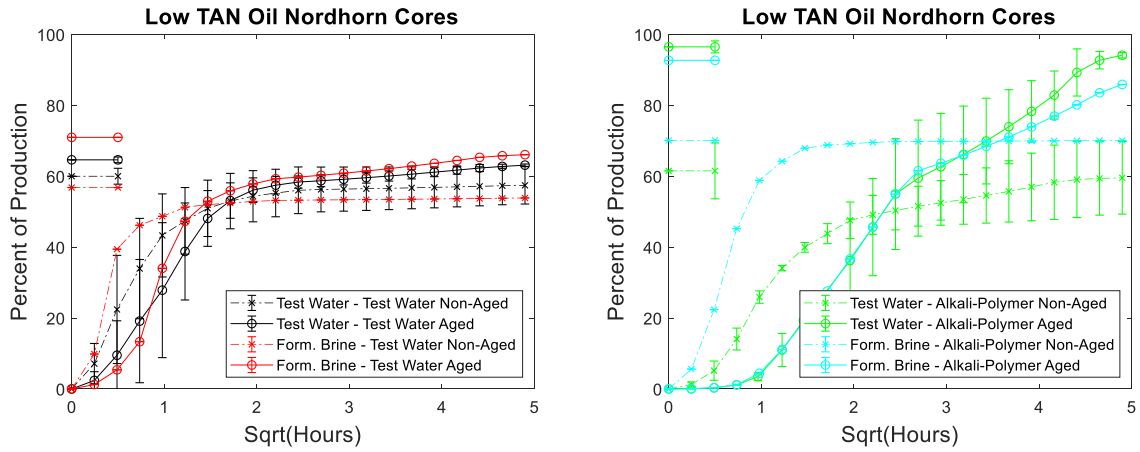

Figure 53 – Percent of production versus square root of time plot for non-aged and aged Nordhorn core plugs saturated with low TAN oil (water composition comparison) at 60°C [Alkali: 7g/L Na_2CO_3, Polymer: 2000 ppm FLOPAAM 3630S]

As it can be seen, the production behaviour is similar for all cases, excerpt non-aged alkali-polymer experiment. What deserves attention is the same production profiles in case of aged cores with implementation of alkali-polymer solution. The process of wettability alteration due to anionic surfactant creation does not happen in this case. Due to this fact, the divalent cation bridging effect of wettability alteration does not appear. As a result, there are no differences between saturation of core plugs with high or low divalent ion concentration brine.

4.4.4 Nordhorn and Keuper Core Plugs - Mineralogy Effect

Similar set of experiments were performed using Keuper outcrop core in order to study the effect of clay minerals on the wettability alteration process. Core plugs were initially saturated with formation brine -containing high amount of divalent ions-. After the saturation with oil, core plugs were submerged into test water and alkali-polymer solution. The observed oil production behaviour is presented on Figure 54.

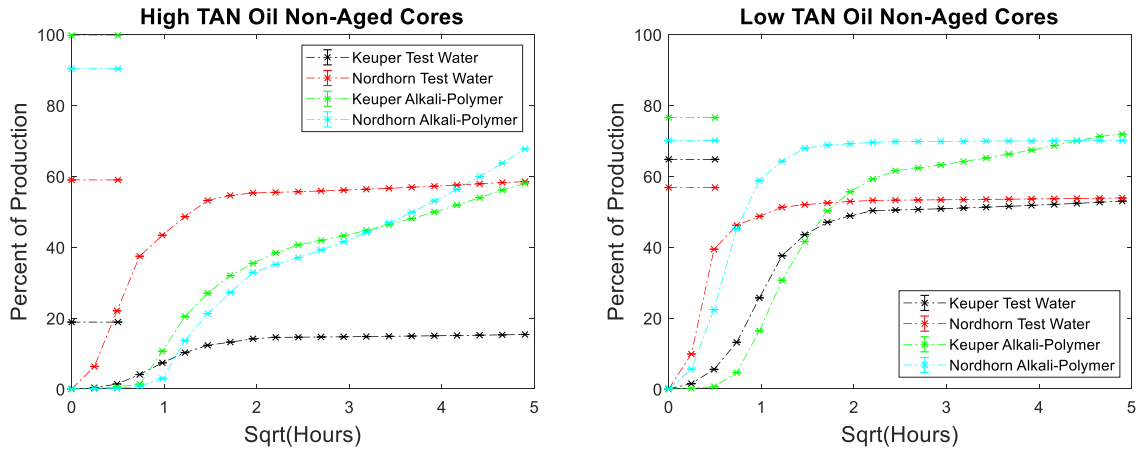

Figure 54 – Percent of production versus square root of time plot for non-aged Nordhorn and Keuper core plugs for high Tan oil (left) and low TAN oil (right) at 60°C [Alkali: 7g/L Na_2CO_3, Polymer: 2000 ppm FLOPAAM 3630S]

The obtained results point out on the wettability alteration even when the core was not aged. Thus, the effect of oil total acid number is more indicative. For high TAN oil, Keuper core plugs showed significant decrease in both production rate and ultimate oil recovery when test water is used as a displacing fluid. At the same time, the production is similar to Nordhorn core plug in case of alkali-polymer application. This fact suggests that even without ageing period, polar components of the crude oil covered the clay mineral surfaces. This resulted in the oil-wet state of the core. However, during the application of alkali-polymer solution, the oil-wetness was back returned to water-wet state. As a result, a higher ultimate recovery was achieved. At the same time, small capillary forces led to a slow production. A large difference in case of test water application can be also related to high value of heterogeneity of the Keuper outcrop core. It brings additional complexity to spontaneous imbibition data interpretation.

Data obtained during experiments with low TAN oil also indicated wettability alteration. A slower production rate for Keuper core plug is detected. This proves the oil-wet state of the core after ageing. The lower ultimate oil recovery for Nordhorn core plugs can be explained by “snap-off” effect in water-wet system, leading to higher residual oil saturation. Another remarkable point is the minor improvement of oil recovery with alkali-polymer solution. As it was proved by IFT measurements, the low TAN oil fails to reduce interfacial tension to ultra-low values. Chandra S. (2003) has reported, that there exists a critical value of IFT, above which, the wettability alteration does not occur [72]. Not reaching the critical IFT value, the oil droplet detachment does not happen. Consequently, a smaller ultimate production is obtained.

The set of experiments presented below were carried out in order to check the possible effect that ageing can cause on Keuper outcrop during the spontaneous imbibition process. Figure 55 gives an information about oil production behaviour from aged and non-aged Keuper samples and compares it to Nordhorn sample results discussed before.

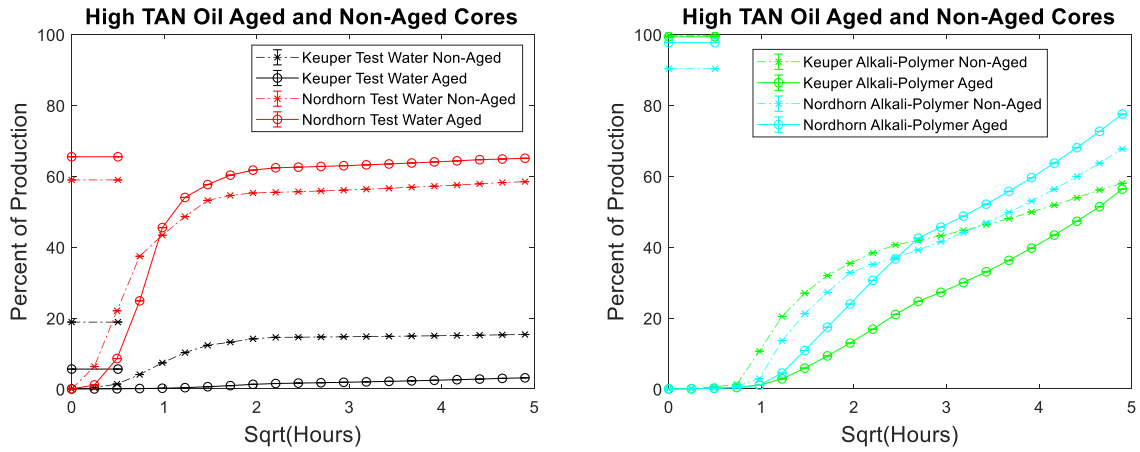

Figure 55 – Percent of production versus square root of time plot for non-aged and aged Keuper and Nordhorn core plugs saturated with high TAN oil at 60°C [Alkali: 7g/L Na_2CO_3, Polymer: 2000 ppm FLOPAAM 3630S]

Results obtained from the aged core plugs confirmed wettability changes. Minimal oil production was observed during the spontaneous imbibition evaluation of aged Keuper core plug using test water as a displacing fluid. This represents a significant wettability change towards oil-wet state. Similarly, applying alkali-polymer solution, oil production rate also dropped significantly -suggesting oil-wet behaviour-, but the ultimate oil recovery was the largest. This fact can be explained by previously described principle of anionic surfactant – mineral surface reaction. Note that similar observations were obtained while evaluating with the low TAN oil (see Figure 56).

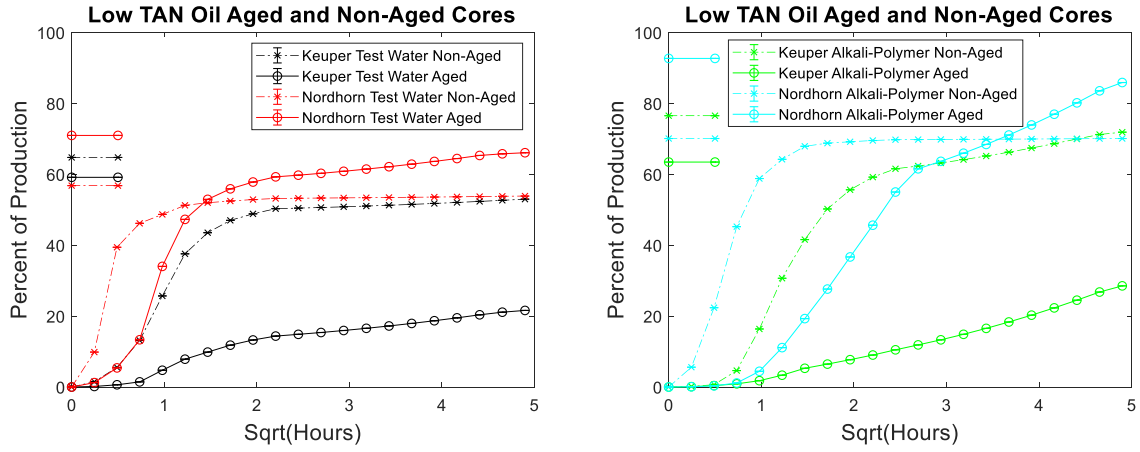

Figure 56 – Percent of production versus square root of time plot for non-aged and aged Keuper and Nordhorn core plugs saturated with low TAN oil at 60°C [Alkali: 7g/L Na_2CO_3, Polymer: 2000 ppm FLOPAAM 3630S]

One important overall observation is that significant shift in core sample wettability was observed for the Keuper outcrop. The observations are mainly based on the profile of the oil production plot. Both aged Keuper core plugs showed much slower production rate and ultimate oil recovery, which is the indicator of strongly oil-wet system. The alkali-polymer application again fails to improve oil recovery for low TAN oil.

4.4.5 Spontaneous Imbibition Summary

Summarizing all experimental observations stated for the spontaneous imbibition data, the following conclusion could be drawn:

1. The Total acid number (TAN) of oil plays a significant role in the spontaneous imbibition process. Generation of anionic surfactants “in-situ” promotes wettability alteration during the imbibition process. The observed effect of TAN number was minor when experiments were performed in water-wet core plugs. The results led to a small decrease in oil production rate due to decrease in IFT and, consequently capillary forces. At the same time, the high TAN oil ultimate recovery was significantly increased in cases with aged (neutral to oil-wet) core plugs.
2. Ageing of core samples saturated with crude oil lead to a shift in wettability towards oil-wet state. The observed Wettability alteration during ageing was affected by the core plug mineralogy. On one hand, for the evaluated Nordhorn samples (minor clay minerals), wettability shifted from water-wet to slightly neutral-wet state. On the other hand, Keuper core plugs depicted a much more significant wettability change. The initially water-wet to neutral-wet core plugs became strongly oil-wet after ageing. Similar observations of the aging impact were reported by Ehrlich et al. (1974) [7];
3. Neutral-wet state delivers the highest ultimate (final) oil recovery. This might appear due to both: oil detachment from the mineral surfaces and, at the same time, a small extent of oil “snap-off”;
4. In the current study, while assessing the high TAN oil, the application of alkaline solution always resulted in higher ultimate oil recovery comparing to other displacing fluids. Moreover, the application of polymer together with alkali negatively affects the oil recovery process during spontaneous imbibition;
5. For the low TAN oil assessment, the application of all solutions in water-wet cores provided similar production behaviour. Improvement of oil production was solely observed in aged core plugs with alkali and alkali-polymer solutions as imbibing fluid. This is directly linked to wettability alteration from water-wet to neutral-wet system;
6. Presence of divalent ions in brine (used for initial saturation) has a minor effect on core plugs with low clay content. In contrast, core plugs with a large amount of clay minerals were largely affected by brine composition. It was found out, that the presence of divalent ions promotes oil-wetness during ageing process as well as boosts back wettability alteration in presence of anionic surfactants.

5 Data Interpretation and Simulations

In this chapter, an effort to analyse the production behaviour by means of capillary suction phenomenon is attempted. First, the capillary diffusion equation was solved analytically to describe the oil production rate. Further, the problem was solved numerically in order to obtain saturation profiles in the core plug over time.

5.1 Analytical Solution

The aspect of capillary suction and its analytical solution is introduced in the Chapter 2.4.5. The results of analytical approach for all experiments are presented in this section.

5.1.1 Non-aged Nordhorn Core Plugs - Oil Type Comparison

Data obtained during the first 24 hours of oil production was transfer into a normalized oil saturation plot. The analytical solution was solved for capillary diffusion coefficient, which gives the best match to observed data (see Figure 57).

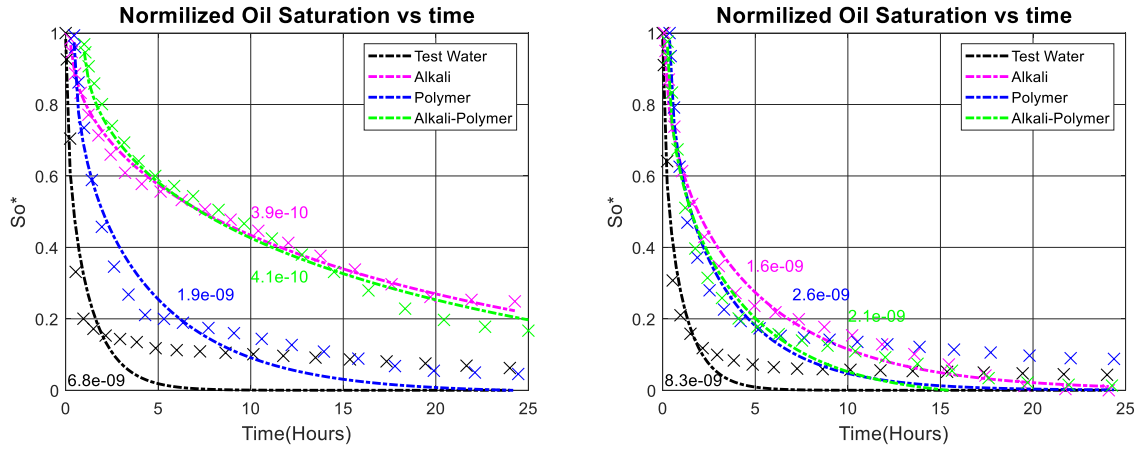

Figure 57 – Normalized oil saturation versus time plot for Nordhorn non-aged core plugs saturated with high TAN (left) and low TAN oil (right) [Alkali: 7g/L Na_2CO_3, Polymer: 2000 ppm FLOPAAM 3630S]

As in can be noted from the Figure 57 on one hand the alkali and alkali-polymer solution show a reasonable fit to the constant capillary diffusion coefficient solution. On the other hand, the test water and polymer cases show a strong mismatch to the data. According to the literature, the analytical solution better holds for early time steps. A reason of mismatching could be the assumption of constant capillary diffusion coefficient. Diffusion coefficient is a complex parameter that depends on capillary pressure, fluid mobility and saturation. All of these parameters change during the imbibition process.

The objective of this study was to find out the range of saturation, where the capillary diffusion coefficient is constant that allows evaluating capillary forces acting at a certain period of

imbibition process. Therefore, it was decided to match only the first production data as long as the analytical solution replicates the experimental data (see Figure 58).

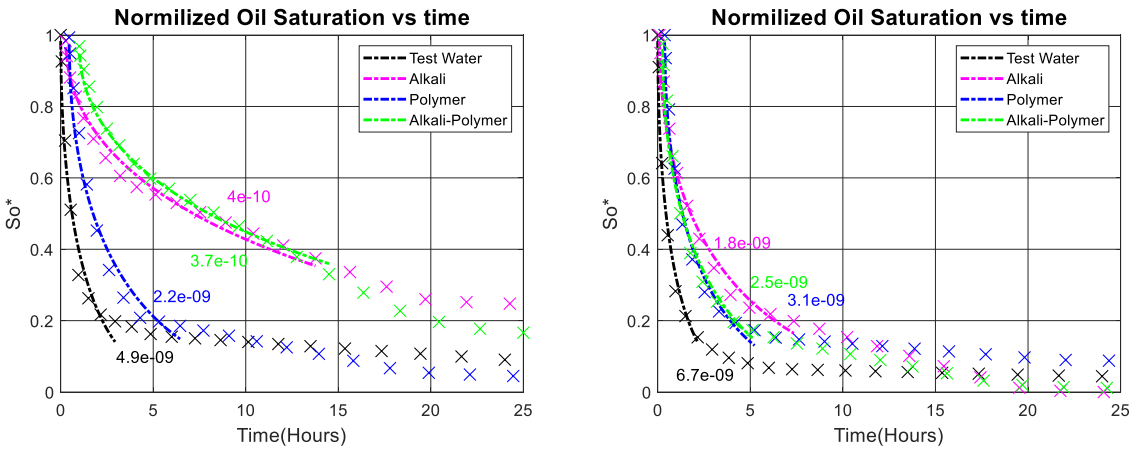

Figure 58 – Best fit of normalized oil saturation versus time plot for Nordhorn non-aged core plugs saturated with high TAN (left) and low TAN oil (right) [Alkali: 7g/L Na_2CO_3, Polymer: 2000 ppm FLOPAAM 3630S]

Few points can be drawn while analysing Figure 58:

- Capillary diffusion coefficient stays constant over a large saturation range. Only later production does not follow analytical solution for constant capillary diffusion.
- Comparison of the obtained coefficients reflects the imbibition rate with the application of different chemical agents. The slowest imbibition rate is detected with the use of alkali solution. This effect is related to the capillary forces reduction due to ultra-low IFT in the system.
- Capillary diffusion coefficients for test water and polymer are similar for both oil types, whereas for alkali and alkali-polymer solutions, the coefficients are smaller for the high TAN oil case.
- Small diffusion coefficients of the high TAN oil are in agreement with IFT measurement results. The largest reduction in interfacial tension and, consequently, capillary force was observed for evaluations with alkali and alkali-polymer and high TAN oil.

Estimated values of capillary diffusion coefficients were used further for calculation of the dP_c/dS_w values, which are linked to wetting state of the system. Additionally, these values were implemented in numerical simulation case in order to obtain saturation distribution inside the core plug.

5.1.2 Nordhorn Core Plugs - Ageing Effect

The capillary diffusion equation was solved for the aged core plugs. It was observed that the assumption of constant capillary diffusion coefficient could not be held for a large saturation

range, when the wettability state tends towards oil-wet. The imbibition rate at initial oil production period is much slower for the oil-wet state core plugs. Therefore, a smaller capillary diffusion coefficient is required in order to fit the observed data (see Figures 59, 62).

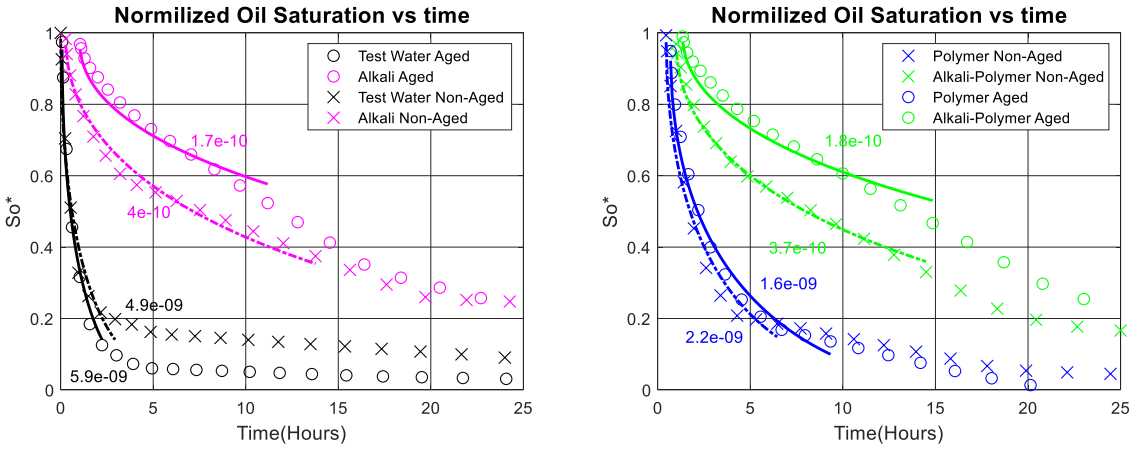

Figure 59 – Best fit of normalized oil saturation versus time plot for Nordhorn non-aged and aged core plugs saturated with high TAN oil [Alkali: 7g/L Na_2CO_3, Polymer: 2000 ppm FLOPAAM 3630S]

As previously described, capillary diffusion coefficient is a function of water saturation. Defined values of this coefficient are valid only for a certain range of saturation, which is different for each test. Figure 60 shows the values of diffusion coefficients as a function of water saturation of the core plug. Other than capillary diffusion coefficient, it is important to compare residual oil saturation values after imbibition test, where $P_c = 0$.

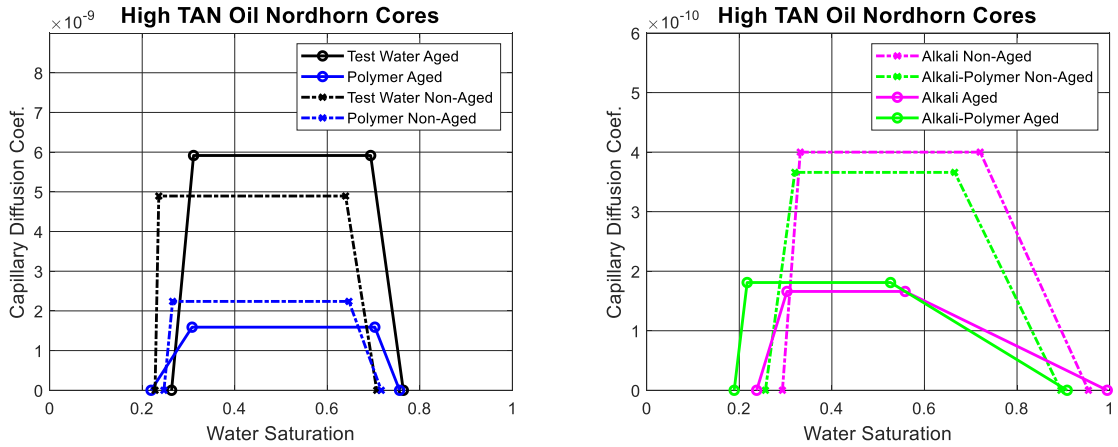

Figure 60 – Capillary diffusion coefficient [in m^2/s] as a function of water saturation for Nordhorn non-aged and aged core plugs saturated with high TAN oil [Alkali: 7g/L Na_2CO_3, Polymer: 2000 ppm FLOPAAM 3630S]

As it can be seen from the graph (figure 60), ageing of the core plugs leads to similar change in the capillary diffusion coefficient function. Only in case of test water -used as a displacing

fluid- the capillary diffusion coefficient showed a higher value for aged core plug. Another remarkable feature is the decrease in residual oil saturation for all aged core cases.

Capillary diffusion coefficients cannot be directly compared for different examples due to the various permeability and oil mobility. On those bass, an equation (10) was solved for dP_c/dS_w in order to compare the results (see Figure 61). Values presented for dP_c/dS_w, indicate the slope of the capillary pressure curve in a range of the saturation, at which capillary diffusion coefficient stays constant. During the computation, the end-point phase permeabilities were used for simplification.

Independently of correcting core plug permeability and/or fluid mobilities, values obtained for dP_c/dS_w help supporting the observations described before. Nothing that only test water showed a faster imbibition with higher capillary forces acting in the system.

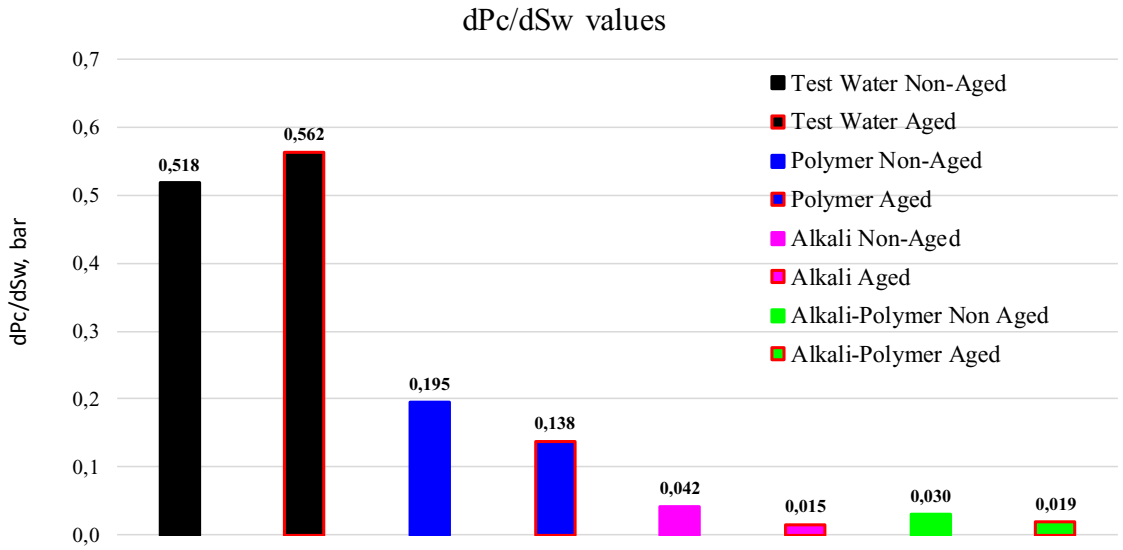

Figure 61 – Values of dP_c/dS_w for Nordhorn non-aged and aged core plugs saturated with high TAN oil [Alkali: 7g/L Na_2CO_3, Polymer: 2000 ppm FLOPAAM 3630S]

Figure 62 shows an interpretation of data from experiments with low TAN oil. One can see from the graph, that the capillary diffusion coefficient was reduced for all aged core plug cases. The highest reduction in imbibition rate was observed for alkali-polymer solution used as a displacing fluid.

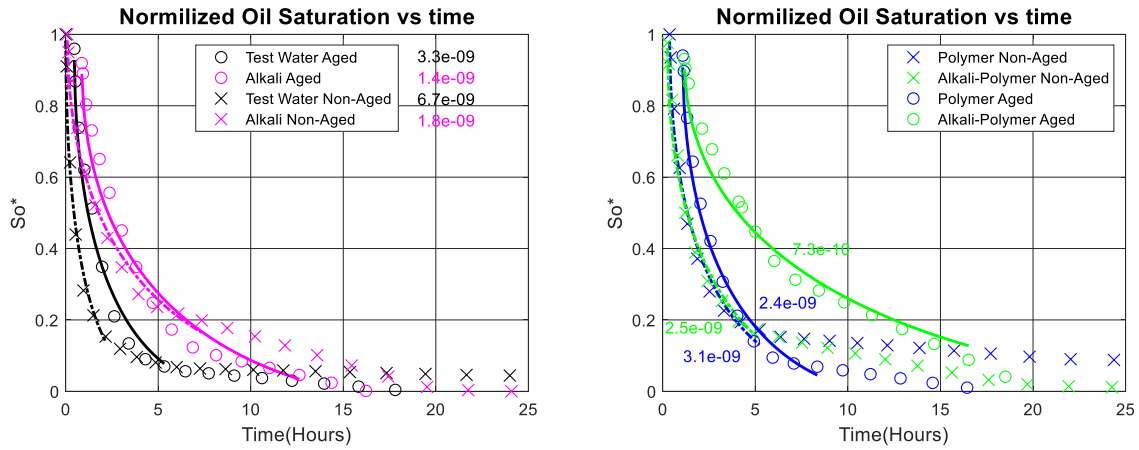

Figure 62 – Best fit of normalized oil saturation versus time plot for Nordhorn non-aged and aged core plugs saturated with low TAN oil [Alkali: 7g/L Na_2CO_3, Polymer: 2000 ppm FLOPAAM 3630S]

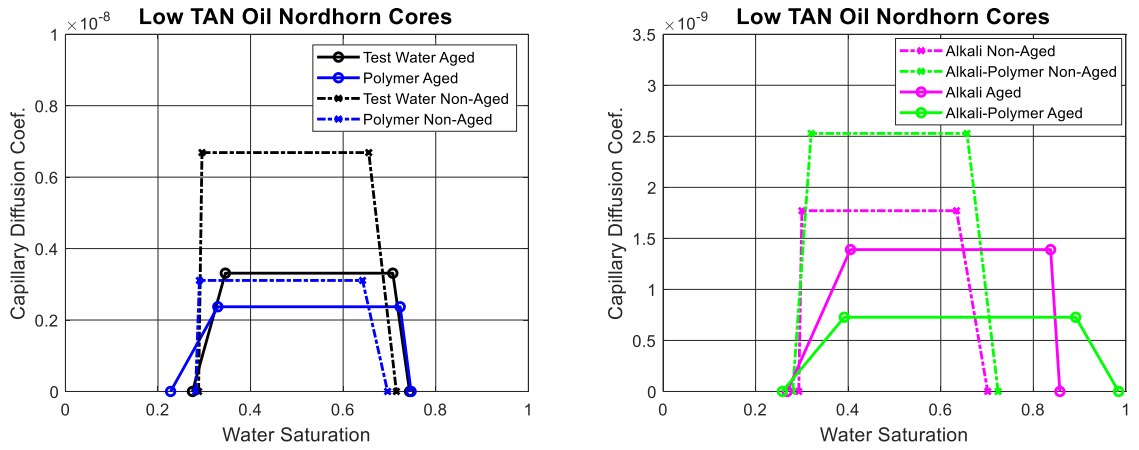

Figure 63 – Capillary diffusion coefficient [in m^2/s] as a function of water saturation for Nordhorn non-aged and aged core plugs saturated with low TAN oil [Alkali: 7g/L Na_2CO_3, Polymer: 2000 ppm FLOPAAM 3630S]

The capillary diffusion function in case of low TAN oil application changes similarly for cases with all displacing fluids. One can detect, that ageing leads to reduction of capillary diffusion coefficient and shift of the residual oil saturation towards smaller values.

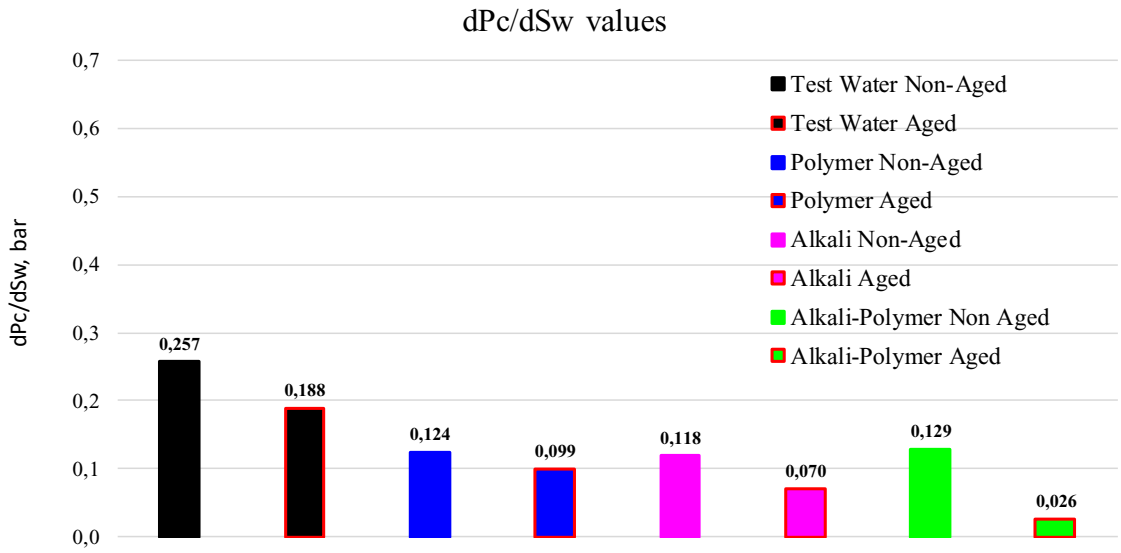

Figure 64 – Values of dP_c/dS_w for Nordhorn non-aged and aged core plugs saturated with low TAN oil [Alkali: 7g/L Na_2CO_3, Polymer: 2000 ppm FLOPAAM 3630S]

Comparing the values obtained for dP_c/dS_w (low and high TAN oil) led to some remarks:

- Higher values were observed for alkali and alkali-polymer solutions when using the low TAN oil. Suggesting that capillary forces act stronger in the case of low TAN oil. One possible explanation is the strong IFT reduction, when alkali reacts with the high amount of natural acids in case of high TAN oil.
- The obtained value of dP_c/dS_w for test water was much smaller than for the high TAN oil, one assumptions relates to the mobility of oil.
- The low TAN oil has also a smaller viscosity, which affect the imbibition process. In all investigations with low TAN oil, the dP_c/dS_w values reduced on ~25% after ageing.

As afore mentioned, this parameter (dP_c/dS_w) is directly related to capillary forces acting in the core plug. The smaller capillary forces during imbibition process can be treated as an indication of wettability alteration. Many parameters affect the value of dP_c/dS_w, therefore, it cannot be directly taken as a wettability alteration parameter, since is just and indicator/marker.

5.1.3 Nordhorn Core Plugs - Water Composition Effect

Similar analysis was performed for the experiments when core plugs were initially saturated with high divalent ion concentration brine. The results of imbibition tests and its comparison to previous data are presented on the Figure 65. One can see, that there are only minor differences between saturation change between core plugs, which were saturated with formation brine and test water in case of high TAN oil. For the low TAN oil, the biggest difference is observed for imbibition process with alkali-polymer solution. The imbibition rate in this case is very high.

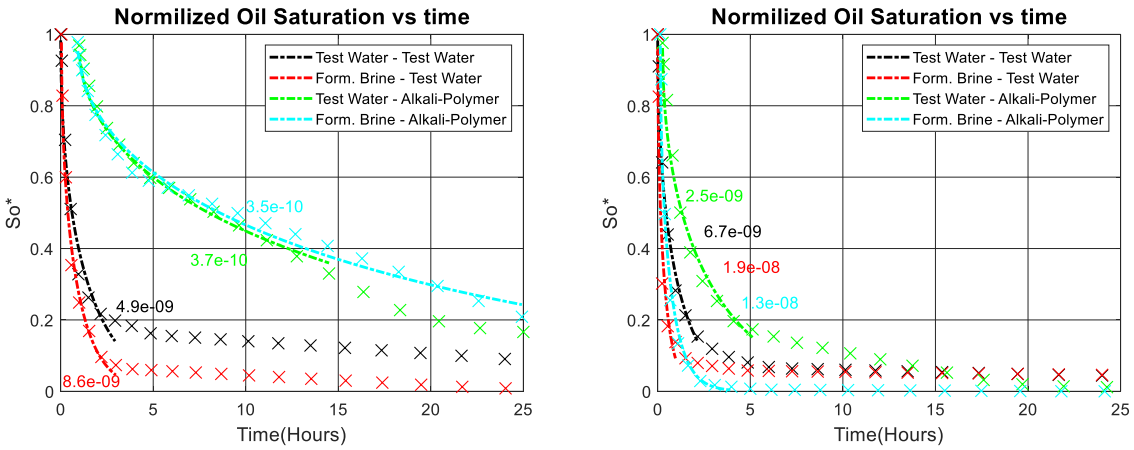

Figure 65 – Best fit of normalized oil saturation versus time plot for non-aged Nordhorn core plugs saturated with high TAN (left) and low TAN oil (right) (Brine composition effect) [Alkali: 7g/L Na_2CO_3, Polymer: 2000 ppm FLOPAAM 3630S]

Subsequently, another set of experiments with aged core plugs were performed and analyzed. The normalized oil saturation plot for aged and non-aged core plugs is displayed on the Figure 66. Results suggest minor effect of ageing of core plugs (submerged into test water). There is a slight decrease in imbibition rate for aged core plugs, which stays in the uncertainty range due to the measurement. The biggest effect of divalent ions can be observed for the case of aged core plug (submerged into alkali-polymer solution). Only the first few hours, imbibition rate for aged core plug is slower, increasing consequently.

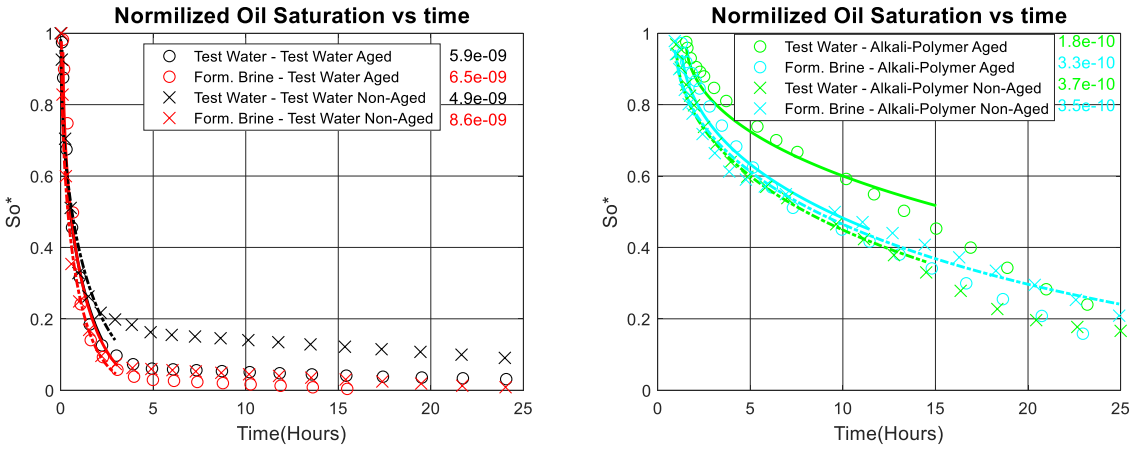

Figure 66 – Best fit of normalized oil saturation versus time plot for aged and non-aged Nordhorn core plugs saturated with high TAN oil (Brine composition effect) [Alkali: 7g/L Na_2CO_3, Polymer: 2000 ppm FLOPAAM 3630S]

Capillary diffusion coefficients computed for aged and non-aged core plugs turned out to be very similar (see figure 67). For core plugs initially saturated with test water, the difference

was significant. This fact reveals a great impact of presence of the divalent ions in the formation brine. After the ageing process, the core plug wettability was shifted towards oil-wet state. When no divalent ions present in the system, anionic surfactants are not capable to change the wetting state back towards water-wet or this process happens slowly. Divalent ions help anionic surfactant to change the wetting state of the core plug towards water-wet by bridging the surfactant to the mineral surfaces. This process was described in detail along chapter 4.4.3.

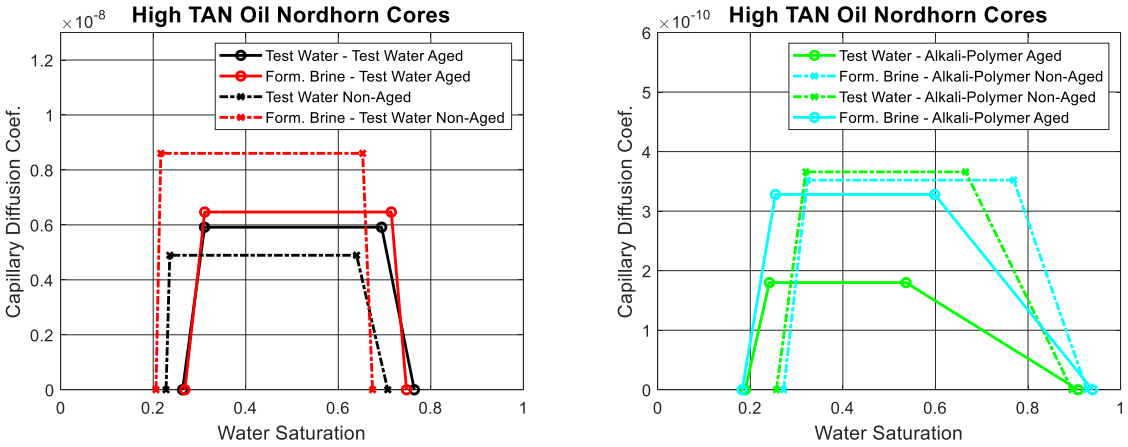

Figure 67 – Capillary diffusion coefficient [in m^2/s] as a function of water saturation for Nordhorn non-aged and aged core plugs saturated with high TAN oil (Brine composition effect) [Alkali: 7g/L Na_2CO_3, Polymer: 2000 ppm FLOPAAM 3630S]

Analysing the capillary diffusion function, one can see a change in case of aged and non-aged core plugs initially saturated with formation brine. Even when the change if oil production rate is very similar, the fit of capillary diffusion coefficient exposes the change in wetting state of the core plug. Only a slight change in capillary diffusion coefficient function is observed for aged and non-aged samples, which were saturated with formation brine and tested with alkali-polymer solution.

The analysis of dP_c/dS_w values (figure 68) show that the highest capillary forces act in case of formation brine used for pre-saturation. Moreover, only a very slight effect of ageing is observed for both, test water and alkali-polymer case, when formation brine is used for initial saturation.

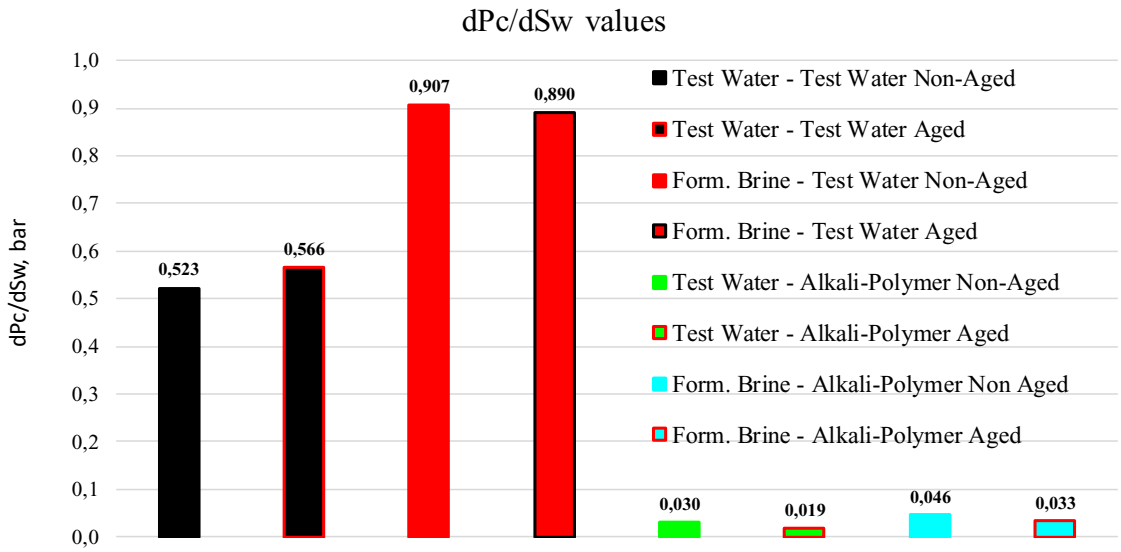

Figure 68 – Values of dP_c/dS_w for Nordhorn non-aged and aged core plugs saturated with high TAN oil [Alkali: 7g/L Na_2CO_3, Polymer: 2000 ppm FLOPAAM 3630S]

Figure 69 shows normalized oil saturation change with time for aged and non-aged Nordhorn core plugs saturated with low TAN oil. In all cases, ageing resulted in a slower fluid imbibition and oil production. Additionally, it can be seen, that alkali-polymer solution does not affect the wettability of the core plug even in case of presence of divalent ions. Capillary diffusion coefficient function can be seen on the Figure 70.

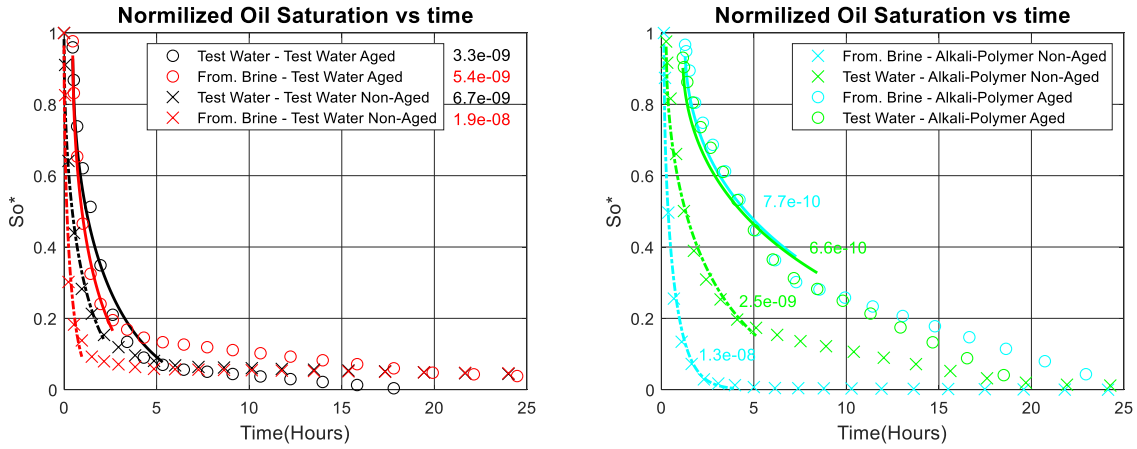

Figure 69 – Best fit of normalized oil saturation versus time plot for aged and non-aged Nordhorn core plugs saturated with low TAN oil (Brine composition effect) [Alkali: 7g/L Na_2CO_3, Polymer: 2000 ppm FLOPAAM 3630S]

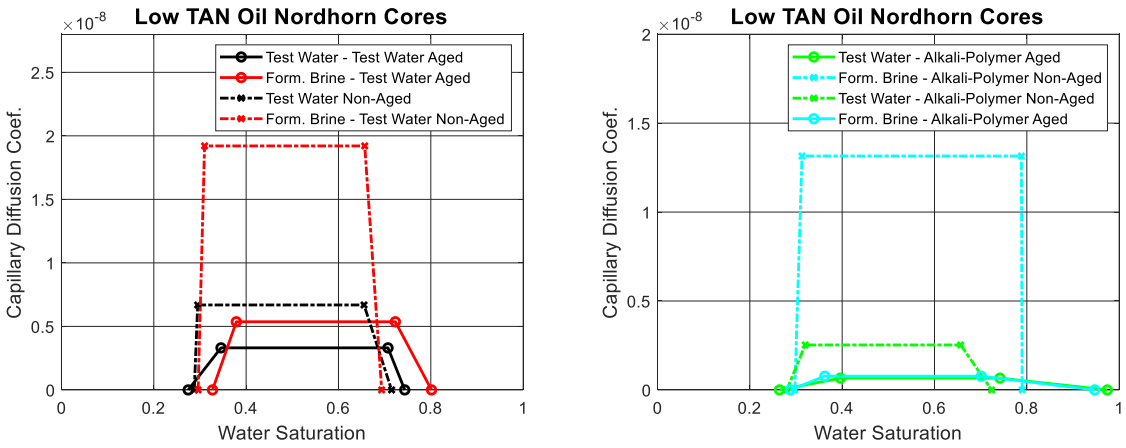

Figure 70 – Capillary diffusion coefficient [in m^2/s] as a function of water saturation for Nordhorn non-aged and aged core plugs saturated with low TAN oil (Brine composition effect) [Alkali: 7g/L Na_2CO_3, Polymer: 2000 ppm FLOPAAM 3630S]

From the capillary diffusion coefficient function, a large shift in case of aged core plugs was observed. Another valuable outcome of this test is the effect of brine composition on ageing process. A much stronger change in the capillary diffusion function was noticed, when the brine with divalent ions present in the system. This suggests a stronger wettability alteration due to oil polar compounds – divalent ion – mineral surface bridging.

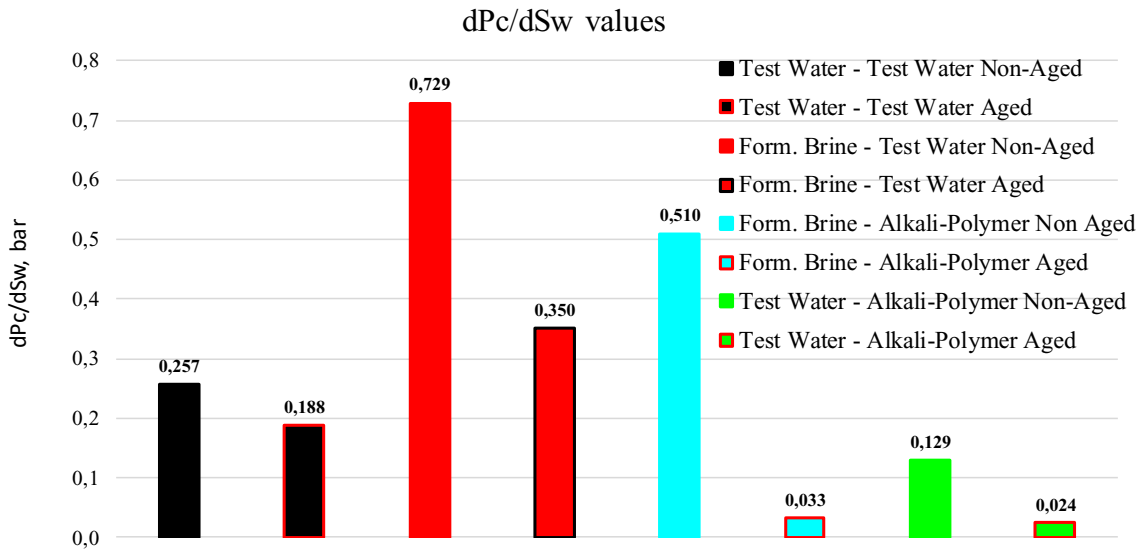

Figure 71 – Values of dP_c/dS_w for Nordhorn non-aged and aged core plugs saturated with low TAN oil [Alkali: 7g/L Na_2CO_3, Polymer: 2000 ppm FLOPAAM 3630S]

Even though the core plug permeability and fluid mobilities were accounted for, a large reduction of the parameter dP_c/dS_w is observed for all cases, when low TAN oil was used. This reduction indicates a strong alteration of core plug wettability towards the oil-wet state.

5.1.4 Nordhorn and Keuper Core Plugs - Mineralogy Effect

In this section summarizes and discusses the experiments where the largest change in wettability were expected. The effect of clay minerals combined with brine with divalent ions, led to remarkable results regarding oil production rate and ultimate recovery. First, the normalized oil saturation plots of the non-aged Nordhorn and Keuper core plugs are presented on the Figure 72.

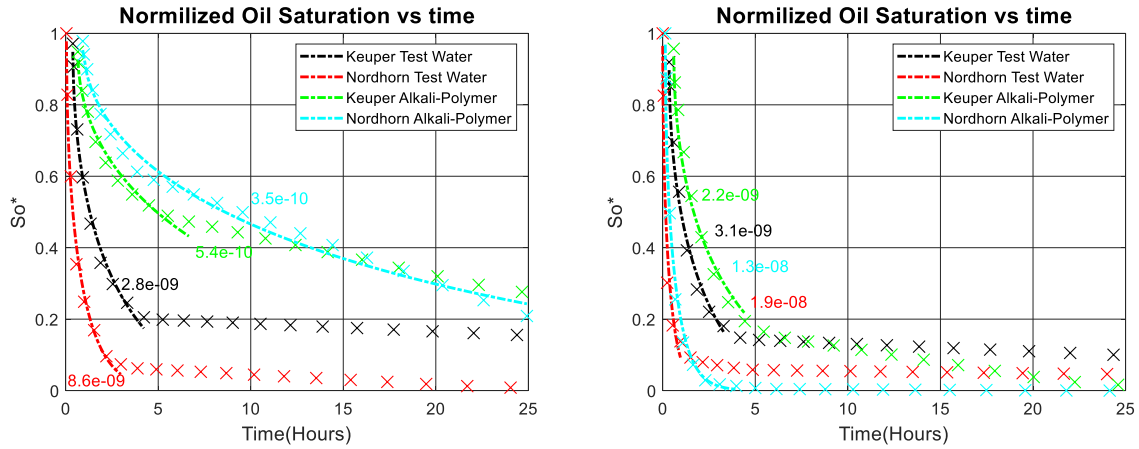

Figure 72 – Best fit of normalized oil saturation versus time plot for non-aged Nordhorn and Keuper core plugs saturated with high TAN (left) and low TAN oil (right) (Mineralogy effect) [Alkali: 7g/L Na_2CO_3, Polymer: 2000 ppm FLOPAAM 3630S]

As per the observations, in a general sense the Keuper core plugs exhibited slower rate of imbibition. This can be related to core plug permeability. In all cases, the usage of alkali-polymer as a displacing fluid led to slower oil production. Due to the so called ultra-low IFT between alkali-polymer and high TAN oil, the reduction of capillary forces and, finally, the imbibition rate is more significant, comparing to low TAN oil. The further comparison of these cases with aged core plugs might reveal more interdependencies.

Figure 73 shows the normalized oil plot for aged and non-aged Nordhorn and Keuper core plugs saturated with formation brine and high TAN oil. The plot presents a noteworthy result. While for Nordhorn core plugs, the effect of ageing is not significant, only minor changes in imbibition rate was observed, the Keuper core plugs are strongly affected by ageing process. This fact leads to a conclusion, that the core plug mineralogy is an important parameter, which tremendously affect the process of wettability alteration due to ageing and implementation of chemical solutions.

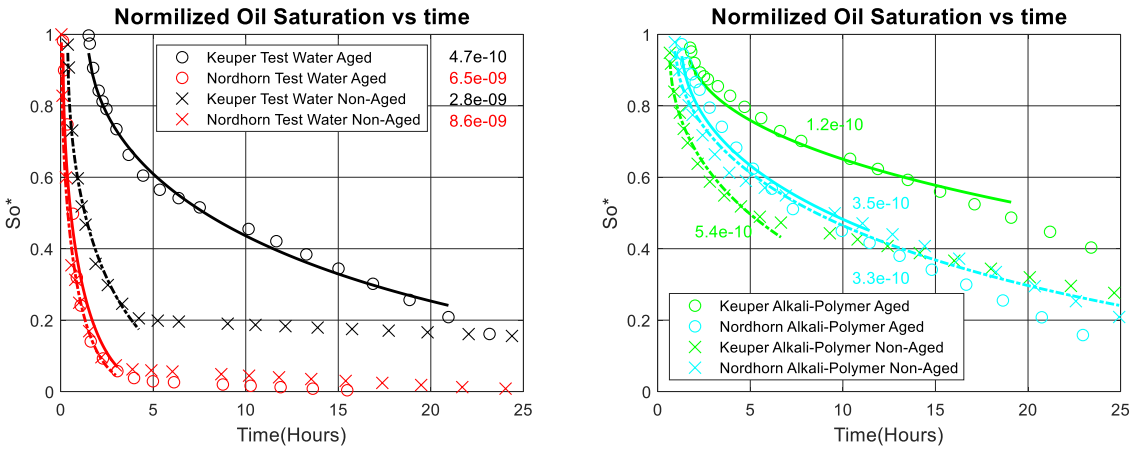

Figure 73 – Best fit of normalized oil saturation versus time plot for aged and non-aged Nordhorn and Keuper core plugs saturated with high TAN oil (Mineralogy effect) [Alkali: 7g/L Na_2CO_3, Polymer: 2000 ppm FLOPAAM 3630S]

A very strong influence of clay minerals on ageing process can be detected from Figure 74. A significant decrease in capillary diffusion coefficient together with small range of water saturation, where this capillary coefficient fits observed data and large value of residual oil saturation indicate a strongly oil-wet behaviour of the aged Keuper core plug comparing to non-aged case. In case of alkali-polymer solution evaluation using Keuper core plugs, a substantial decrease in capillary diffusion coefficient can be also observed. Similarly, a value of residual oil saturation is smaller for aged Keuper core plug than for non-aged one. This behaviour illustrates an initial oil-wet behaviour of the core plug, which is tuned towards water-wet state due to alkali-polymer application.

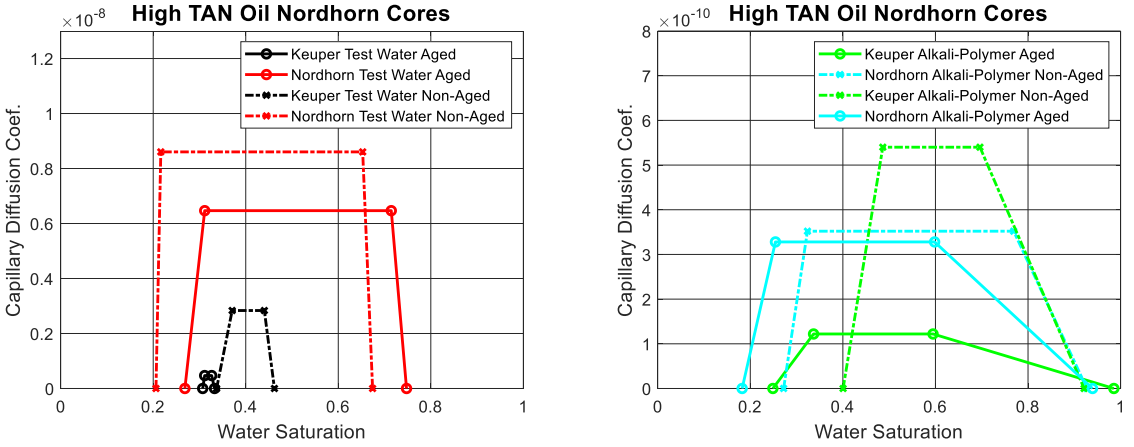

Figure 74 – Capillary diffusion coefficient [in m^2/s] as a function of water saturation for non-aged and aged Nordhorn and Keuper core plugs saturated with high TAN oil (Mineralogy effect) [Alkali: 7g/L Na_2CO_3, Polymer: 2000 ppm FLOPAAM 3630S]

The evaluation of dP_c/dS_w (Figure 75) is crucial when Keuper core plugs are used because of its high value of heterogeneity. Despite that fact, the calculated values of dP_c/dS_w confirm the considerable effect of clay minerals on wettability alteration process. While the Nordhorn core plugs show only slight decrease in dP_c/dS_w values after ageing, the same parameters for Keuper core plugs decrease in approximately 9 times.

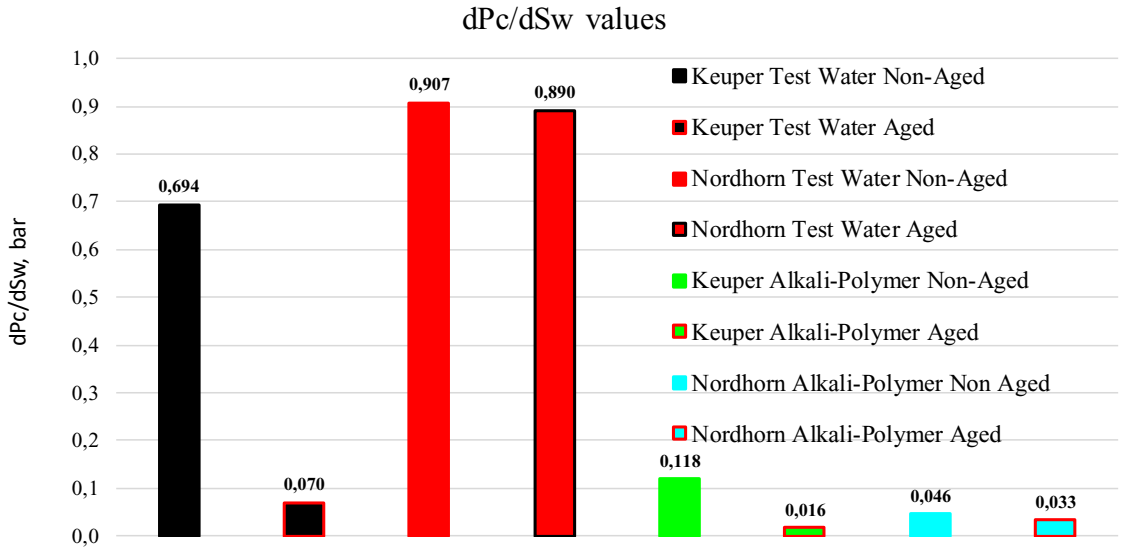

Figure 75 – Values of dP_c/dS_w for non-aged and aged Nordhorn and Keuper core plugs saturated with high TAN oil [Alkali: 7g/L Na_2CO_3, Polymer: 2000 ppm FLOPAAM 3630S]

Figure 76 depicts similar cases with the use of low TAN oil. Similar effect as in the case of high TAN oil, can be observed in this set of experiments. Ageing affects more significantly the Keuper core plugs with high content of clay minerals. In all cases, the reduction of imbibition rate was observed.

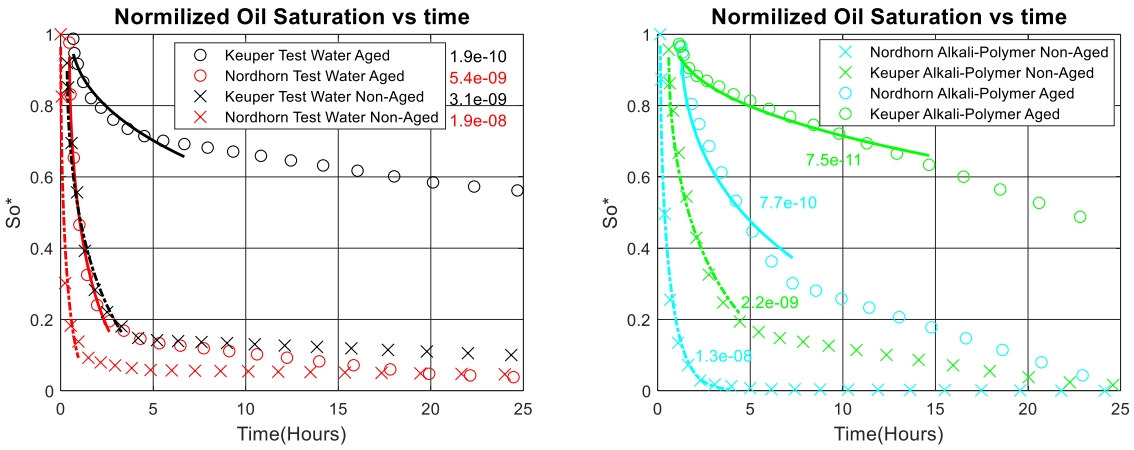

Figure 76 – Best fit of normalized oil saturation versus time plot for aged and non-aged Nordhorn and Keuper core plugs saturated with low TAN oil (Mineralogy effect) [Alkali: 7g/L Na_2CO_3, Polymer: 2000 ppm FLOPAAM 3630S]

Due to the ageing process, the capillary diffusion coefficient function strongly decreased comparing to non-aged cases. Another remarkable feature is that much higher residual oil saturation was observed for aged Keuper core plugs in comparison to Nordhorn samples. This can be a result of the strongly oil-wet state of the Keuper core plugs, whereas, the Nordhorn samples exhibit only a neutral-wet state. This observation is in agreement with the literature Ehrlich, R. et al. (1974) and Dong, H. et al. (2008), where the most beneficial wetting state is not water-wet nor oil-wet, but something in between. Moreover, Figure 78 shows a very large reduction in dP_c/dS_w values are estimated in case of low TAN oil application.

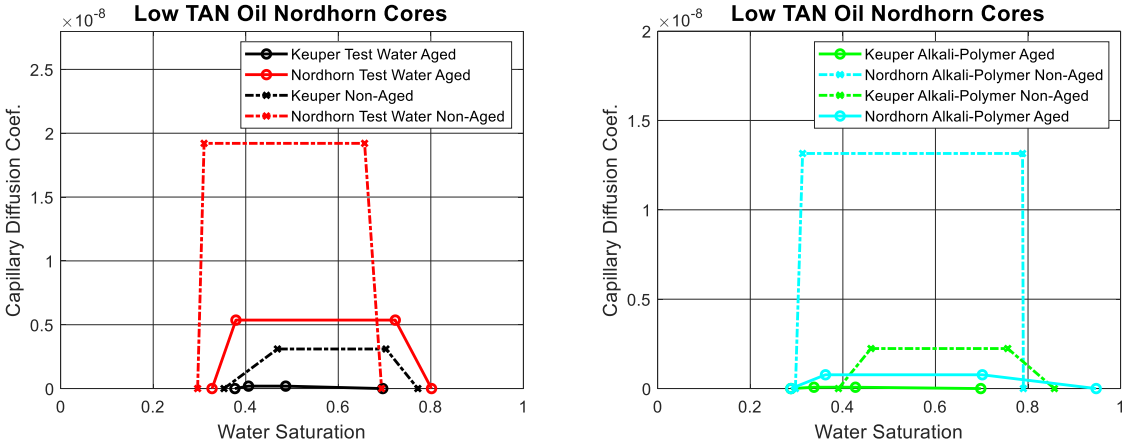

Figure 77 – Capillary diffusion coefficient [in m^2/s] as a function of water saturation for non-aged and aged Nordhorn and Keuper core plugs saturated with low TAN oil (Mineralogy effect) [Alkali: 7g/L Na_2CO_3, Polymer: 2000 ppm FLOPAAM 3630S]

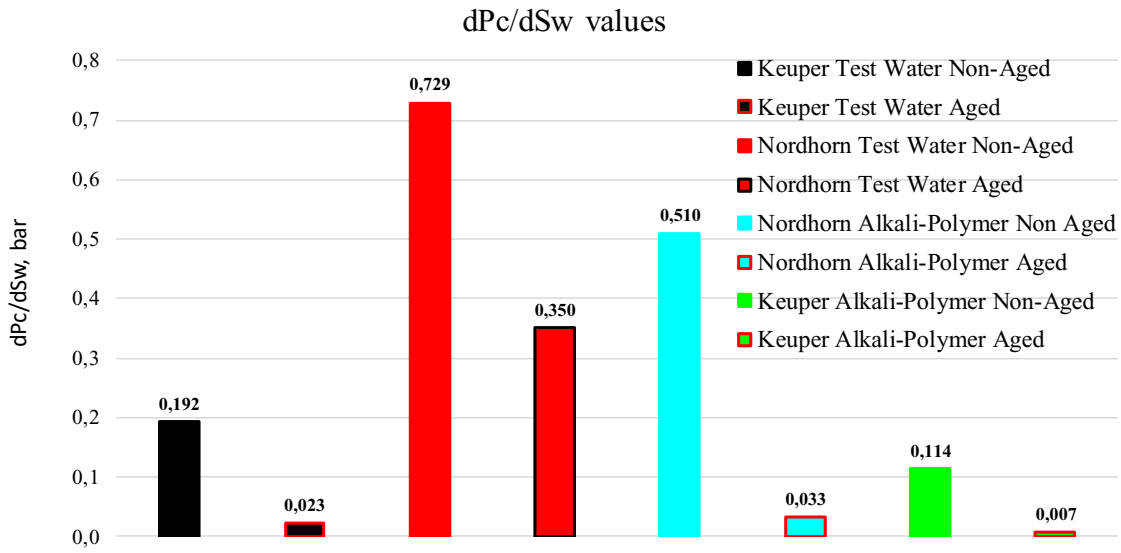

Figure 78 – Values of dP_c/dS_w for non-aged and aged Nordhorn and Keuper core plugs saturated with low TAN oil [Alkali: 7g/L Na_2CO_3, Polymer: 2000 ppm FLOPAAM 3630S]

Figure 78 shows a very large reduction in dP_c/dS_w values are estimated in case of low TAN oil application.

5.2 Numerical Solution (Constant D_c)

For the purpose of obtaining saturation profiles within the core plug, the capillary diffusion equation was solved numerically. The setup of numerical model is described in the Chapter 2.4.5. For numerical simulation, the same capillary diffusion coefficients as from analytical solution were used. This allows to check the correctness of numerical model setup. Only cases with the largest change in wettability due to ageing and implementation of alkali-polymer was solved numerically, namely, the cases with aged and non-aged Keuper core plugs saturated with high divalent ion composition brine and high TAN oil (see analytical solution in the Chapter 5.1.4).

Numerical simulation was performed for a constant capillary diffusion coefficient, defined analytically. This allows to compare and verify the numerical configuration/arrangement. For all simulations, the results obtained from numerical model follow exact behaviour of analytical solution and observed data during the experiments. Figure 79 shows the normalized oil saturation change as observed during the experiment, from analytical solution and from numerical calculations. All cases show reasonable match.

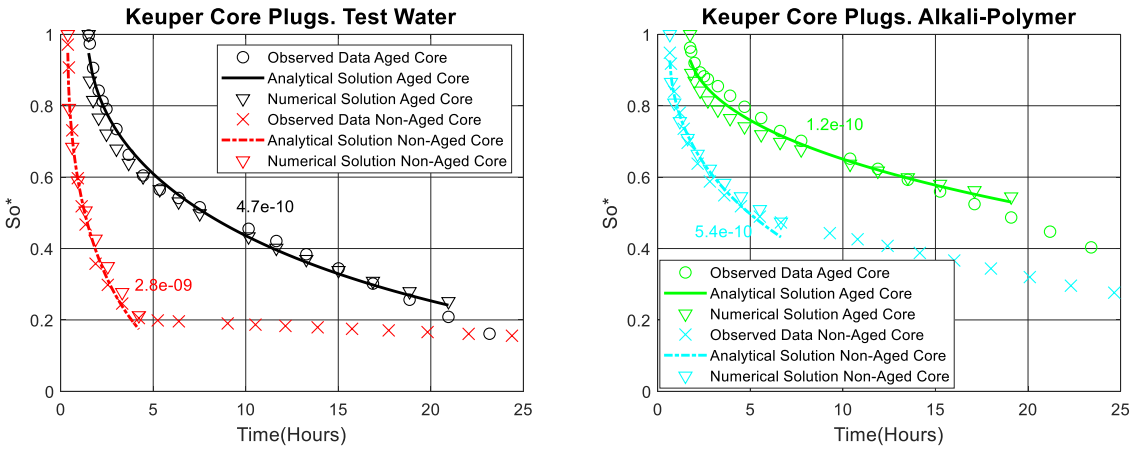

Figure 79 –Normalized oil saturation versus time plot for aged and non-aged Keuper core plugs saturated with high TAN [Alkali: 7g/L Na_2CO_3, Polymer: 2000 ppm FLOPAAM 3630S]

Having verified the correctness of the numerical simulation model, the data can be used to plot saturation profiles. Figure 80 depicts the saturation profiles along two planes: vertically (A-A') and horizontally (B-B') through the middle of the core plug for non-aged and aged Keuper core plug submerged into test water.

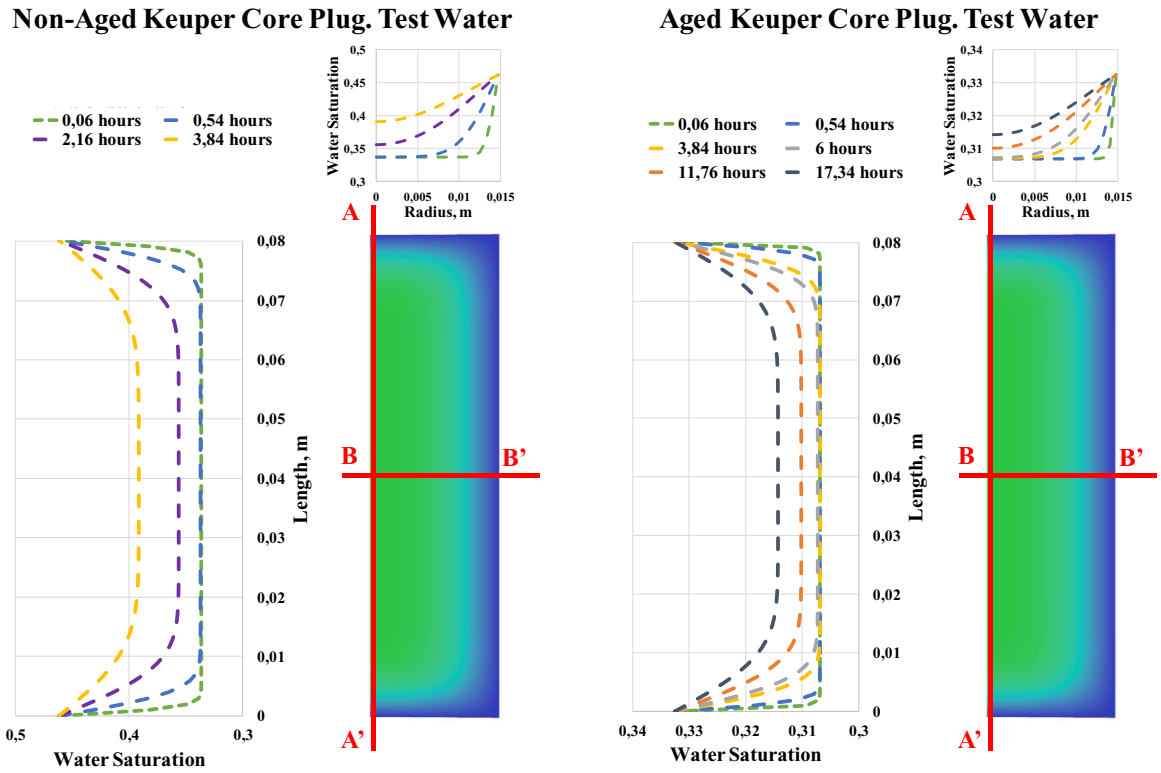

Figure 80 –Water saturation profiles for different time steps after the start of spontaneous imbibition test for non-aged (left) and aged (right) Keuper core plug saturated with high TAN (Test Water)

Figure 80 helps to detect how water imbibition process happens within the core plug. One can note, that for non-aged core plug, the water reaches the center of the core plug approximately after 2 hours, while for aged core plug, this values reaches around 10 hours. The imbibition process in case of aged core plug happens much slower than in non-aged case. During first minutes after the start of the test, the water saturation close to the open surfaces of the core plug rises drastically, after that, the saturation change slows down because of smaller local saturation gradient. Another outcome of this numerical simulation case is similar saturation profiles at the point of time, when the capillary diffusion coefficient does not hold constant value anymore. This happens when the saturation in the middle of the core plug reaches approximately the half of the saturation, which can be recovered. After that, there is no enough oil supply to hold the same production rate, which lead to slowing down of the production and, consequently, imbibition rate.

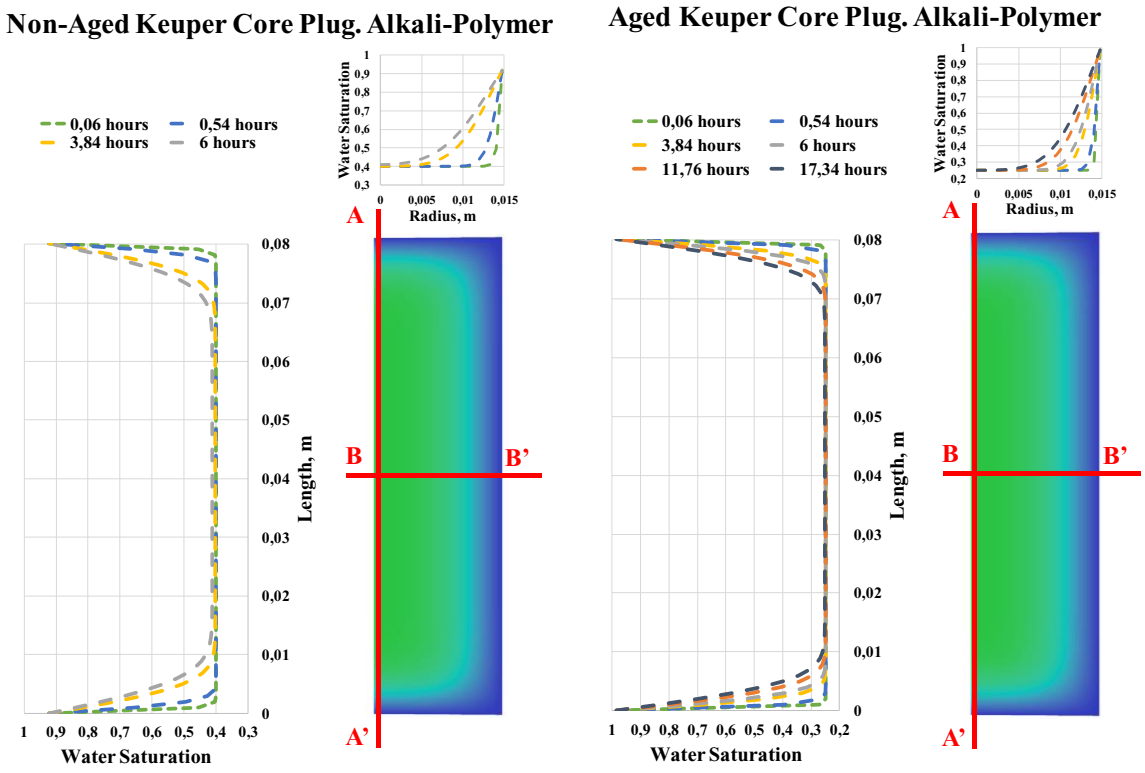

Figure 81 –Water saturation profiles for different time steps after the start of spontaneous imbibition test for non-aged (left) and aged (right) Keuper core plug saturated with high TAN (Alkali-Polymer) [Alkali: 7g/L Na_2CO_3, Polymer: 2000 ppm FLOPAAM 3630S]

Looking at the saturation profile in case of testing with alkali-polymer solution, a significantly slower imbibition rate is observed. The water saturation in the middle of the core plug start to change after 6 hours of imbibition for non-aged and 17 hours for aged Keuper core plug. At the time, when the imbibition process does not hold constant capillary diffusion coefficient,

approximately at the distant of half-radius from the center, the saturation is still at its initial value. In case of aged core plugs with alkali-polymer solution, the imbibition rate is much slower than in case of non-aged core plug. It can be seen from the saturation profile along the radius. The saturation profile in this case is steeper and main saturation changes happen close to the surfaces, which are open to flow. For non-aged core plug, the saturation change occurs much deeper in the core plug, closer to the center.

6 Summary and Conclusions

Conclusions have been grouped according the main addressed topics throughout the investigation. Topics include interfacial tension, spontaneous imbibition, analytical evaluation and numerical simulation evaluation. By using a complementary evaluation and cross analysis the topics helped on the ***Understanding of Wettability Changes during Alkali-Polymer***

I. ***Interfacial Tension***

- The decrease of IFT for high TAN oil is more significant, which reaches the ultra-low equilibrium value in a range of 0.01 mN/m. For low TAN oil, initially low value of IFT (~0.4 mN/m) was monotonically rising over 300 minutes of investigation with almost linear trend until ~1 mN/m.
- Interfacial tension between oils and test water stay constant with time in a range between 1 and 3,5 mN/m for high TAN oil and 2 to 4,5 mN/m for low TAN oil
- Addition of polymer to the test water and alkali solution causes a slight increase in the measured IFT values. Addition of polymer to the alkali solution leads to diminishing the effect of IFT reduction and an increase of the observed IFT pick value.

II. Spontaneous Imbibition

Oil Type Comparison

- Regardless the TAN number of oil, the imbibition rate is larger using Test Water as a displacing fluid. For the polymer, it was slowed down due to resulting higher viscosity. For alkali and alkali-polymer, the slower imbibition is explained by the IFT reduction.
- Non-aged core plugs: low TAN oil- all chemical solutions provided similar ultimate recovery; high TAN oil- the use of alkali and alkali-polymer solutions led to a larger amount of produced oil.

Effect of Core Ageing

- Using test water and polymer as displacing fluids reflected slower production rate only within the first hour of imbibition evaluation. Other cases exhibit significantly slower initial production rate.
- The smaller ultimate oil production for non-aged (water-wet) core plugs can be explained by the oil droplet snap-off phenomenon. Submerging more oil-wet core plugs into different solutions, the invading fluid enters the middle of the pore throat, displacing larger amount of oil, then in case of water-wet core.
- Wettability alteration due to alkali application: Fluid enters large pores and displaces oil from the neutral (oil) wet core plug. The drop in interfacial tension causes wettability alteration. Invading fluid starts to spread around the inner surface of the pore throats. It leads to oil detachment from the mineral surfaces

- The residual oil saturation is decreased for all aged Nordhorn core cases comparison to non-aged samples.

Effect of Brine Composition

- There are not significant changes in oil production rate and ultimate oil recovery, when formation brine or test water were used for initial saturation in case of non-aged (water-wet) core samples
- For aged (neutral to oil wet) core plugs saturated with high TAN oil, a higher production rate can be detected if formation water is used for primary saturation and the alkali-polymer solution as a displacing fluid.
- For low TAN oil, the divalent ions do not play a role in case of aged cores with implementation of alkali-polymer solution.

Effect of Core Mineralogy

- Core samples containing high clay content exhibited neutral to oil-wet behaviour even when the core was not aged
- For high TAN oil, Keuper (high clay content) core plugs showed significant decrease in production rate and ultimate oil recovery, indicating of strongly oil-wet system.
- During the application of alkali-polymer solution with high TAN oil, the oil-wet sample was returned to water-wet state. A higher ultimate recovery was achieved.
- In case of low TAN oil, a minor improvement of oil recovery with alkali-polymer solution. The oil droplet detachment does not happen
- Core plug mineralogy tremendously affects the process of wettability alteration due to ageing and implementation of chemical solutions.

III. Analytical Description

- Capillary diffusion coefficient stays constant over a large saturation range for non-aged core plugs. Only later production does not follow analytical solution for constant capillary diffusion.
- A much stronger change in the capillary diffusion function was noticed, when the brine with divalent ions present in the system. This suggests a stronger wettability alteration due to oil polar compounds – divalent ion – mineral surface bridging
- A significant decrease in capillary diffusion coefficient together with large value of residual oil saturation indicate a strongly oil-wet behaviour of the aged Keuper core.
- In case of alkali-polymer solution evaluation using Keuper core plugs, a value of residual oil saturation is smaller for aged Keuper core plug than for non-aged one. This behaviour illustrates an initial oil-wet behaviour of the core plug, which is tuned towards water-wet state due to alkali-polymer application

IV. Numerical Simulation Description

- For non-aged core plug, the water reaches the center of the core plug approximately after 2 hours, while for aged core plug, this values reaches around 10 hours
- During first minutes after the start of the test, the water saturation close to the open surfaces of the core plug rises drastically, after that, the saturation change slows down because of smaller local saturation gradient.
- Testing with alkali-polymer, the water phase saturation in the middle of the core plug start to change after 6 hours of imbibition for non-aged and 17 hours for aged Keuper core plug
- For non-aged core plug, the saturation change occurs much deeper in the core plug, closer to the center.

7 References

[1] Clemente, J., 2015, “How Much Oil Does the World Have Left?”, Journal Forbes

[2] Sheng, J.J., 2011, “Modern Chemical Enhanced Oil Recovery”

[3] Anderson, W.G., 1986, “Wettability Literature Survey- Part 1: Rock/Oil/Brine Interactions and the Effect of Core Handling on Wettability”, SPE 13932.

[4] McPhee, C., et. al., 2013, "Best Practice Core Analysis Guide", Wintershall

[5] Jadhunandan, P.P. et. al., 1999, “Effect of wettability on waterflood recovery for crude-oil/brine/rock interactions and oil recovery”

[6] Yuan, S., et. al., 1998, “Effects of Important Factors on Alkali/Surfactant/Polymer Flooding”, SPE 50916

[7] Ehrlich,R., et al., 1974, “Alkaline Waterflooding for Wettability Alteration – Evaluating a Potential Field Application”, Journal of Petroleum Technology

[8] Spinler, E.A., et. al., 2000, “Surfactant Induced Wettability Alteration in Porous Media”, Fundamentals and Applications in the Petroleum Industry

[9] Ayirala, S.C, 2002, “Surfactant-Induced relative permeability modifications fpr oil recovery enhancement”, A Master Thesis, Louisiana State University

[10] Ayirala, S.C, 2004, “Beneficial effects of wettability Altering Surfactant in Oil/wet Fractured reservoirs”, 8th International symposium on reservoir wettability and its effect on oil recovery

[11] https://www.glossary.oilfield.slb.com/en/Terms/w/wettability.aspx

[12] Raza, S.H., 1968, “Wettability of Reservoir Rocks and its Evaluation”

[13] Dong H. et. al., 2008, “The Effect of Wettability on Oil Recovery of Alkaline/Surfactant/Polymer Flooding”, SPE 102564

[14] Nutting, P.G., 1934, “Some Physical and Chemical Properties of Reservoir Rocks Bearing on the Accumulation and Discharge of Oil”, AAPG, Tusla

[15] Marsden, S.S., 1965, “The Wettability of the Bradford Sand, II; Pyrolysis Chromatography Study”

[16] Katz, D.L., 1942 “Possibility of Secondary Recovery for the Oklahoma City Wilcox Sand”, SPE 942028

[17] Chilingar, 1983 G.V. and Yen, T.F., “Some Notes on Wettability and Relative Permeabilities of Carbonate Reservoir Rocks, II”

[18] Cram, P.J., 1972, “Wettability Studies with Non-Hydrocarbon Constituents of Crude Oil”

[19] Denekas, M.O. et. al., 1959, “Effect of Crude Oil Components on Rock Wettability”

[20] Hall, A.C., 1983, “Stability of Aqueous Wetting Films in Athabasca Tar Sands”, SPEJ

[21] Melrose, J.C., 1982, “Interpretation of Mixed Wettability Sates in Reservoir Rocks”, SPE 10971

[22] Lowe, A.C., 1973, “On the Wetting of Carbonate Surfaces by Oil and Water”, AIME

[23] Berezin, V.M., 1982, “Adsorption of Asphaltenes and Tar from Petroleum by Sandstone”, SPE 11800

[24] Treiber, L.E., et. al., 1972, „A Laboratory Evaluation of the Wettability of Fifty Oil Producing Reservoirs“, SPEJ

[25] Dos Santos, R.G., et. al., 2006, „Contact angle measurements and wetting behavior of inner surfaces of pipelines exposed to heavy crude oil and water“, Journal of Petroleum Science and Engineering

[26] León-Pabón, J.A., et. al., 2014, “Experimental Comparison for the Calculation of Rock Wettability Using the Amott-Harvey Method and a New Visual Method”

[27] Morrow, N.R., 1975, “The Effects of Surface Roughness On Contact: Angle With Soecial Reference to Petroleum Recovery”, PETSOC-75-04-04

[28] Ma, S., et. al., 1996, “Effect of Contact Angle on Drainage and Imbibition in Regular Polygonal Tubes”, Colloids and Surfaces A: Physicochemical and Engineering Aspects

[29] Hamilton, W., 2000, “Oil and Gas in Austria”

[30] Butt., H-J., 2003, “Phyysics and Chemistry of Interfaces”

[31] Emery, L.W., 1970, “Caustic Slug Injection in the Singleton Field”

[32] Shiyi, Y., 1998, “Effects of Important Factors on Alkali/Surfactant/Polymer Flooding”, SPE50916

[33] Skripnik, A.G., 2012, “Experimental Studies of Oil Recovery After Alkali-Surfactant-Polymer (ASP) Flooding with West Salym Cores”, SPE162063

[34] Tong, Z. S., et. al., 1998, “A Study of Microscopic Flooding Mechanisms of Surfactant/Alkali/Polymer”, SPE39662

[35] Anon., 2018, “Machinery Lubrication”

[36] Arihara, N., et. al., 1999, “Oil Recovery Mechanisms of Alkali-Surfactant-Polymer Flooding”, SPE 54330

[37] Vonnegut, B., 1942, “Rotating Bubble Method for Determination of Surface and Interfacial Tension”

[38] Gong, X., 2017, “Understanding the wettability of nanometer-thick room temperature ionic liquids on solid surfaces”

[39] Schumi, B., et. al., 2019, “Alkali-Co-Solvent_Polymer Flooding of High TAN Number Oil: Using Phase Experiments, Micro-Models and Corefloods for Injection Agent Selection”, SPE195504-MS

[40] Lüftenegger, M., Clemens, T., 2017, “Chromatography Effects in Alkali Surfactant Polymer Flooding”, SPE185793-MS

[41] Leitenmuller, V., et. al., 2018, “Microemulsion Formation & Its Effect on Rheology Using Carbonate-Based Alkalis for AP or ASP Floods in the Matzen Field”, SPE190434-MS

[42] www.kruss-scientific.com

[43] www.Anton-Paar.com

[44] Lake, L.W, 1989, “Enhanced Oil Recovery”

[45] Glatz, G., 2013, “A Primer on Enhanced Oil Recovery”, Stanford University

[46] Eremin, N., Nazarova, L. N., 2003, “Enhanced Oil Recovery Methods”

[47] Pye, D.J., 1964, “Improved secondary recovery by control of water mobility”

[48] Bataweel, M.A., 2012, “Rheological Study for Surfactant-Polymer and Novel Alkali-Surfactant-Polymer Solutions”, SPE150913

[49] Dong, H., 2008, “The Effect of Wettability on Oil Recovery of Alkaline/Surfactant/Polymer Flooding”, SPE102564

[50] Juarez-Morejon, J.L., et. al., 2017, “Spontaneous Imbibition as Indicator of Wettability Change During Polymer Flooding”, EAGE

[51] De Gennes, P.G., 1971, “Reptation of a Polymer Chain in the Presence of Fixed Obstacles”, The Journal of Chemical Physics

[52] Jennings, H.Y., 1974, "A Caustic Waterflooding Process for Heavy Oils", J.Pet.Tech

[53] McWorther, D.B., Sunada, D.K., 1990, "Exact Integral Solution for Two-Phase Flow"

[54] Chen, J., et. al., 1995, "Theoretical Investigation of Countercurrent Imbibition in Fractured Reservoir Matrix Blocks", SPE 29141

[55] Kashchiev, D., Firoozabadi, A., 2003, "Analytical Solution for 1D Countercurrent Imbibition in Water-Wet Media", SPE-87333-PA

[56] Stoll, W.M., et. al., 2008, "Toward Field-Scale Wettability Modification- The Limitations of Diffusive Transport", SPE Reservoir Evaluation and Engineering

[57] Chevalier, T., et. al., 2018, "A Novel Experimental Approach for Studying Spontaneous Imbibition Process with Alkaline Solutions"

[58] Crank, J., 1976, "The Mathematics of Diffusion (2nd Edition)", Oxford

[59] Sheng, J.J., 2105, "Investigation of Alkaline-Crude Oil Reaction", Petroleum

[60] Wael, A., et. al., 2007, "Fundamentals of Wettability"

[61] Pudji, P.J., 1990, "Effects of Brine Composition, Crude Oil, and Aging Conditions on Wettability and Oil Recovery", Dissertation

[62] Hujer, W., et. al., 2017, "EOR by Alkali Flooding in the Vienna Basin: First Experimental Results of Alkali/Mineral Reactions in Reservoir Rocks", SCA 2017-053

[63] Awolayo, A.N., et. al., 2018, "Brine-Dependent Recovery Processes in Carbonate and Sandstone Petroleum Reservoirs: Review of Laboratory-Field Studies, Interfacial Mechanisms and Modeling Attempts"

[64] Mohnot, S. M., et. al., 1987, "A Study of Mineral/Alkali Reactions", SPE13032

[65] Mohnot, S. M., et. al., 1989, "A Study of Mineral/Alkali Reactions - Part 2"

[66] Sharma, M. M., Jang, L. K., Yen, T. F., 1989, "Transient Interfacial Tension Behaviour of Crude-Oil/Caustic Interfaces" Society of Petroleum Engineers: doi:10.2118/12669

[67] Arnold, P., 2018, "Experimental Investigation of interfacial Tension for Alkaline Flooding". Master Thesis

[68] deZabala, E.F., 1986, "A Nonequilibrium Description of Alkaline Waterflooding"

[69] Sarquez, J.F.R, et. al., 2019, "Long-term Polymer Degradation in High pH Solutions and Polymer Effect on Alkali-oil Phases"

[70] Salehi, M., 2009, " Enhancing the Spontaneous Imbibition Process in Naturally Fractured Reservoirs through Wettability Alteration using Surfactants: Mechanistic Study and Feasibility of using Biosurfactnats "

[71] Abe, A.A., 2005, "Relative Permeability and Wettability Implications of Dilute Surfactants at Reservoir Conditions"

[72] Chandra, S., et. al., 2003, "Effect of Brine Dilution and Surfactant Concentration on Spreading and Wettability", SPE80273

[73] Sharma, M. M., et. al., 1989, "Transient Interfacial Tension Behavior of Crude-Oil/Caustic Interfaces", SPE

[74] Haagh, M.E.J., et. al., 2017, "Salinity-Dependent Contact Angle Alteration in Oil/Brine/Silicate Systems: the Critical Role of Divalent Cations"

[75] Wei, J., et. al., 2011, "A Study on Alkali Consumption Regularity in Minerals of Reservoirs During Alkali(NaoH)/Surfactant/Polymer Flooding in Daqing Oilfield"

[76] EOR lecture handout, Montan University, Leoben

List of Tables

Table 1: Contact angle to wettability state relationship [4] 15

Table 2: Amott-Harvey wetting indices 18

Table 3: USBM wetting indices 19

Table 4: Oil properties 36

Table 5: Brine properties and composition 37

Table 6: Chemical solution properties 38

Table 7: Average Properties of the Core plug used in this work 39

Table 8: Overall Comparison for Phase permeability and saturation data of the cores used in this work 42

List of Figures

Figure 1: Capillary desaturation curve [44] 4
Figure 2: Representation of the mobility ratio effect on sweep efficiency [45] 5
Figure 3: Creation of in-situ surfactants 6
Figure 4: Wettability change due to polymer application [50] 7
Figure 5: Young's equation schematics 8
Figure 6: Shape of spinning drop related to interfacial tension 9
Figure 7: Water-wet rock storage and flow behaviour 11
Figure 8: Oil-wet rock storage and flow behaviour 11
Figure 9: Wettability change due to polar molecule adsorption (a) and organic matter precipitation (b) 12
Figure 10: Sessile drop contact angle measurements [26] 14
Figure 11: Capillary pressure curve 15
Figure 12: Schematic of Amott-Harvey test [4] 17
Figure 13: Capillary pressure curve for primary imbibition (red) and secondary drainage (blue) 18
Figure 14: Axial numerical mesh with the top-view (top) and side-view (bottom) and applied boundary conditions 21
Figure 15: Anton Paar Density Meter [43] 23
Figure 16: Anton Paar Rheometer [43] 24
Figure 17: Torque error check before device calibration 25
Figure 18: Torque error check after device calibration 25
Figure 19: Used spinning drop tensiometer [42] 26
Figure 20: Components of the IFT measurements device 26
Figure 21: Photo of Nordhorn (left) and Keuper outcrop rock (right) 27
Figure 22: SEM results on Nordhorn Outcrop Core [62] 28
Figure 23: This-section analysis of Nordhorn outcrop rock 28
Figure 24: Soxhlet extraction apparatus 29
Figure 25: Boyle's porosimeter schematics 30
Figure 26: N2 permeability measurement device 30
Figure 27: Pre-saturation setup schematics 31
Figure 28: Core Pre-saturation setup equipment 31

Figure 29: Water permeability measurement (i.e. Core NH-113) 32

Figure 30: Oil permeability measurement (i.e. Core NH-117) 33

Figure 31: Amott cell schematic 34

Figure 32: Amott cell in the oven 35

Figure 33: Steady-shear viscosity of polymer (left) and alkali-polymer (right) versus shear rate at 25°C 38

Figure 34: Steady-shear viscosity of polymer (left) and alkali-polymer (right) versus shear rate at 60°C 38

Figure 35: Porosity-N2 permeability cross-plot for Nordhorn (left) and Keuper core plugs (right) 39

Figure 36: Cross-plot permeability to Water and Gas for Nordhorn (left and Keuper core plugs (right) 40

Figure 37: Cross-plot permeability to Water and Gas without outliers for Nordhorn (left) and Keuper samples (right) 40

Figure 38: Cross-plot permeability to Gas and Oil for Nordhorn (left) and Keuper core plugs (right) 41

Figure 39: Cross-plot permeability to Gas and Oil without outliers for Nordhorn (left) and Keuper samples (right) 41

Figure 40: Swirr versus Kro cross-plot for Nordhorn (left) and Keuper core plugs (right) 42

Figure 41: IFT measurement for 16-TH (left) and Saint Ulrich oil (right) at 60°C [Alkali: 7g/L Na_2CO_3, Polymer: 2000 ppm FLOPAAM 3630S] 44

Figure 42: IFT measurement for high TAN (left) and low TAN oil (right) with Test Water at 60°C 45

Figure 43: IFT measurement for high TAN (left) and low TAN oil (right) with Alkali Solution at 60°C [Alkali: 7g/L Na_2CO_3] 45

Figure 44: IFT measurement for high TAN (left) and low TAN oil (right) with Polymer at 60°C [Polymer: 2000 ppm FLOPAAM 3630S] 46

Figure 45: IFT measurement for high TAN (left) and low TAN oil (right) with Alkali-Polymer at 60°C [Alkali: 7g/L Na_2CO_3, Polymer: 2000 ppm FLOPAAM 3630S] 47

Figure 46: Performed spontaneous imbibition tests and studied parameters 48

Figure 47: Percent of production versus square root of time plot for Nordhorn core plugs using high TAN oil (left) and low TAN oil (right) at 60°C [Alkali: 7g/L Na_2CO_3, Polymer: 2000 ppm FLOPAAM 3630S] 49

Figure 48: Percent of production versus square root of time plot for Nordhorn non-aged and aged core plugs saturated with high TAN oil at 60°C [Alkali: 7g/L Na_2CO_3, Polymer: 2000 ppm FLOPAAM 3630S] 50

Figure 49: Percent of production versus square root of time plot for Nordhorn non-aged and aged core plugs saturated with low TAN oil at 60°C [Alkali: 7g/L Na_2CO_3, Polymer: 2000 ppm FLOPAAM 3630S] 51

Figure 50: Percent of production versus square root of time plot for non-aged Nordhorn core plugs (water composition comparison) for high Tan oil (left) and low TAN oil (right) at 60°C [Alkali: 7g/L Na_2CO_3, Polymer: 2000 ppm FLOPAAM 3630S].....52

Figure 51: Percent of production versus square root of time plot for non-aged and aged Nordhorn core plugs saturated with high TAN oil (water composition comparison) at 60°C [Alkali: 7g/L Na_2CO_3, Polymer: 2000 ppm FLOPAAM 3630S].....52

Figure 52: Schematic process of wettability alteration due to anionic surfactant formation 53

Figure 53: Percent of production versus square root of time plot for non-aged and aged Nordhorn core plugs saturated with low TAN oil (water composition comparison) at 60°C [Alkali: 7g/L Na_2CO_3, Polymer: 2000 ppm FLOPAAM 3630S].....54

Figure 54: Percent of production versus square root of time plot for non-aged Nordhorn and Keuper core plugs for high Tan oil (left) and low TAN oil (right) at 60°C [Alkali: 7g/L Na_2CO_3, Polymer: 2000 ppm FLOPAAM 3630S] 55

Figure 55: Percent of production versus square root of time plot for non-aged and aged Keuper and Nordhorn core plugs saturated with high TAN oil at 60°C [Alkali: 7g/L Na_2CO_3, Polymer: 2000 ppm FLOPAAM 3630S] 56

Figure 56: Percent of production versus square root of time plot for non-aged and aged Keuper and Nordhorn core plugs saturated with low TAN oil at 60°C [Alkali: 7g/L Na_2CO_3, Polymer: 2000 ppm FLOPAAM 3630S] 56

Figure 57: Normalized oil saturation versus time plot for Nordhorn non-aged core plugs saturated with high TAN (left) and low TAN oil (right) [Alkali: 7g/L Na_2CO_3, Polymer: 2000 ppm FLOPAAM 3630S].....58

Figure 58: Best fit of normalized oil saturation versus time plot for Nordhorn non-aged core plugs saturated with high TAN (left) and low TAN oil (right) [Alkali: 7g/L Na_2CO_3, Polymer: 2000 ppm FLOPAAM 3630S] 59

Figure 59: Best fit of normalized oil saturation versus time plot for Nordhorn non-aged and aged core plugs saturated with high TAN oil [Alkali: 7g/L Na_2CO_3, Polymer: 2000 ppm FLOPAAM 3630S] 60

Figure 60: Capillary diffusion coefficient as a function of water saturation for Nordhorn non-aged and aged core plugs saturated with high TAN oil [Alkali: 7g/L Na_2CO_3, Polymer: 2000 ppm FLOPAAM 3630S].....60

Figure 61: Values of dP_c/dS_w for Nordhorn non-aged and aged core plugs saturated with high TAN oil [Alkali: 7g/L Na_2CO_3, Polymer: 2000 ppm FLOPAAM 3630S] 61

Figure 62: Best fit of normalized oil saturation versus time plot for Nordhorn non-aged and aged core plugs saturated with low TAN oil [Alkali: 7g/L Na_2CO_3, Polymer: 2000 ppm FLOPAAM 3630S]..62

Figure 63: Capillary diffusion coefficient as a function of water saturation for Nordhorn non-aged and aged core plugs saturated with low TAN oil [Alkali: 7g/L Na_2CO_3, Polymer: 2000 ppm FLOPAAM 3630S]....62

Figure 64: Values of dP_c/dS_w for Nordhorn non-aged and aged core plugs saturated with low TAN oil [Alkali: 7g/L Na_2CO_3, Polymer: 2000 ppm FLOPAAM 3630S] 63

Figure 65: Best fit of normalized oil saturation versus time plot for non-aged Nordhorn core plugs saturated with high TAN (left) and low TAN oil (right) (Brine composition effect) [Alkali: 7g/L Na_2CO_3, Polymer: 2000 ppm FLOPAAM 3630S]....64

Figure 66: Best fit of normalized oil saturation versus time plot for aged and non-aged Nordhorn core plugs saturated with high TAN oil (Brine composition effect) [Alkali: 7g/L Na_2CO_3, Polymer: 2000 ppm FLOPAAM 3630S] 64

Figure 67: Capillary diffusion coefficient as a function of water saturation for Nordhorn non-aged and aged core plugs saturated with high TAN oil (Brine composition effect) [Alkali: 7g/L Na_2CO_3, Polymer: 2000 ppm FLOPAAM 3630S]....65

Figure 68: Values of dP_c/dS_w for Nordhorn non-aged and aged core plugs saturated with high TAN oil [Alkali: 7g/L Na_2CO_3, Polymer: 2000 ppm FLOPAAM 3630S] 66

Figure 69: Best fit of normalized oil saturation versus time plot for aged and non-aged Nordhorn core plugs saturated with low TAN oil (Brine composition effect) [Alkali: 7g/L Na_2CO_3, Polymer: 2000 ppm FLOPAAM 3630S] 66

Figure 70: Capillary diffusion coefficient as a function of water saturation for Nordhorn non-aged and aged core plugs saturated with low TAN oil (Brine composition effect) [Alkali: 7g/L Na_2CO_3, Polymer: 2000 ppm FLOPAAM 3630S]....67

Figure 71: Values of dP_c/dS_w for Nordhorn non-aged and aged core plugs saturated with low TAN oil [Alkali: 7g/L Na_2CO_3, Polymer: 2000 ppm FLOPAAM 3630S] 67

Figure 72: Best fit of normalized oil saturation versus time plot for non-aged Nordhorn and Keuper core plugs saturated with high TAN (left) and low TAN oil (right) (Mineralogy effect) [Alkali: 7g/L Na_2CO_3, Polymer: 2000 ppm FLOPAAM 3630S]....68

Figure 73: Best fit of normalized oil saturation versus time plot for aged and non-aged Nordhorn and Keuper core plugs saturated with high TAN oil (Mineralogy effect) [Alkali: 7g/L Na_2CO_3, Polymer: 2000 ppm FLOPAAM 3630S] 69

Figure 74: Capillary diffusion coefficient as a function of water saturation for non-aged and aged Nordhorn and Keuper core plugs saturated with high TAN oil (Mineralogy effect) [Alkali: 7g/L Na_2CO_3, Polymer: 2000 ppm FLOPAAM 3630S]....69

Figure 75: Values of dP_c/dS_w for non-aged and aged Nordhorn and Keuper core plugs saturated with high TAN oil [Alkali: 7g/L Na_2CO_3, Polymer: 2000 ppm FLOPAAM 3630S]....70

Figure 76: Best fit of normalized oil saturation versus time plot for aged and non-aged Nordhorn and Keuper core plugs saturated with low TAN oil (Mineralogy effect) [Alkali: 7g/L Na_2CO_3, Polymer: 2000 ppm FLOPAAM 3630S] 71

Figure 77: Capillary diffusion coefficient as a function of water saturation for non-aged and aged Nordhorn and Keuper core plugs saturated with low TAN oil (Mineralogy effect) [Alkali: 7g/L Na_2CO_3, Polymer: 2000 ppm FLOPAAM 3630S].....71

Figure 78: Values of dP_c/dS_w for non-aged and aged Nordhorn and Keuper core plugs saturated with low TAN oil [Alkali: 7g/L Na_2CO_3, Polymer: 2000 ppm FLOPAAM 3630S] 72

Figure 79: Normalized oil saturation versus time plot for aged and non-aged Keuper core plugs saturated with high TAN [Alkali: 7g/L Na_2CO_3, Polymer: 2000 ppm FLOPAAM 3630S] 73

Figure 80: Water saturation profiles for different time steps after the start of spontaneous imbibition test for non-aged (left) and aged (right) Keuper core plug saturated with high TAN (Test Water)73

Figure 81: Water saturation profiles for different time steps after the start of spontaneous imbibition test for non-aged (left) and aged (right) Keuper core plug saturated with high TAN (Alkali-Polymer) [Alkali: 7g/L Na_2CO_3, Polymer: 2000 ppm FLOPAAM 3630S].....74